GENETIC ALTERATIONS IN PROSTATE CANCER: EVALUATING THEIR BIOMARKER POTENTIAL AND ROLES IN THERAPEUTIC RESPONSE AND RESISTANCE

By
Samantha Danielle Torquato

A dissertation submitted to Johns Hopkins University in conformity with the requirements for the degree of Doctor of Philosophy

Baltimore, Maryland
August 2018

ABSTRACT

Prostate cancer (PCa) continues to be a leading cause of cancer-related death in United States men due to the subset of patients who develop metastatic disease. In spite of recent advances, two substantial clinical challenges remain today: identifying who is at risk for (1) metastatic recurrence and (2) developing resistance to current therapies. In order to address these two main challenges, three novel approaches were taken to evaluate the potential of PCa genetic alterations as biomarkers and the roles that these genetic alterations have in therapeutic response and resistance. For our first study, genetic aberrations discovered by the next-generation sequencing (NGS) of patients' primary tumor DNA (which was isolated from radical prostatectomy samples) were probed for by droplet digital PCR (ddPCR) in the corresponding patient's plasma-derived cell-free DNA (cfDNA) isolated before radical prostatectomy. Determining if it is possible to assess the genetic landscape of primary PCa by liquid biopsy, may ultimately lead to the discovery of biomarkers for disease risk stratification as well as the ability to better predict disease outcomes and treat localized PCa patients. For our second study, metastatic castration-resistant prostate cancer (mCRPC) patients were prospectively enrolled in order to validate gene alterations, such as androgen receptor (*AR*) ligand-binding domain (LBD) mutations and/or *AR* copy number (CN) gain, detected in cfDNA as markers of enzalutamide and abiraterone resistance. Here, we show that *AR* LBD missense mutations are associated with a shorter progression-free survival (PFS). In addition, loss of the tumor protein p53 (*TP53*) gene and defects in the phosphoinositide 3-kinase

(PI3K) pathway are associated with a worse overall survival (OS). In our third study, the CRISPR/Cas9 system was used to generate an isogenic panel of PCa cell lines, containing both individual and multiple hotspot *AR* LBD mutations. The findings from these *in vitro* models will illuminate the biological role that these genetic alterations have in resistance to contemporary next-generation therapies, such as abiraterone and enzalutamide. Taken together, our studies provide valuable insight on how to better identify which PCa patients are at risk for developing lethal disease and resistance to current treatments.

Thesis Advisor: Paula J. Hurley, Ph.D.

Thesis Readers: Paula J. Hurley, Ph.D.

Srinivasan Yegnasubramanian, M.D., Ph.D.

ACKNOWLEDGEMENTS

There are several people I wish to acknowledge for the support they have given me throughout my graduate school career. Without the following colleagues, friends and family, this dissertation would not have been possible.

First, I would like to thank my thesis advisor, Dr. Paula J. Hurley. Over the past four years, you have taught me what it takes to be an effective principle investigator, to run a productive laboratory, and to succeed in science. Thank you for having an open-door policy, which allowed for a constant exchange of scientific ideas. I would also like to thank Dr. Ben H. Park for inviting me to your laboratory in order to learn cutting-edge science firsthand and for welcoming me into your home for all of the major holidays. I would like to acknowledge the members of my thesis committee: Dr. Srinivasan Yegnasubramanian, Dr. John T. Isaacs, and Dr. Shawn E. Lupold. Every aspect of my thesis project would not have been as successful without your mentorship and wisdom.

The members of the Hurley Laboratory have contributed to my graduate school experience by sharing their technical talents and scientific knowledge as well as providing moral support and loyal friendships. Robert Hughes (Rob), you have been more than a colleague, classmate, and friend; I finally know what it's like to have a big brother. Rebecca Miller (Becky), thank you for the countless hours you spent ordering supplies so that I could complete my thesis project and for being a good listener.

The members of the Park Laboratory have been a supportive influence throughout graduate school, always willing to share their expertise and teach me

new techniques. Dr. W. Brian Dalton, the scientific discussions we had over the years greatly enriched my Ph.D. experience, and Chapter 3 of this dissertation would not have been possible without your guidance. Dr. Natasha Hunter, the patient room was truly not as fun until we started working together, and Chapter 1 of this dissertation would not have been possible without you.

I would also like to thank the administrators of Cellular and Molecular Medicine (CMM) for making my dreams come true when I was accepted into this Ph.D. program. Dr. Rajini Rao and Dr. Robert A. Casero, Jr., thank you for your advice and inspiration throughout my graduate school experience. To Colleen Graham and Leslie Lichter, you are two of the strongest and fiercest women I know; thank you for all of the laughs, hugs, and unconditional support. To my CMM classmates: from our first Thanksgiving to our trip to see the cherry blossoms in DC, from our coating ceremony to the many weddings, I want to say thank you for making graduate school memorable. To Jessica Miciak (Jess), thank you for the sisterly love you have shown me; this journey would not have been the same without you and your humor. To Ruchama Steinberg (Roo), when you meet someone from home, it doesn't seem like home is that far away. Thank you for being a true friend and trustworthy confidant.

Lastly, this dissertation is dedicated to my family. Mom and Dad, thank you for your unconditional love and for all of the sacrifices you have made so that I could achieve my dreams and accomplish all of my personal and professional goals. To my sister, Melissa, I am grateful for your unwavering belief in me and for all of the times you have motivated me to continue moving forward. To my

grandparents, thank you for your endless love and encouragement as well as the constant reminder that you are proud of me. I would not be where I am today without all of you.

TABLE OF CONTENTS

Preface

Chapters

LIST OF TABLES

Chapter 3

LIST OF FIGURES

1 Genetic Alterations as Potential Biomarkers for Localized Prostate Cancer

Introduction

Prostate Cancer (PCa) and PCa Screening

PCa is the second most common cancer in men worldwide [1]. It is estimated that in 2018, PCa will be diagnosed in 164,690 men in the United States alone and that 29,430 men will die of this disease, which is equivalent to 9% of the total cancer-related deaths in United States men [2]. This high incidence of PCa can be attributed to multiple genetic and demographic factors, such as age, family history, and race [3]. However, due to advances in PCa screening, the five-year relative survival rate for PCa, regardless of race and disease stage at diagnosis, is 99% [2].

The Prostate-Specific Antigen (PSA) blood test has allowed for the early detection of PCa. In fact, regular PSA screening aids in the diagnoses of men with prostatic carcinoma, on average, 10-12 years earlier in their natural history of the disease than those men who remain unscreened [4-7]. Thus, due to the PSA blood test, the majority of initially detected PCa (~90%) is still localized disease [4]. Today, it is widely acknowledged that the PSA blood test can detect high levels of circulating PSA that may be present due to noncancerous conditions of the prostate, such as inflammation. Therefore, the PSA blood test alone cannot be used as a reliable diagnostic tool for primary PCa, but can still assist in the monitoring of disease progression once the disease has been confirmed [8].

Localized PCa and Disease Risk Stratification

Localized PCa is a clinically and molecularly heterogeneous disease, which is best highlighted by the fact that some patients are cured of their indolent disease with initial therapy, while others will die from their more aggressive cancers [9]. It is due to this subset of aggressive and metastatic cancers that PCa remains a leading cause of death. Over the past two decades, many researchers have attempted to gain a better understanding of who is at risk for metastatic disease in order to positively impact clinical disease management. Earlier research efforts focused on developing accurate disease risk stratification systems, relying on both clinical and pathological parameters. These initial systems, which involved Gleason grading or assessing free PSA levels alone, have been shown to be severely deficient in predicting disease outcomes [10-12]. Today, enhanced risk stratification systems, such as five-grade grouping and the Prostate Health Index (PHI), exist [13, 14]; however, due to the heterogeneous nature of PCa, these systems do not have perfect predictive abilities. Thus, molecular and genetic features of localized PCa are still being studied with the intention of further improving the ability to distinguish between indolent and aggressive disease in the clinic.

Genetic Landscape of Primary PCa

Multiple studies have identified genetic alterations (such as mutations, copy number variations, rearrangements and fusions) in primary PCa, aiming to determine if the genomic status of a tumor could be used to additionally

differentiate between low- and high-risk disease [15-22]. In 2015, a comprehensive molecular profiling study of primary PCa found that 74% of tumors could be assigned to one of seven genomically distinct subtypes (Figure 1.1) [9]. The mutually exclusive subtypes defined by this study were fusions in 1) ETS-related gene (*ERG*), 2) ETS variant 1 (*ETV1*), 3) ETS variant 4 (*ETV4*), 4) Friend leukemia virus integration 1 (*FLI1*) and mutations in 5) Speckle-type BTB/POZ protein (*SPOP*), 6) Forkhead box A1 (*FOXA1*), 7) Isocitrate dehydrogenase 1 (NADP+) (*IDH1*) [9].

Fusions between *ERG* or the other members of the ETS family of transcription factors and the promoters of androgen receptor (AR)-targeted genes are extremely common in localized PCa. In fact, the *TMPRSS2:ERG* gene fusion is the most common genetic alteration in primary PCa, occurring in 40-50% of tumors [9, 23, 24]. However, multiple studies in the past decade have shown that *TMPRSS2:ERG* gene fusions do not significantly correlate with long-term patient outcomes, the risk of biochemical recurrence, or even PCa-specific mortality [25, 26].

While somatic point mutations are less common in PCa than in other solid malignancies, genetic mutations have been discovered in recent years. *SPOP* missense mutations occur in up to 15% of clinically localized PCa, making *SPOP* one of the most commonly mutated genes in primary PCa [9, 16, 17, 27]. The *SPOP* gene encodes for a substrate-binding adapter protein that provides specificity to a CUL3-based E3 ubiquitin ligase [28]. To date, multiple oncogenic substrates of SPOP have been discovered, such as DEK [29], tripartite motif-

containing 24 (TRIM24) [29, 30], and AR [31, 32]. The Y87, F102, W131, and F133 residues are located in the SPOP protein's MATH domain, are important for substrate-binding, and are the most commonly mutated residues in primary PCa [16, 28]. In 2017, Blattner et al. showed with a conditional mouse model that mutated SPOP drives prostate tumorigenesis *in vivo* by activating both AR and phosphatidylinositol-4,5-bisphosphate 3-kinase (PI3K)/mechanistic target of rapamycin (mTOR) signaling [33].

The *FOXA1* gene encodes for a transcription factor that has been previously shown to target the *AR* [34], to be required for prostate epithelial cell differentiation [35], to play a role in PCa oncogenesis [36], and to promote cell cycle progression in castration-resistant prostate cancer (CRPC) [37]. In multiple studies, it has been found that *FOXA1* mutations occur in about 4% of localized PCa [9, 16, 38]. Mutations in *FOXA1* have been found in its DNA-binding domain, Forkhead domain, and C-terminal trans-activating domain [9, 16, 38]. Today, it is still unclear if these mutations impact FOXA1's binding to its DNA targets or interaction with its transcriptional coregulators [9, 16]. Meanwhile, the *IDH1* gene encodes for the cytoplasmic form of IDH [39]. *IDH1* mutations have been shown to occur in only 1 to 3% of primary PCa and significantly correlate with early onset disease [9, 39, 40].

The following genes have also been discovered to be consistently altered in primary PCa across multiple studies; however, they do not necessarily form mutually exclusive subgroups. The oncogene PI3K-alpha (*PIK3CA*) and the tumor suppressor phosphatase and tensin homolog (*PTEN*), both of which are

genes in the PI3K/mTOR pathway, have been found to be altered in 4% and 17% of localized PCa, respectively [9, 16]. Interestingly, *PTEN* gene deletion is an established prognostic biomarker in PCa, as it is reproducibly associated with poor outcomes [41-43]. Other tumor suppressor genes harboring aberrations in primary PCa are lysine methyltransferase 2D (*KMT2D*; 3%) and tumor protein p53 (*TP53*; 7%) [9, 16]. In the past decade, *TP53* mutations have been shown to significantly contribute to tumor recurrence in PCa [44]. Lastly, lysine demethylase 6A (*KDM6A*; < 2%), mediator complex subunit 12 (*MED12*; 5%), and sodium voltage-gated channel alpha subunit 11 (SCN11A; 5%) genetic aberrations have also been identified in localized disease. A recent study concluded that genetic alterations in epigenetic regulators and chromatin remodelers, such as *KMT2D* and *KDM6A*, are significantly enriched in metastatic tumors when compared to primary tumors, implying that these genetic alterations could be potential biomarkers for high-risk disease [45]. While aberrations in a few of the aforementioned genes are known to contribute to poor outcomes in PCa patients, the significance of the other previously discussed genetic alterations as they relate to PCa progression is still unclear [9, 16].

Tissue vs. Liquid Biopsies

Today, tissue biopsies are collected from patients for diagnostic purposes; however, the molecular and genetic landscape of primary and metastatic tumor biopsies can also be evaluated. In fact, Gerlinger et al. (2012) characterized multiple tumor specimens obtained from the same patient and determined that

there were spatial (genomic differences between separate regions of the same tumor) and temporal (genomic differences between the primary tumor and recurrences) heterogeneities amongst this patient's samples [46]. Thus, tissue samples provide a limited view of a tumor's genomic makeup at only one point in time. In addition, tissue biopsies are extremely invasive and can have high complication rates [47].

In recent years, liquid biopsies have been considered as the replacement for tissue biopsies as they better capture genomic heterogeneity of a given patient's disease and allow for consistent monitoring throughout the natural history of one's disease [47, 48]. Additionally, liquid biopsies are minimally invasive and easily obtainable [47]. One type of liquid biopsy is the collection of a patient's blood so that circulating cell-free DNA (cfDNA) can be isolated and examined for diagnostic genetic aberrations. Since it has been previously shown that the amount of circulating cfDNA correlates with disease burden [49] and that a portion of cfDNA is tumor-derived [50], it is thought that liquid biopsies will have the ability to benefit all stages of cancer therapy (i.e. from assisting in the early diagnosis of primary disease to predicting treatment response in patients with metastatic disease).

Liquid Biopsies for Primary PCa

In the past decade, many studies have discovered how plasma-derived cfDNA from metastatic PCa patients can be utilized to predict disease recurrence and treatment response [51-59]. However, there has been very little research

concerning the use of cfDNA in order to diagnose early PCa, determine biomarkers that risk-stratify localized disease, or even improve prognostic abilities before patients receive surgery and/or radiation. In fact, since the majority of primary PCa is still contained within the prostate itself when initially diagnosed and circulating cfDNA correlates with disease burden, it is unknown if cfDNA is even reliably detectable in localized PCa patients or those with a low disease burden.

The primary goal of this study was to determine if genetic aberrations discovered by the next-generation sequencing (NGS) of patients' primary tumor DNA (which was isolated from radical prostatectomy samples) could also be found by droplet digital PCR (ddPCR) in the corresponding patient's plasma-derived cfDNA isolated before radical prostatectomy. The secondary aim of this study was to determine if the same genetic aberrations discovered in the primary tumor DNA and pre-radical prostatectomy, plasma-derived cfDNA samples could additionally be probed for by ddPCR in the corresponding patient's plasma-derived cfDNA isolated after radical prostatectomy. The findings from this study will determine if it is possible to assess the genetic landscape of primary PCa by liquid biopsy. Ultimately, this study could lead to the usage of a noninvasive technique in order to discover potential biomarkers for disease risk stratification as well as better predict disease outcomes and treat patients with localized PCa.

Materials and Methods

Patients and Sample Collection

  This biomarker study was approved by the Johns Hopkins Medicine Institutional Review Board (IRB). All patients provided written informed consent prior to enrollment. Eligibility criteria included patients diagnosed with localized PCa who had no documented metastatic disease by either computed tomography (CT) or by bone scans with technetium-99mm-labeled methylene diphosphonate. Patients were enrolled between May 2013 and March 2014 at the Johns Hopkins Hospital (Baltimore, MD). The 17 patients enrolled in this study had histologically confirmed prostate adenocarcinoma and radical prostatectomies. Radical prostatectomy samples were formalin-fixed and paraffin-embedded (FFPE). In a dedicated bleach- and ultraviolet (UV)-cleaned hood, primary tumor DNA was isolated from the FFPE samples using QIAamp® DNA FFPE Tissue Kit (Qiagen; Cat. #56404) as per the manufacturer's protocol. To limit cross-contamination of samples, no more than four patient samples were processed at a time.

  Blood was collected before and after radical prostatectomy for all 17 subjects. Clinical follow-up data, including patient PSA levels, were also obtained before and after radical prostatectomy for all 17 subjects.

Plamsa and cfDNA Isolations from Blood Samples

Three, 10mL blood samples were collected in Streck BCT tubes pre- and post-surgery for each patient. Blood was stored at room temperature and then processed for plasma isolation within 24 hours. To optimize patient sample integrity and to limit DNA contamination, plasma was extracted in a bleach- and UV-cleaned hood specifically for plasma extraction in a room dedicated for blood processing, storage, and cfDNA isolation. Plasma was extracted from blood by centrifugation for 10 minutes at 1500 x g followed by a second centrifugation for 10 minutes at 3000 x g as previously described [60-63]. Plasma was stored at -80°C in 1.5mL aliquots. In a dedicated bleach- and UV-cleaned hood, cfDNA was extracted from plasma using the QIAamp® Circulating Nucleic Acid Kit (Qiagen; Cat. #55114) as per the manufacturer's protocol. To limit cross-contamination, samples were processed individually.

Deep NGS

GeneRead™ DNAseq Custom Mix and Match Targeted Panel V2 (Qiagen; 47 genes; 352,096 bases; Table 1.1) was used to prepare libraries of the primary tumor DNA isolated from the FFPE samples for NGS as per the manufacturer's protocol. NGS libraries were prepared in a dedicated bleach- and UV-cleaned hood. Primary tumor DNA was quantified using Qiagen's QIAseq™ DNA QuantiMIZE Assay (DNQC-100Y-F) as per the manufacturer's protocol. Between 0.8 and 13.0ng of primary tumor DNA was used for library generation. Samples were PCR-amplified using Qiagen's GeneRead™ DNAseq Panel PCR

Reagent V2 (Cat. #181942) for 22 cycles as per the manufacturer's protocol.

PCR panel amplicons were purified using AMPure XP beads (Beckman Coulter,

Cat. #A63880) and then quantified by the Agilent 2100 Bioanalyzer. Qiagen's

GeneRead™ DNA Library Prep I Kit (Cat. #180435) and GeneRead™ Adapter I

Set A and B 12-plex (Cat. #180985 and #180986, respectively) were used to

construct all libraries according to the manufacturer's instructions. Purified

libraries were amplified using Qiagen HiFi PCR Master Mix for 5 cycles according

to the manufacturer's protocol. Purified libraries were amplified using Qiagen HiFi

PCR Master Mix for 5 cycles according to the manufacturer's instructions.

Prepared libraries were quantified using QIAseq™ Library Quant Assay (Qiagen;

QSTF-ILZ-F). NGS was performed on the Illumina Hi-Seq with a median on-

target coverage of 701x.

Sequence Alignment and Analysis of Variants

Raw sequencing data was aligned to Human Genome (build

GRCH37.p13/hg19) reference [64] using BWA aligner(v0.7.10) [65]. Post-

alignment data was passed through Picard Tools (V1.125] [66] to assess the

alignment quality. Quality-controlled alignment data was employed to call the

variants using an in-house variant caller, MDLVC, which scans through the

alignment data for raw variants. Resulting raw variant calls were further applied

with various filters including minimum base quality of q25, minimum base depth

of 25, strand bias threshold, and allele frequency of ≥5%. In addition to the above

filters, false positive variant calls arising due to the given sequencing run were

assessed, tracked, and filtered out using two negative controls (i.e. DNA isolated from normal, FFPE prostate tissue) sequenced in this study. Variant calls that were coding silent or that were designated as common in populations by dbSNP [67], EXaC [68], TCGA [69], and ClinVar [70] reference databases were excluded from analyses. ClinVar was used to determine pathogenicity of missense mutations [70]. Missense mutations that were pathogenic or likely pathogenic by ClinVar were used for analyses. High-confidence somatic variants were further annotated with information from COSMIC [71], Mutation Assessor, and cBioPortal [72]. Final variant calls were visualized and assessed further for validity using Integrated Genome Viewer (IGV) [73].

ddPCR

ddPCR for the *SPOP* gene's mutational status was performed as described previously [60]. All cfDNA was first PCR-amplified using Platinum SuperFi™ (Invitrogen) and the following primers (IDT; depending on the given *SPOP* mutation of interest): preAMP-Int6-F1 (GGCTTTGATCTGGTTTTTGCG) and preAMP-Ex7Int7-R1 (GAATACAAGGACTCACCTCG; for F125L mutation only) or preAMP-Int7-R1 (TCAGATCTGGGAACTGCTAG; for W131C and F133L mutations). The annealing temperatures for these primers were 60°C for preAMP-Int6-F1 and preAMP-Ex7Int7-R1 and 55°C for preAMP-Int6-F1 and preAMP-Int7-R1. The following primers (IDT) were used in the ddPCR: (1) For F125L: dd-SPOP-Int6Ex7-F1 (TTTTCCCCACCCCAGAGAG) and dd-SPOP-Ex7-R3 (ATCAGGGAGAAGCCCGTTGG) (2) For W131C and F133L: dd-SPOP-Ex7-

F1 (CCAGAGAGTCAACGGGCAT) and dd-SPOP-Ex7-R1 (GCTTGTCATCAGGGAGAAGC). Dual-labeled (FAM or HEX) fluorescent-quencher hydrolysis probes (IDT) were designed for *SPOP* mutations (F125L, W131C, and F133L) and their respective wild-type loci. The following are the probes that were used for each loci in this ddPCR (with the mutated amino acid in **bold**): (1) F125 region: SPOP-F125-WT (HEX: GGCATATAGGTTTGTGCAAGGCA) and SPOP-F125L-MUT1 (FAM: GGCATATAGG**TTG**GTGCAAGGCA) (2) F131 region: SPOP-W131-WT (HEX: TGCAAGGCAAAGACTGGGGATTCA) and SPOP-W131C-t-MUT1 (FAM: TGCAAGGCAAAGAC**TGT**GGATTCA) or SPOP-W131C-c-MUT2 (FAM: TGCAAGGCAAAGAC**TGC**GGATTCA) (3) F133 region: SPOP-F133-WT (HEX: CAAAGACTGGGGATTCAAGAAATTC) and SPOP-F133L-MUT1 (FAM: CAAAGACTGGGGA**TTG**AAGAAATTC). The following annealing temperatures for these primer and probe combinations are as follows: (1) 55°C (2) 58°C (3) 62°C for mutations W131C (t-mutant), W131C (with c-mutant) and F133L, respectively.

Wild-type male cfDNA was used as a control. The following gBlocks® Gene Fragments were designed (with mutated amino acids in **bold**) and ordered from IDT to act as additional controls for the ddPCR: (1) SPOP-Ex7-WT: 5'-TTCATACACTGACAAGTTGTGGCTTTGATCTGGTTTTTGCGTAACCTTAAATATGACTTTTTTTTTCCCCACCCCAGAGAGTCAACGGGCATATAGGTTTGTGCAAGGCAAAGACTGGGGATTCAAGAAATTCATCCGTAGAGATTTTCTTTTGGATGAGGCCAACGGGCTTCTCCCTGATGACAAGCTTACCCTCTTCTGCGAGGTG

AGTCCTTGTATTCTGCTGAGACTAGCAGTTCCCAGATCTGATGAGTATTGGT

AGACTTAAT-3' (2) SPOP-Ex7-F125L: 5'-

TTCATACACTGACAAGTTGTGGCTTTGATCTGGTTTTTGCGTAACCTTAAATA

TGACTTTTTTTTTCCCCACCCCAGAGAGTCAACGGGCATATAGG**TTG**GTGCA

AGGCAAAGACTGGGGATTCAAGAAATTCATCCGTAGAGATTTTCTTTTGGAT

GAGGCCAACGGGCTTCTCCCTGATGACAAGCTTACCCTCTTCTGCGAGGTG

AGTCCTTGTATTCTGCTGAGACTAGCAGTTCCCAGATCTGATGAGTATTGGT

AGACTTAAT-3' (3) SPOP-Ex7-W131C-1: 5'-

TTCATACACTGACAAGTTGTGGCTTTGATCTGGTTTTTGCGTAACCTTAAATA

TGACTTTTTTTTTCCCCACCCCAGAGAGTCAACGGGCATATAGGTTTGTGCA

AGGCAAAGAC**TGT**GGATTCAAGAAATTCATCCGTAGAGATTTTCTTTTGGAT

GAGGCCAACGGGCTTCTCCCTGATGACAAGCTTACCCTCTTCTGCGAGGTG

AGTCCTTGTATTCTGCTGAGACTAGCAGTTCCCAGATCTGATGAGTATTGGT

AGACTTAAT-3' (4) SPOP-Ex7-W131C-2: 5'-

TTCATACACTGACAAGTTGTGGCTTTGATCTGGTTTTTGCGTAACCTTAAATA

TGACTTTTTTTTTCCCCACCCCAGAGAGTCAACGGGCATATAGGTTTGTGCA

AGGCAAAGAC**TGC**GGATTCAAGAAATTCATCCGTAGAGATTTTCTTTTGGAT

GAGGCCAACGGGCTTCTCCCTGATGACAAGCTTACCCTCTTCTGCGAGGTG

AGTCCTTGTATTCTGCTGAGACTAGCAGTTCCCAGATCTGATGAGTATTGGT

AGACTTAAT-3' (5) SPOP-Ex7-F133L: 5'-

TTCATACACTGACAAGTTGTGGCTTTGATCTGGTTTTTGCGTAACCTTAAATA

TGACTTTTTTTTTCCCCACCCCAGAGAGTCAACGGGCATATAGGTTTGTGCA

AGGCAAAGACTGGGGA**TTG**AAGAAATTCATCCGTAGAGATTTTCTTTTGGAT

GAGGCCAACGGGCTTCTCCCTGATGACAAGCTTACCCTCTTCTGCGAGGTG
AGTCCTTGTATTCTGCTGAGACTAGCAGTTCCCAGATCTGATGAGTATTGGT
AGACTTAAT-3'. ddPCR (Bio-Rad) was performed in a dedicated, UV-equipped
hood and according to the manufacturer's protocol. Total molecules were
quantified by the QX200 Droplet Reader software.

Results

Patient Cohort

In total, 17 patients with localized PCa were enrolled prior to radical
prostatectomy. Patient characteristics are summarized in Table 1.2. The median
age at enrollment for the overall cohort was 62 years. The majority of patients
were of the Caucasian/White racial background and were diagnosed with their
primary PCa in 2013. All patients had a representative pre-surgery samples,
while 4 patients (or 23.5% of patients) did not have a representative post-surgery
sample. The median pre-surgery PSA level for the cohort was 8.1ng/mL and the
median post-surgery PSA level for the cohort was undetectable.

The patient's primary PCa characteristics in this study are summarized in
Table 1.3. Seven (or 41% of) localized PCa patients had a clinical stage of T1c.
The median biopsy and pathological Gleason sums of this cohort were both
equal to eight, while the range of the biopsy and pathological Gleason sums were
both six to 10. Six (or 35% of) patients in this cohort had a pathological stage of

pT2 pN0. Only two (or 12% of) patients had positive lymph nodes. While over

three-quarters of the patients had negative bone scans, the results of the bone

scans for the remaining one-quarter of patients were not recorded in this study.

After surgery, four patients (or 24% of patients) still had a positive surgical

margin.

Genetic Alterations in Localized PCa Patient Cohort

It was discovered by NGS of primary tumor DNA that each of the 17

patients possessed multiple genetic alterations in their respective FFPE, radical

prostatectomy samples. For simplification purposes, Table 1.4 only lists the one

genetic alteration that was chosen for follow-up with ddPCR. Currently, a genetic

alteration has not been chosen for pursuit by ddPCR in two (or 12%) of the

patients. Twenty-seven percent (4/15) of the remaining mutations listed in Table

1.4 were annotated by ClinVar as pathogenic or likely pathogenic. Interestingly,

five patients (or 29% of the total patients in this study) had the following *SPOP*

missense mutations, all of which are found within the MATH domain of the

protein: F125L, W131C, and F133L. While ClinVar annotated three of the *SPOP*-

W131C and F133L mutations as pathogenic or likely pathogenic, it is important to

note that a prior study demonstrated that *SPOP* mutations are not associated

with worse outcomes, such as shorter length of time to biochemical recurrence,

in PCa patients [27].

Two (2/17; 12%) additional patients had *TP53* mutations causing

frameshifts of unknown clinical significance. Another two patients had *KMT2D*

mutations both of which were single nucleotide deletions. Only one (1/17; 6%) patient had a missense mutation in *KDM6A*. However, over 76% of the total read counts for this locus in this patient's NGS library contained this mutation, and so it is possible that this *KDM6A* missense mutation is germline. Interestingly, two patients had one mutation in the following mismatch repair genes: mutS homolog 2 (*MSH2*) and mutL homolog 1 (*MLH1*). While the missense mutation in *MSH2* is of unknown significance, the *MLH1* mutation is involved in splicing and is predicted to have pathogenic consequences [71]. One patient had a neutral missense mutation in *SCN11A* that was found in over 56% of the total read counts, meaning that this patient could also have a germline mutation. One patient had a splice site mutation in the *MED12* gene and another patient had a frameshift mutation in the Fanconi anemia complementation group M (*FANCM*) gene. The FANCM protein is involved in the DNA damage repair pathway, possibly even assisting *BRCA2* [74], however, it is unclear if the particular mutation found in this study's patient sample is of clinical relevance.

Mutational Status of Patient cfDNA by ddPCR

The ddPCR results for the cfDNA analyzed from four patients thus far can be viewed in Figure 1.2. From these results, it was determined that Patients 1, 6, and 9 are not positive for the anticipated *SPOP* mutations that were originally discovered in their primary tumor DNA by NGS. However, the *SPOP*-W131C mutation was found in Patient 14's cfDNA by ddPCR at very low levels. The frequency of this SPOP-W131C mutation in Patient 14 is 0.0002.

Discussion and Future Directions

One limitation of this study is its small sample size (n=17). Thus, the percentages of patients who have a given genetic alteration in this study and the percentage of primary tumors that have the same genetic alteration in the previously mentioned studies available through cBioPortal (Figures 1.1 and 1.3) cannot be compared. For example, in this study five out of the 17 total subjects (29%) had *SPOP* mutations in their primary tumor DNA isolated from the FFPE, radical prostatectomy samples; however, it is estimated that only about 10% of primary tumors available on cBioPortal have genomic aberrations in the *SPOP* gene. If this study consisted of a larger number of consented patients, then the percentage of *SPOP* mutations may not have been so high.

Another limitation of this study is that it is currently in-progress as both aims are still being addressed. All plasma-derived cfDNA samples taken before radical prostatectomies for the remaining 13 patients are being assessed by ddPCR for the presence of each genetic alteration listed in Table 1.4. As for the four patients whose cfDNA was probed by ddPCR for the given *SPOP* mutations discovered by NGS, the mutations of interest were not detected in three of the patients thus far. Meanwhile, Patient 14 was confirmed to contain the mutation of interest in his cfDNA at extremely low levels. Before absolute conclusions can be drawn from these results, the remaining 13 patients' cfDNA samples need to be assessed by ddPCR for the chosen mutation of interest. In addition, all 17 plasma-derived cfDNA samples taken after radical prostatectomy still need to be

18

assessed by ddPCR. The completion of these ddPCRs is imperative for truly

discerning whether or not plasma-derived cfDNA from primary PCa patients can

be reliably utilized to detect genetic alterations at this early stage of the disease.

Ultimately, this small study could discover potential biomarkers for the purpose of

distinguishing between an indolent and aggressive PCa, thereby better predicting

disease outcomes and treatment responses in patients with localized PCa.

Table 1.1: Qiagen Mix and Match Panel

AR	BRCA1	POLH	GLI1
NCOA2	BRCA2	POLE	CDH1
TP53	ATM	POLD1	MET
RB1	ATR	MLH1	SPOP
MYC	CHEK2	MLH3	POU6F2
CDKN1B	PALB2	MSH2	SCN11A
PTEN	NBN	MSH3	GNAS
PIK3CA	CDK12	PMS1	MED12
AKT1	FANCG	PMS2	ZFHX3
AKT2	FANCM	KDM6A	IDH1
APC	ERCC3	KMT2C	IDH2
CTNNB1	ERCC5	KMT2D	

Table 1.2. Patient Characteristics (n=17)

Characteristics	Total Cohort (n=17)
Age of Enrollment, years	
Median (range)	62 (41-73)
Race, n (%)	
Caucasian/White	15 (88.2)
African American/Black	1 (5.9)
Hispanic/Other	1 (5.9)
Year of Diagnosis, n (%)	
2005	1 (5.9)
2011	1 (5.9)
2012	1 (5.9)
2013	13 (76.5)
2014	1 (5.9)
Pre-Surgery Samples, n (%)	
Yes	17 (100)
No	0 (0)
Post-Surgery Samples, n (%)	
Yes	13 (76.5)
No	4 (23.5)
Pre-Surgery PSA, ng/ml	
Median (range)	8.1 (2.4-30)
Post-Surgery PSA, ng/ml	
Median (range)	0 (0-2)

Table 1.3: Patient Primary PCa Characteristics (n=17)

Patient Number	Clinical Stage	Biopsy Gleason Score	Pathologic Stage	Pathologic Gleason Score	Node Positive	Bone Scan	Positive Surgical Margin
T1	T2c	4+4=8	pT3a pN0	4+4=8	0/5	negative	negative
T2	T1c	4+5=9	pT2 pN0	4+5=9	0/9	negative	negative
T3	T3a	4+4=8	pT3b N0	4+5=9	0/11	negative	negative
T4	T1c	3+3=6	pT3a pN0	3+3=6	0/3	negative	positive
T5	T2b	4+3=7	pT3a pN0	4+3=7	0/6	negative	negative
T6	T2a	3+4=7	pT2 pN0	3+4=7	0/7	negative	negative
T7	T3c	5+4=9	pT3b pN0	4+5=9	0/7	negative	positive
T9	T2c	4+5=9	pT2 pN0	4+5=9	0/9	negative	negative
T10	T1c	4+3=7	pT3b pN0	4+3=7	0/18	negative	positive
T12	T1c	4+4=8	pT3b pN0	3+5=8	0/3	N/A	negative
T13	T1c	4+3=7	pT2 pN0	3+4=7	0/2	negative	negative
T14	T1c	4+3=7	pT2 pN0	4+3=7	0/2	N/A	negative
T15	T2b	5+4=9	pT3a pN1	5+4=9	2/8	negative	negative
T16	T2a	4+5=9	pT3a pN0	4+5=9	0/7	negative	negative
T17	T2b	5+5=10	pT3a pN0	5+5=10	0/2	negative	positive
T18	T1c	3+4=7	pT2 pN0	3+4=7	0/11	N/A	negative
T19	T2b N+	4+5=9	pT3a pN1	4+5=9	4/37	N/A	negative

Table 1.4: Genetic Alterations in FFPE, Radical Prostatectomy Samples from Localized PCa Patients

Patient	Gene	Genetic Alteration	Amino Acid Alteration	Wild-type Read Counts	Mutant Read Counts	Percent Mutant
1	SPOP*€	393G>T	W131C	994	116	10.45
2	KMT2D	11220_11222del	3740_3741del	167	10	5.7
3	TP53	341delT	L114fs	180	97	35.0
4	MED12	553+1G>A	splicing	281	10	3.4
5	SCN11A*	2945G>A	R982Q	414	537	56.5
6	SPOP*€	399C>G	F133L	1104	275	19.9
7	TP53	316_317insA	S106fs	917	424	31.6
9	SPOP	393G>C	W131C	1253	500	28.5
10	MSH2	799G>A	V267I	306	30	8.9
12	none					
13	MLH1€	790+1G>A	splicing	374	12	3.1
14	SPOP*€	393G>T	W131C	1662	67	3.88
15	FANCM	619_620insA	E207fs	515	95	15.6
16	none					
17	KMD6A	3349A>C	N1117H	88	287	76.5
18	SPOP	375T>G	F125L	1773	63	3.4
19	KMT2D	16368delC	N5456fs	867	69	7.4

*COSMIC; €(ClinVar Likely Pathogenic/Pathogenic); §(ClinVar Uncertain Significance); ¥(ClinVar Likely Benign); £(ClinVar Not Available)

ERG 37%

ETV1 9%

ETV4 6%

FLI1 2.2%

SPOP 10%

FOXA1 7%

IDH1 1.4%

Genetic Alteration

Inframe Mutation (putative driver)   Inframe Mutation (unknown significance)   Missense Mutation (putative driver)

Missense Mutation (unknown significance)   Truncating Mutation (putative driver)   Fusion   Amplification   Deep Deletion

No alterations

Study of origin

Prostate Adenocarcinoma (Broad/Cornell, Cell 2013)   Prostate Adenocarcinoma (MSKCC, Cancer Cell 2010)

Prostate Adenocarcinoma (TCGA, Cell 2015)

Profiled for copy number alterations

Yes   – No

22

Figure 1.1: The seven genomically distinct subgroups of primary PCa [9, 15, 20], as analyzed by cBioPortal for Cancer Genomics [72, 75].
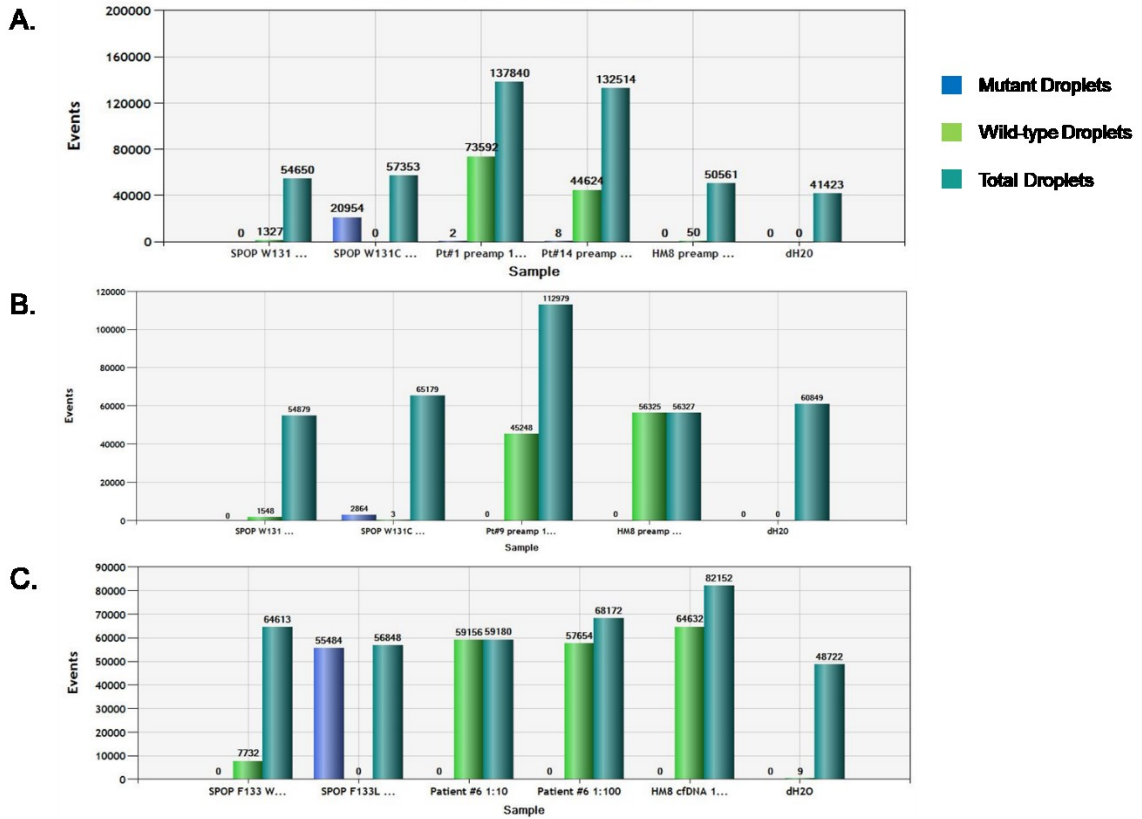
Figure 1.2: Determining the *SPOP* mutational status of patients' cfDNA by ddPCR. ddPCR results for (A) Patients 1 and 14, (B) Patient 9, and (C) Patient 6. SPOP W131 or F133= given SPOP WT gBlock controls; SPOP W131C or F133L=given SPOP mutant gBlock controls; HM8=healthy male control cfDNA; dH2O=water (negative) control.

Study of origin

Profiled for copy number alterations

SPOP 10%

TP53 7%

KMT2D 2.6%

KDM6A 2.8%

MSH2 1.8%

MLH1 0.2%

SCN11A 1%

MED12 2%

FANCM 1%

Genetic Alteration

Inframe Mutation (unknown significance)   Missense Mutation (putative driver)   Missense Mutation (unknown significance)

Truncating Mutation (putative driver)   Truncating Mutation (unknown significance)   Amplification   Deep Deletion

No alterations

Study of origin

Prostate Adenocarcinoma (Broad/Cornell, Cell 2013)   Prostate Adenocarcinoma (MSKCC, Cancer Cell 2010)

Prostate Adenocarcinoma (TCGA, Cell 2015)

Profiled for copy number alterations

Yes   — No

24

Figure 1.3: The general genomic aberration status of primary PCa [9, 15, 20] for the specific genes found altered in this study, as analyzed by cBioPortal for Cancer Genomics [72, 75].

References:

1. Ferlay J, Soerjomataram I, Ervik M, et al. GLOBOCAN 2012 v1.0, Cancer Incidence and Mortality Worldwide: IARC CancerBase No. 11. Lyon, France: *International Agency for Research on Cancer*; 2013.

2. Siegel RL, Miller KD, and Jemal A. Cancer statistics, 2018. *CA: a cancer journal for clinicians*. 2018;68(1):7-30.

3. Al Olama AA, Kote-Jarai Z, Berndt SI, et al. A meta-analysis of 87,040 individuals identifies 23 new susceptibility loci for prostate cancer. *Nature genetics*. 2014;46(10):1103-1109.

4. Penney KL, Stampfer MJ, Jahn JL, Sinnott JA, Flavin R, Rider JR, Finn S, Giovannucci E, Sesso HD, Loda M, et al. Gleason grade progression is uncommon. *Cancer research*. 2013;73(16):5163-8.

5. Draisma G, Etzioni R, Tsodikov A, Mariotto A, Wever E, Gulati R, et al. Lead time and overdiagnosis in prostate-specific antigen screening: importance of methods and context. *Journal of the National Cancer Institute*. 2009;101(6):374-383.

6.   Finne P, Fallah M, Hakama M, Ciatto S, Hugosson J, de Koning H, et al. Lead-time in the European Randomised Study of Screening for Prostate Cancer. *European journal of cancer*. 2010;46(17):3102-3108.

7.   Savage CJ, Lilja H, Cronin AM, Ulmert D, Vickers AJ. Empirical estimates of the lead time distribution for prostate cancer based on two independent representative cohorts of men not subject to prostate-specific antigen screening. *Cancer epidemiology biomarkers & prevention*. 2010;19(5):1201-1207.

8.   Haythorn MR and Ablin RJ. Prostate-specific antigen testing across the spectrum of prostate cancer. *Biomarkers in medicine*. 2011;5(4):515-26.

9.   Cancer Genome Atlas Research N. The Molecular Taxonomy of Primary Prostate Cancer. *Cell*. 2015;163:1011-25.

10.   Cooperberg MR, Broering JM, and Carroll PR. Risk assessment for prostate cancer metastasis and mortality at the time of diagnosis. *Journal of the National Cancer Institute*. 2009;101(12):878-87.

11.   D'Amico AV, Whittington R, Malkowicz SB, Schultz D, Blank K, et al. Biochemical outcome after radical prostatectomy, external beam radiation therapy, or interstitial radiation therapy for clinically localized prostate cancer. *JAMA*. 1998;280(11):969-74.

12.   Kattan MW, Eastham JA, Stapleton AM, et al. A preoperative nomogram for disease recurrence following radical prostatectomy for prostate cancer. *Journal of the National Cancer Institute*. 1998;90(10):766-71.

13.   Epstein JI, Zelefsky MJ, Sjoberg DD, Nelson JB, et al. A Contemporary Prostate Cancer Grading System: A Validated Alternative to the Gleason Score. *European urology*. 2016;69(3):428-35.

14.   Loeb S and Catalona WJ. The Prostate Health Index: a new test for the detection of prostate cancer. *Therapeutic advances in urology*. 2014;6(2):74-7.

15.   Baca SC, Prandi D, Lawrence MS, Mosquera JM, Romanel A, Drier Y, Park K, Kitabayashi N, MacDonald TY, Ghandi M, et al. Punctuated evolution of prostate cancer genomes. *Cell*. 2013;153(3):666-77.

16.   Barbieri CE, Baca SC, Lawrence MS, Demichelis F, Blattner M, Theurillat JP, White TA, Stojanov P, Van Allen E, Stransky N, et al. Exome sequencing identifies recurrent SPOP, FOXA1 and MED12 mutations in prostate cancer. *Nature genetics*. 2012;44(6):685-9.

17.   Berger MF, Lawrence MS, Demichelis F, Drier Y, Cibulskis K, Sivachenko AY, Sboner A, Esgueva R, Pflueger D, Sougnez C, et al. The genomic complexity of primary human prostate cancer. *Nature*. 2011;470(7333):214-20.

18.   Lapointe J, Li C, Giacomini CP, Salari K, Huang S, et al. Genomic profiling reveals alternative genetic pathways of prostate tumorigenesis. *Cancer research*. 2007;67(18):8504-10.

19.   Pflueger D, Terry S, Sboner A, Habegger L, Esgueva R, Lin PC, Svensson MA, Kitabayashi N, Moss BJ, MacDonald TY, et al. Discovery of non-ETS gene fusions in human prostate cancer using next-generation RNA sequencing. *Genome research*. 2011;21(1):56-67.

20.   Taylor BS, Schultz N, Hieronymus H, Gopalan A, Xiao Y, Carver BS, Arora VK, Kaushik P, Cerami E, Reva B, et al. Integrative genomic profiling of human prostate cancer. *Cancer cell*. 2010;18(1):11-22.

21.   Tomlins SA, Laxman B, Dhanasekaran SM, Helgeson BE, Cao X, Morris DS, Menon A, Jing X, Cao Q, Han B, et al. Distinct classes of chromosomal rearrangements create oncogenic ETS gene fusions in prostate cancer. *Nature*. 2007;448(7153):595-9.

22.   Wang XS, Shankar S, Dhanasekaran SM, Ateeq B, Sasaki AT, Jing X, Robinson D, Cao Q, Prensner JR, Yocum AK, et al. Characterization of KRAS rearrangements in metastatic prostate cancer. *Cancer discovery*. 2011;1(1):35-43.

23.   Tomlins SA, Rhodes DR, Perner S, Dhanasekaran SM, Mehra R, Sun XW, Varambally S, Cao X, Tchinda J, Kuefer R, et al. Recurrent fusion of TMPRSS2 and ETS transcription factor genes in prostate cancer. *Science*. 2005;310(5748):644-8.

24.   Tomlins SA, Bjartell A, Chinnaiyan AM, Jenster G, Nam RK, Rubin MA, Schalken JA. ETS gene fusions in prostate cancer: from discovery to daily clinical practice. *European journal of urology*. 2009;56(2):275-86.

25.   Gopalan A, Leversha MA, Satagopan JM, Zhou Q, Al-Ahmadie HA, Fine SW, Eastham JA, Scardino PT, Scher HI, Tickoo SK, et al. TMPRSS2-ERG gene fusion is not associated with outcome in patients treated by prostatectomy. *Cancer research*. 2009;69(4):1400-6.

26.   Pettersson A, Graff RE, Bauer SR, Pitt MJ, Lis RT, Stack EC, Martin NE, Kunz L, Penney KL, Ligon AH, et al. The TMPRSS2:ERG rearrangement, ERG expression, and prostate cancer outcomes: a cohort study and meta-analysis. *Cancer epidemiology, biomarkers & prevention*. 2012;21(9):1497-509.

27.   Blattner M, Lee DJ, O'Reilly C, et al. SPOP mutations in prostate cancer across demographically diverse patient cohorts. *Neoplasia*. 2014;16(1):14-20.

28.   Mani, R-S. The emerging role of speckle-type POZ protein (SPOP) in cancer development. *Drug discovery today*. 2014;19(9):1498-1502.

29.   Theurillat JP, Udeshi ND, Errington WJ, et al. Prostate cancer. Ubiquitylome analysis identifies dysregulation of effector substrates in SPOP-mutant prostate cancer. *Science*. 2014;346(6205):85-89.

30.   Groner Anna C, Cato L, de Tribolet-Hardy J, et al. TRIM24 is an oncogenic transcriptional activator in prostate cancer. *Cancer cell*. 2016;29(6):846-858.

31.   An J, Wang C, Deng Y, et al. Destruction of full-length androgen receptor by wild-type SPOP, but not prostate-cancer-associated mutants. *Cell reports*. 2014;6(4):657-669.

32.   Geng C, Rajapakshe K, Shah SS, et al. Androgen receptor is the key transcriptional mediator of the tumor suppressor SPOP in prostate cancer. *Cancer research*. 2014;74(19):5631-5643.

33.   Blattner M, Liu D, Robinson BD, et al. SPOP mutation drives prostate tumorigenesis in vivo through coordinate regulation of PI3K/mTOR and AR signaling. *Cancer cell*. 2017;31(3):436-451.

34.   Gao N, Zhang J, Rao MA, Case TC, et al. The role of hepatocyte nuclear factor-3 alpha (Forkhead Box A1) and androgen receptor in transcriptional regulation of prostatic genes. *Molecular endocrinology*. 2003;17(8):1484-507.

35.   Gao N, Ishii K, Mirosevich J, Kuwajima S, et al. Forkhead box A1 regulates prostate ductal morphogenesis and promotes epithelial cell maturation. *Development*. 2005;132(15):3431-43.

36.   Jin HJ, Zhao JC, Ogden I, Bergan RC, Yu J. Androgen receptor-independent function of FoxA1 in prostate cancer metastasis. *Cancer research*. 2013;73(12):3725-36.

37.   Zhang C, Wang L, Wu D, Chen H, et al. Definition of a FoxA1 Cistrome that is crucial for G1 to S-phase cell-cycle transit in castration-resistant prostate cancer. *Cancer research*. 2011;71(21):6738-6748.

38.   Grasso CS, Wu YM, Robinson DR, Cao X, et al. The mutational landscape of lethal castration-resistant prostate cancer. *Nature*. 2012;487(7406):239-43.

39.   Ghiam AF, Cairns RA, Thoms J, et al. IDH mutation status in prostate cancer. *Oncogene*. 2012;31(33):3826.

40.   Kang MR, Kim MS, Oh JE, et al. Mutational analysis of IDH1 codon 132 in glioblastomas and other common cancers. *International journal of cancer.* 2009;125(2):353-5.

41.   Lotan TL, Heumann A, Rico SD, Hicks, J, et al. PTEN loss detection in prostate cancer: comparison of PTEN immunohistochemistry and PTEN FISH in a large retrospective prostatectomy cohort. *Oncotarget*. 2017;8(39):6556676.

42.   Yoshimoto M, Cunha IW, Coudry RA, Fonseca, FP, et al. FISH analysis of 107 prostate cancers shows that PTEN genomic deletion is associated with poor clinical outcome. *British journal of cancer*. 2007;97(5):678-685.

43.   Krohn A, Diedler T, Burkhardt L, Mayer PS, De Silva C, et al. Genomic deletion of PTEN is associated with tumor progression and early PSA recurrence in ERG fusion-positive and fusion-negative prostate cancer. *The American journal of pathology*. 2012;181(2):401-12.

44.   Ecke TH, Schlechte HH, Schiemenz K, Sachs MD, et al. TP53 gene mutations in prostate cancer progression. *Anticancer research*. 2010;30(5):1579-86.

45.   Armenia J, Wankowicz SAM, Liu D, Gao J, Kundra R, et al. The long tail of oncogenic drivers in prostate cancer. *Nature genetics*. 2018;50(5):645-651.

46.   Gerlinger M, Rowan AJ, Horswell S, et al. Intratumor heterogeneity and branched evolution revealed by multiregion sequencing. The *New England journal of medicine*. 2012;366(10):883-92.

47.   Donaldson J and Park BH. Circulating Tumor DNA: Measurement and Clinical Utility. *Annual review of medicine*. 2018;69:223-234.

48.   De Mattos-Arruda L, Weigelt B, Cortes J, et al. Capturing intra-tumor genetic heterogeneity by de novo mutation profiling of circulating cell-free tumor DNA: a proof-of-principle. *Annals of oncology*. 2014;25(9):1729-35.

49.   Leon SA, Shapiro B, Sklaroff DM, and Yaros MJ. Free DNA in the serum of cancer patients and the effect of therapy. *Cancer research*. 1977;37(3):646-50.

50.   Stroun M, Anker P, Maurice P, Lyautey J, et al. Neoplastic characteristics of the DNA found in the plasma of cancer patients. *Oncology*. 1989;46(5):318-322.

51.   Mahon KL, Qu W, Devaney J, Paul C, et al. Methylated Glutathione S-transferase 1 (mGSTP1) is a potential plasma free DNA epigenetic marker of prognosis and response to chemotherapy in castrate-resistant prostate cancer. *British journal of cancer*. 2014;111(9):1802-1809.

52.   Azad AA, Volik SV, Wyatt AW, Haegert A, et al. Androgen Receptor Gene Aberrations in Circulating Cell-Free DNA: Biomarkers of Therapeutic Resistance in Castration-Resistant Prostate Cancer. *Clinical cancer research: an official journal of the American Association for Cancer Research.* 2015;21(10):2315-2324.

53.   Lallous N, Volik SV, Awrey S, Leblanc E, et al. Functional analysis of androgen receptor mutations that confer anti-androgen resistance identified in circulating cell-free DNA from prostate cancer patients. *Genome biology*. 2016;17:10.

54.   Salvi S, Casadio V, Conteduca V, et al. Circulating cell-free AR and CYP17A1 copy number variations may associate with outcome of metastatic castration-resistant prostate cancer patients treated with abiraterone. *British journal of cancer*. 2015;112(10):1717-1724.

55.   Carreira S, Romanel A, Goodall J, et al. Tumor clone dynamics in lethal prostate cancer. *Science translational medicine*. 2014;6(254):254ra125.

56.	Romanel A, Gasi Tandefelt D, Conteduca V, et al. Plasma AR and abiraterone-resistant prostate cancer. *Science translational medicine*. 2015;7(312):312re10.

57.	Annala M, Vandekerkhove G, Khalaf D, Taavitsainen S, et al. Circulating tumor DNA genomics correlate with resistance to abiraterone and enzalutamide in prostate cancer. *Cancer discovery*. 2018.

58.	Horning AM, Awe JA, Wang CM, Liu J, Lai Z, et al. DNA methylation screening of primary prostate tumors identifies SRD5A2 and CYP11A1 as candidate markers for assessing risk of biochemical recurrence. *Prostate*. 2015;75(15):1790-1801.

59.	Torquato S, Pallavajjala A, Goldstein A, Toro PV, et al. Genetic Alterations Detected in Cell-free DNA are Associated with Enzalutamide and Abiraterone Resistance in Castration-resistant Prostate Cancer. [Submitted]

60.	Goldstein A, Valda Toro P, Lee J, Silberstein JL, Nakazawa M, Waters I, Cravero K, Chu D, Cochran RL, Kim M, et al. Detection fidelity of AR mutations in plasma derived cell-free DNA. *Oncotarget*. 2017.

61.	Beaver JA, Jelovac D, Balukrishna S, Cochran RL, et al. Detection of cancer DNA in plasma of patients with early-stage breast cancer. *Clinical cancer research: an official journal of the American Association for Cancer Research*. 2014;20(10):2643-50.

62.	Chu D, Paoletti C, Gersch C, VanDenBerg DA, Zabransky DJ, et al. ESR1 Mutations in Circulating Plasma Tumor DNA from Metastatic Breast Cancer

Patients. *Clinical cancer research: an official journal of the American Association for Cancer Research*. 2016;22(4):993-9.

63.   Toro PV, Erlanger B, Beaver JA, Cochran RL, VanDenBerg DA, et al. Comparison of cell stabilizing blood collection tubes for circulating plasma tumor DNA. *Clinical biochemistry*. 2015;48(15):993-8.

64.   http://hgdownload.soe.ucsc.edu/goldenPath/hg19.

65.   Li H, and Durbin R. Fast and accurate long-read alignment with Burrows-Wheeler transform. *Bioinformatics*. 2010;26(5):589-95.

66.   Picard tools hbgip.

67.   Database of Single Nucleotide Polymorphisms (dbSNP). Bethesda (MD): National Center for Biotechnology Information NLoMdBIAfh.

68.   Lek M, Karczewski KJ, Minikel EV, Samocha KE, Banks E, Fennell T, O'Donnell-Luria AH, Ware JS, Hill AJ, Cummings BB, et al. Analysis of protein-coding genetic variation in 60,706 humans. *Nature*. 2016;536(7616):285-91.

69.   Tomczak K, Czerwinska P, and Wiznerowicz M. The Cancer Genome Atlas (TCGA): an immeasurable source of knowledge. *Contemporary oncology (Pozn)*. 2015;19(1A):A68-77.

70.   Landrum MJ, Lee JM, Benson M, Brown G, Chao C, Chitipiralla S, Gu B, Hart J, Hoffman D, Hoover J, et al. ClinVar: public archive of interpretations of clinically relevant variants. *Nucleic acids research*. 2016;44(D1):D862-8.

71.   Forbes SA, Beare D, Gunasekaran P, Leung K, Bindal N, Boutselakis H, Ding M, Bamford S, Cole C, Ward S, et al. COSMIC: exploring the world's

knowledge of somatic mutations in human cancer. *Nucleic acids research*.

2015;43(Database issue):D805-11.

72.   Gao J, Aksoy BA, Dogrusoz U, Dresdner G, et al. Integrative analysis of

complex cancer genomics and clinical profiles using the cBioPortal. *Science

signaling*. 2013;6(269):pl1.

73.   Thorvaldsdottir H, Robinson JT, and Mesirov JP. Integrative Genomics

Viewer (IGV): high-performance genomics data visualization and exploration.

Briefings in bioinformatics. 2013;14(2):178-92.

74.   Gari K, Décaillet C, Stasiak AZ, Stasiak A, Constantinou A. The Fanconi

anemia protein FANCM can promote branch migration of Holliday junctions and

replication forks. *Molecular cell*. 2008;29(1):141-8.

75.   Cerami E, Gao J, Dogrusoz U, et al. The cBio cancer genomics portal: an

open platform for exploring multidimensional cancer genomics data. *Cancer

discovery*. 2012;2(5):401-4.

2

Genetic Alterations Detected in Cell-free DNA are Associated with Enzalutamide and Abiraterone Resistance in Castration-resistant Prostate Cancer

Abstract

PURPOSE. Androgen receptor (*AR*) gene alterations, including ligand-binding domain (LBD) missense mutations and copy number (CN) gain, as predictive markers of resistance to enzalutamide and abiraterone in men with metastatic castration-resistant prostate cancer (mCRPC) have yet to be fully established. The goal of this study was to validate *AR* gene alterations detected in cell-free DNA (cfDNA) as markers of enzalutamide and abiraterone resistance in mCRPC patients.

METHODS. Patients with mCRPC (n=62) were prospectively enrolled between 2014 and 2018. Blood was collected prior to therapies: enzalutamide (n=25), abiraterone (n=35), or concurrent enzalutamide and abiraterone (n=2) and at progression. Deep next-generation sequencing (NGS) was used to analyze cfDNA for sequence variants and CN status in *AR* and 46 additional cancer-associated genes. The primary endpoints were PSA response, progression-free survival (PFS), and overall survival (OS).

RESULTS. Elevated tumor-specific cfDNA (ctDNA) was associated with a worse PSA response (HR: 3.17; 95%CI: 1.11-9.05; *P*=0.031), PFS (HR: 1.76; 95%CI: 1.03-3.01; *P*=0.039), and OS (HR: 2.92; 95%CI: 1.40-6.11; *P*=0.004). *AR* LBD missense mutations (HR: 2.51; 95%CI: 1.15-5.72; *P*=0.020) were associated with a shorter PFS in multivariable models. *AR* CN gain was associated with a shorter

PFS; however, significance was lost in multivariable modeling (*P*=0.060). Genetic alterations in tumor protein p53 (*TP53*; HR: 2.70; 95%CI: 1.27-5.72; *P*=0.009) and phosphoinositide 3-kinase (PI3K) pathway defects (HR: 2.62; 95%CI: 1.12-6.10; *P*=0.026) were associated with a worse OS.

CONCLUSION. These findings support that high ctDNA, *AR* LBD hotspot missense mutations, and, to a limited extent, *AR* CN gain are associated with a worse response to next-generation anti-androgen therapies and that ctDNA burden, *TP53* loss, and PI3K pathway defects are associated with worse OS in men with mCRPC.

Introduction

Prostate cancer remains a leading cause of cancer-related death in US men due to the subset of patients who develop metastatic disease. Most patients with metastatic prostate cancer respond initially to contemporary androgen deprivation therapies (ADT), but eventually progress to mCRPC. Next-generation therapies targeting the androgen-AR axis, such as abiraterone and enzalutamide, have improved survival outcomes for men with mCRPC [1-4], but both primary and acquired resistance to these drugs continue to be a substantial clinical challenge. Thus, there is a need to identify robust biomarkers to guide therapy decisions for patients with mCRPC, especially given the availability of

various non-hormonal therapies (i.e. chemotherapy, immunotherapy, and bone-targeted therapy).

Resistance mechanisms to therapies targeting the androgen-AR axis are not fully understood; however, some forms of resistance likely involve *AR* gene alterations, including amplification and mutations. *AR* gene alterations are rare in primary prostate cancers with a reported incidence of less than 2% of cases [5-7]. In contrast, *AR* gene alterations are highly prevalent in mCRPC with a combined frequency of 50-60% [8-11], thereby, supporting their association with resistance to androgen-AR axis therapies [12, 13]. Moreover, amplification of *AR* occurs far more commonly than *AR* LBD missense mutations in mCRPC (approximately 50% vs. 15% of cases) with some cases exhibiting multiple *AR* alterations [10]. Thus, *AR* gene alterations may be relevant biomarkers for decision-making in clinical practice.

Metastatic tissue biopsies as a sole means to determine and follow changes in *AR* status is impractical, and thus cfDNA is gaining traction as a minimally invasive and easily obtainable tumor biopsy surrogate. Prior studies using cfDNA from the blood to evaluate the association of *AR* gene aberrations with resistance to abiraterone and enzalutamide are inconclusive [14-17]. Elevated *AR* levels in cfDNA as measured by CN gain [18, 19] and/or amplification [20], or detection of two or more *AR* mutations [20] have been associated with worse outcomes when men are treated with therapies such as abiraterone and enzalutamide. In contrast, neither *AR* CN gain nor *AR* LBD mutations were significantly associated with time to progression on abiraterone

and enzalutamide therapies in multivariate models [17]. Thus, the role of *AR* gene aberrations in mediating resistance to androgen-AR axis therapies has not been fully determined and definitive prospective studies are needed for clinical validation.

AR gene alterations are only detected in a subset of patients who have either primary or acquired resistance to androgen-AR axis therapies, thereby highlighting the need to determine other mechanisms that may mediate resistance. The *AR* splice variant, *AR*-V7, is associated with resistance to enzalutamide and abiraterone [21-23] and is also associated with increased *AR* CN [24]. In addition to *AR*, alterations in other genes such as *TP53*, phosphatase and tensin homolog (*PTEN*), and breast cancer gene 2 (*BRCA2*) are enriched in lethal prostate cancer [8-11]. Recent studies support that lineage plasticity from an AR-dependent to an AR-independent state through loss of *TP53* and retinoblastoma-associated protein 1 (*RB1*) mediates resistance to androgen-AR axis therapies [25-27]. Consistent with this, *TP53* defects have been shown to be associated with worse outcomes with abiraterone and enzalutamide therapies [17]. Similar to *TP53*, *PTEN* may promote a less AR-dependent state to mediate castrate-resistance [28-31]. The role of *BRCA2* and other homology-directed repair (HDR) genes in mediating resistance to enzalutamide and abiraterone has not been definitively determined. While it has been reported that truncating mutations in *BRCA2* and ataxia-telangiectasia mutated gene (*ATM*) are associated with a shorter time to progression on enzalutamide and abiraterone

[17], other studies indicate that HDR defects may be associated with a better response to therapy [32, 33].

The primary goal of this study was to validate *AR* LBD mutations and/or *AR* CN gain detected in cfDNA as predictive markers to enzalutamide and abiraterone resistance in patients with mCRPC. The secondary goal was to determine if mutations in other genes enriched in lethal prostate cancer such as *TP53*, *PTEN*, and *BRCA2* were associated with response to enzalutamide and abiraterone. In this study, high ctDNA burden was significantly associated with PSA response, PFS, and OS. Study findings also validate that *AR* LBD mutations are significantly associated with a shorter PFS, even after controlling for factors such as ctDNA burden. Pre-therapy *AR* CN gain was significantly associated with both a shorter PFS and a worse OS, but lost significance when controlled for ctDNA burden. *TP53* loss and defects in the PI3K pathway were both associated with worse OS.

Results

Patient Cohort

Patient characteristics are summarized in Table 2.1. Pre-therapy PSA, PSA response, and PFS were not significantly different between patients on abiraterone and enzalutamide (Table 2.1; Figure 2.1A-C). Approximately one-quarter of patients had prior abiraterone or enzalutamide. Prior abiraterone or

enzalutamide was not significantly associated with PSA response (P=0.146), PFS (P=0.620) or OS (P=0.284) (Tables 2.2 and 2.3; Figure 2.1D). ClinVar-annotated pathogenic or likely pathogenic mutations and/or CN alterations [34] were detected in cfDNA from 89% of patients prior to therapy initiation and in 92% of patients at progression (Figures 2.2A-D and 2.3).

ctDNA

Total cfDNA concentration prior to therapy was associated with PSA (P=0.002; Figure 2.4A). Deep NGS was used to analyze cfDNA for CN variation and mutations in 47 cancer-associated genes (Table 1.1). Nearly all patients (61/62) had detectable CN variation(s) and/or mutation(s) with an allelic frequency above the 1% cutoff (Figure 2.2B-C). High allelic fractions of ctDNA have been associated with poor prognosis [14, 17, 20]. High ctDNA burden was detected in approximately 44% of patients prior to therapy. High ctDNA burden was significantly associated with a worse PSA response (OR: 3.17; 95%CI: 1.11-9.05; P=0.031) by logistic regression analyses (Table 2.2). High ctDNA burden was associated with a shorter median time to progression (14.0 weeks vs. 34.0 weeks; P=0.022) and a shorter PFS (HR: 1.76; 95% CI: 1.03-3.01; P=0.039) using proportional hazards modeling (Table 2.3; Figure 2.5A). High ctDNA burden was also significantly associated with a shorter median survival (62.7 weeks vs. 134.9 weeks; P=0.003) and a worse OS (HR: 2.92; 95%CI: 1.40-6.11; P=0.004) using proportional hazards modeling (Table 2.3; Figure 2.6A). Other clinical variables such as prior abiraterone or enzalutamide therapy, PSA, age,

and visceral metastases were not significantly associated with PSA response, PFS, or OS in univariate analyses (Tables 2.2 and 2.3).

AR

Prior studies evaluating the associations between *AR* gene alterations, including CN gain and LBD missense mutations, with therapeutic outcomes are conflicting [14, 15, 17-20, 35]. *AR* CN gain was detected in approximately half of patients prior to therapy and at progression (Figures 2.2C-D and 2.3; Table 2.4). *AR* CN gain was not significantly associated with PSA response (*P*=0.119; Table 2.2; Figure 2.5B), but was associated with a shorter median time to progression (16.1 weeks vs. 34.0 weeks; *P*=0.013) and a shorter median survival (62.7 weeks vs. 144.9 weeks; *P*=0.002) (Figures 2.5C and 2.6B). Using proportional hazards modeling, PFS (HR: 2.07; 95%CI: 1.20-3.57; *P*=0.009) and OS (HR: 3.26; 95%CI: 1.52-7.11; *P*=0.002) were shorter in patients with *AR* CN gain; however, significance was lost upon inclusion of ctDNA burden in multivariable modeling (Figures 2.5C and 2.6B; Table 2.3).

Pathogenic *AR* LBD missense mutations were detected in cfDNA from 13% of patients prior to therapy initiation and in an additional 15% of evaluable patients at progression who were *AR* LBD missense mutation-negative prior to therapy (Figures 2.2C-D and 2.5D; Table 2.5). Using logistic regression analyses, pre-therapy pathogenic *AR* LBD missense mutations neared significance for a worse PSA response rate (*P*=0.072; Table 2.2). Pre-therapy pathogenic *AR* LBD missense mutations were significantly associated with a

worse ≥ 30% decline in PSA (OR: 6.00; 95%CI: 1.10-32.76; *P*=0.039; Table 2.2;

Figure 2.5E), that remained significant when controlled for other factors including

prior abiraterone or enzalutamide therapy (*P*=0.048), pre-therapy PSA (*P*=0.044),

or ctDNA burden (*P*=0.039) in multivariable logistic regression analyses (Tables

2.2 and 2.5).

Median time to progression was significantly shorter in patients who had

an *AR* LBD missense mutation than in *AR* LBD mutation-negative patients (11.4

weeks vs. 28.7 weeks; *P*=0.021; Figure 2.5F). Using proportional hazards

modeling, *AR* LBD missense mutations detected prior to therapy were

significantly associated with a shorter time to progression (HR: 2.39; 95%CI:

1.11-5.14; *P*=0.026) even when controlled for ctDNA burden (*P*=0.020; Table

2.3). However, *AR* LBD mutations were not significantly associated with a worse

OS (*P*=0.364; Table 2.3).

AR CN gain and *AR* LBD missense mutations were not mutually exclusive

in cfDNA (Figure 2.2C). Collective *AR* alterations, including CN gain and LBD

missense mutations, were significantly associated with a shorter PFS and OS,

but significance was lost upon inclusion of ctDNA burden in multivariable

modeling (Table 2.3).

Interestingly, two *AR* mutations at different allelic frequencies (T878A at

9.4% and L702H at 1.5%) were detected in one patient progressing on

abiraterone plus prednisone who also had *AR* CN gain (Figure 2.2C; Table 2.4).

Studies support that the *AR* L702H mutation mediates an acquired response to

glucocorticoids thereby providing rationale to switch from prednisone to

dexamethasone [14, 20, 36]. In support of this notion, replacement of prednisone with dexamethasone resulted in a greater than 80% PSA decline for this patient (Figure 2.4B).

TP53 and RB1

Genetic alterations in *TP53* are highly enriched in lethal prostate cancer [8-11]; and have recently been shown to be associated with worse PFS and OS in patients treated with abiraterone and enzalutamide [17]. *TP53* was highly altered in patients' cfDNA (Figures 2.2C-D and 2.6C); however, *TP53* defects (pathogenic mutations and/or CN loss) were not associated with PSA response (P=0.602) or PFS (P=0.314; Tables 2.2 and 2.3). Conversely, median OS was shorter in patients with a *TP53* defect compared to patients without a detectable *TP53* defect (68.1 weeks vs. 134.9 weeks; P=0.001; Figure 2.6D). Using proportional hazards modeling, *TP53* defects were associated with worse OS (HR: 3.19; 95%CI: 1.53- 6.64; P=0.002) that remained significant after adjusting for clinical variables including ctDNA (P=0.009), prior abiraterone or enzalutamide (P=0.003), or PSA (P=0.001) (Tables 2.3 and 2.6). Patients with both *TP53* and *RB1* defects had an even shorter median OS compared to patients with a *TP53* defect alone or to patients with intact *TP53* (35.4 weeks vs. 77.4 weeks vs. 157.7 weeks; P<0.001; Figure 2.6E). *TP53* defects in conjunction with *RB1* defects were associated with worse OS (HR: 4.50; 95%CI: 1.79-11.28; P=0.001) that remained significant after adjusting for ctDNA burden (P=0.002) (Table 2.3).

PI3K and wingless-type MMTV integration site (WNT) Pathways

PI3K pathway defects involving genetic alterations in *PTEN* (CN loss and/or truncating mutations) and phosphatidylinositol-4,5-bisphosphate 3-kinase catalytic subunit alpha (*PIK3CA*; CN gain) were detected in nearly one-quarter of patients prior to therapy (Figure 2.2C-D). Patients with PI3K pathway defects prior to therapy had a significantly shorter median survival (49.4 weeks vs. 134.9 weeks; *P*<0.001) and a worse OS (HR: 3.64; 95%CI: 1.69-7.86; *P*=0.001), even after controlling for ctDNA burden (*P*=0.026) (Figure 2.6F; Tables 2.3 and 2.7). PI3K pathway alterations were also associated with a worse PSA response that remained significant after adjusting for ctDNA burden (HR: 8.53; 95%CI: 2.09-34.81; *P*=0.003). WNT pathway defects involving genetic alterations in adenomatous polyposis coli (*APC*; CN loss and truncating mutations) and beta-catenin (*CTNNB1*; CN gain and pathogenic missense mutations) were detected in 15% of patients prior to therapy (Figure 2.2C-D). WNT pathway defects were associated with a worse OS (HR: 2.92; 95%CI: 1.28-6.68; *P*=0.011) using proportional hazards modeling; however, significance was lost after controlling for ctDNA burden (*P*=0.051) (Figure 2.6G; Table 2.3).

BRCA1, BRCA2, and ATM

Men with lethal prostate cancer are more likely to have germline mutations in DNA repair genes [37, 38]; however, the association of *BRCA1*, *BRCA2*, *ATM*, and other HDR gene defects with response to androgen-AR axis therapies such as abiraterone and enzalutamide is conflicting [17, 32, 33]. Approximately one-

third of patients had germline and/or somatic deleterious mutations in or CN loss

of *BRCA1*, *BRCA2*, or *ATM* prior to therapy with some patients having more than

one mutation (Figures 2.2C-D and 2.7A-C), a prevalence that is consistent with

published literature [17]. Collective ClinVar deleterious missense mutations,

truncating mutations, and/or CN loss in *BRCA2*, *BRCA1*, or *ATM* were not

significantly associated with PSA response (P=0.417), PFS (P=0.855), or OS

(P=0.326) (Tables 2.2 and 2.3). Analysis of truncating mutations in *BRCA1*,

BRCA2, and *ATM* did not improve prognostic significance.

Discussion

Liquid biopsies using cfDNA as a tumor analyte are rapidly being

developed for cancer diagnostics of solid tumors [39-41]. When obtained

concurrently, plasma-derived cfDNA is highly concordant with tissue biopsies

from prostate [42] and other [43] cancers for tumor-specific genetic alterations.

Liquid biopsies using cfDNA are advantageous over traditional tissue biopsies for

numerous clinical reasons including ease of accessibility and the ability to

provide a global "snapshot" of the mutational landscape. Furthermore, cfDNA

better recapitulates tumor heterogeneity than single-site biopsies and can be

used sequentially to monitor cancer dynamics. Clinical development of cfDNA

has the potential to advance prostate cancer precision medicine [44].

Mechanisms of resistance to abiraterone and enzalutamide likely involve alterations to androgen-AR axis signaling. Prior studies have indicated that collective genetic aberrations to *AR*, including CN gain and mutations, are associated with worse outcomes in patients on abiraterone or enzalutamide therapies [14, 15]. The value of *AR* LBD mutations alone as a predictive marker for response to enzalutamide and abiraterone in patients with mCRPC has yet to be fully established. A prior study showed that mCRPC patients harboring two or more *AR* mutations had worse outcomes on enzalutamide [20]. An additional retrospective study showed that *AR* mutations (L702H and T878A) were associated with shorter PFS and OS in post-docetaxel mCRPC patients on enzalutamide or abiraterone [19]. In a recently reported prospective study, missense mutations in the *AR* LBD were not associated with time to progression on abiraterone or enzalutamide therapies in treatment naïve mCRPC patients [17]. We found that ClinVar pathogenic/likely pathogenic *AR* LBD missense mutations detected in cfDNA prior to enzalutamide and abiraterone therapies were significantly associated with a shorter time to progression that was independent of PSA, prior therapy, or ctDNA fraction. Discrepancies between study findings may be due to several factors including prior therapy, study therapy, specific *AR* LBD mutation, *AR* amplification, and disease burden. Due to their low prevalence, *AR* LBD missense mutations are often combined for analyses; however, studies support that *AR* LBD missense mutations have distinct functional properties that mediate therapy resistance including ligand promiscuity and agonistic activity [25, 36]. Future prospective studies and meta-

analyses will be necessary to determine fully the roles individual mutations in drug resistance. Overall, our findings support that the presence or absence of pathogenic *AR* LBD missense mutations detected in cfDNA by NGS may afford clinical utility as predictive markers of response to enzalutamide and abiraterone therapies; however, large-scale, multi-center prospective validation is necessary to determine their biomarker potential.

Recent reports also indicate that *AR* CN gain as a single marker is associated with worse outcomes in mCRPC patients on abiraterone and enzalutamide [19, 20]. A retrospective study of three biomarker protocols reported that *AR* CN gain was significantly associated with worse PFS and OS in men treated with enzalutamide or abiraterone for mCRPC [19]. A similar report showed that *AR* CN gain was associated with significantly worse PSA response and PFS in patients on enzalutamide [20]. Consistent with prior reports, our study showed that *AR* CN gain was significantly associated with shorter PFS and OS. However, significance was lost when controlling for high ctDNA burden in multivariable modeling. Consistent with our findings, a recent report also indicates that *AR* CN gain is not significantly associated with time to progression in multivariable modeling [17]. Clearly, further prospective studies are needed to assess the clinical utility of *AR* CN gain as a predictive biomarker for therapeutic response to enzalutamide and abiraterone in patients with mCRPC.

In our study, *TP53* and PI3K pathway defects were associated with worse OS. Deregulation of these pathways likely mediates resistance to androgen-AR axis therapies. Concurrent *TP53* and *RB1* defects are highly enriched in AR-

49

independent neuroendocrine mCRPC compared to adenocarcinoma mCRPC [45]. Combined *TP53* and *RB1* loss has been shown to promote lineage switching from an AR-dependent to an AR-independent state [25-27], and consequent resistance to AR-targeted therapies. Similar to *TP53*, genetic alterations in *PTEN* are enriched in mCRPC compared to metastatic castration-sensitive prostate cancer and localized prostate cancer [11]. Studies suggest that *PTEN* loss may mediate castration resistance by downregulating AR [28-31], thereby supporting a rationale for combined inhibition of PI3K and AR in *PTEN*-deficient mCRPCs [46, 47].

The association of pathogenic mutations in HDR genes, such as *BRCA1*, *BRCA2*, and *ATM*, with response to abiraterone and enzalutamide therapy is conflicting. A recent clinical trial in patients with mCRPC suggested that genetic alterations in HDR genes detected by NGS of metastatic biopsy tissue may be associated with longer PFS when on abiraterone therapy [32]. Concordant findings were observed in a second study that suggested that mCRPC patients harboring a germline *BRCA1/2* or *ATM* mutation may also have improved outcomes to abiraterone and enzalutamide [33]. In contrast, a recent study showed that truncating mutations in *BRCA2* and *ATM* detected in cfDNA were associated with a shorter time to progression on abiraterone and enzalutamide therapies in treatment naïve mCRPC patients [17]. In our study, collective somatic and germline genetic alterations, including ClinVar pathogenic mutations and/or CN loss, in *BRCA1*, *BRCA2*, and *ATM* were not associated with PSA response, PFS, or OS. Truncating mutations alone in *BRCA1*, *BRCA2*, and *ATM*

were also not associated with worse outcomes to enzalutamide and abiraterone. Association differences may reflect variables such as sample size, prior treatment status, disease burden, disease heterogeneity, somatic vs. germline, and single vs. dual loss. Certainly, further prospective investigation is needed to determine the clinical significance of HDR mutations as predictive markers to abiraterone and enzalutamide therapies.

In the current study, many patients had detectable alterations that could serve as potential therapeutic targets. Prior studies have shown that mCRPC patients with either germline or somatic mutations in HDR genes had significant responses to olaparib [48] and to abiraterone plus veliparib [32]. Over one-quarter of patients in our study had a deleterious germline or somatic *BRCA1*, *BRCA2*, or *ATM* mutation detected prior to therapy or at progression suggesting that these patients may benefit from therapies targeting poly (ADP-ribose) polymerase (PARP) or platinum-based chemotherapy [32, 48, 49]. In addition, immunotherapy trials have been largely unsuccessful in men with mCRPC [50], however, rare responders have been reported [51]. A seminal clinical trial showed that microsatellite instable cancers caused by mismatch repair (MMR) gene deficiency were sensitive to PD-1 blockade perhaps due to the formation of neoantigens resulting from increased mutational burden [52]. Inactivation of MMR genes and elevated mutational burden have been detected in some men with aggressive prostate cancers [37, 53, 54]. One patient in our study had a detectable noncanonical MMR gene mutation in his cfDNA and a correspondingly high mutational burden suggesting that he may be an ideal candidate for

checkpoint immunotherapy. This study supports that cfDNA may be a useful analyte for directing clinical decisions in prostate cancer precision medicine.

Several limitations to our study exist. Notably, the small sample size precluded multivariable analyses incorporating more than two variables and analyses by therapy subgroup. Larger prospective studies will be needed to validate our findings. Samples were obtained from two hospitals, and future prospective studies would benefit from inclusion of a larger number of institutions. A final limitation was our inability to evaluate *AR* splice variants, including *AR*-V7, due to the requirement of circulating tumor cells or whole-blood RNA; presence of *AR*-V7 is certainly another established mechanism of primary and acquired resistance to next-generation hormonal therapies [21-23]. Future studies should aim to simultaneously analyze the full complement of *AR* aberrations, including gene mutations, amplifications, genomic structural rearrangements, and mRNA splice variants from a single liquid biopsy.

In summary, our findings indicate ctDNA burden is highly associated with worse outcomes to enzalutamide and abiraterone. In addition, pathogenic *AR* LBD missense mutations are associated with a shorter time to progression on abiraterone and enzalutamide in men with mCRPC. *TP53* loss, especially in the context of concurrent *RB1* defects, and PI3K pathway defects are associated with a worse OS. These studies provide the rationale for larger prospective multi-institutional studies to further assess the clinical utility of integrating genetic alterations detected in cfDNA for optimal management of metastatic prostate cancer.

Materials and Methods

Patients

This prospectively collected biomarker study was approved by the Johns Hopkins Medicine Institutional Review Board (IRB). All patients provided written informed consent prior to enrollment. Eligibility criteria included patients diagnosed with mCRPC who were about to begin either abiraterone or enzalutamide therapy. Seventy patients were prospectively enrolled between September 2014 and June 2017 at the Johns Hopkins Hospital (Baltimore, MD) and Sibley Memorial Hospital (Washington, D.C.) and followed through April 2018. Patients had histologically confirmed prostate adenocarcinoma, progressive disease despite ADT, and documented metastatic disease by computed tomography (CT) or bone scan with technetium-99mm-labeled methylene diphosphonate. Of the 70 enrolled patients with mCRPC who were about to begin either abiraterone or enzalutamide therapy, three patients were excluded due to concurrent treatment with other therapies (Veliparib or Docetaxel). Five eligible patients were excluded due to the absence of clinical follow-up data. Blood and clinical follow-up data were obtained for the remaining 62 patients. Blood was collected prior to initiation of therapy for all patients with most pre-therapy samples collected within one week prior to start of therapy (median collection day was on the day of therapy initiation). Patients were treated with enzalutamide (n=25), abiraterone + prednisone (n=35), or concurrent enzalutamide plus abiraterone + prednisone (n=2).

Study Endpoints

Study endpoints were PSA response, PFS, and OS. PSA response was defined by a ≥ 50% decline in PSA from pre-therapy baseline PSA. A ≥ 30% decline in PSA from pre-therapy baseline PSA was also evaluated. Progression was defined by an increase in PSA by ≥ 25% above the baseline or nadir PSA, radiographic progression, or death from prostate cancer. PSA increase by ≥ 25% above the baseline or nadir PSA was confirmed by a subsequent PSA increase, radiographic progression, death from prostate cancer, or physician-determine change of therapy. PFS was defined by the time to the first of the following events: an increase in PSA by ≥ 25% compared to baseline or nadir PSA, radiographic progression, or death from prostate cancer. Blood was also collected following PSA increase from nadir prior to change in therapy for 26 of the 35 patients who had a decrease in PSA following therapy and then progressed as determined by an increase in PSA by ≥ 25% above the baseline or nadir PSA, radiographic progression, or death from prostate cancer.

Plasma and cfDNA Isolations from Blood Samples

Three, 10mL blood samples were collected in Streck BCT tubes prior to therapy initiation and if applicable, at progression. Please refer to the same subsection in Chapter 1's Materials and Methods section for all remaining protocol details.

Deep NGS

NGS libraries were prepared from cfDNA similarly to the protocol in the same subsection of Chapter 1's Materials and Methods section. Between 0.5 and 40.0ng of cfDNA was used for library generation. Additional differences between these study protocols include the following: samples were PCR-amplified using Qiagen's GeneRead™ DNAseq Panel PCR Reagent V2 for 18-22 cycles depending on input cfDNA concentration and only the GeneRead™ Adapter I Set A 12-plex was used to construct all libraries. Prepared libraries were then quantified using two QIAseq™ Library Quant Assay Kits (Qiagen; QSTF-ILZ-F or NGTF-ILZ-R). Lastly, the median on-target coverage for these cfDNA libraries was 6,631x.

Sequence Alignment and Analysis of Variants

Please refer to the same subsection in Chapter 1's Materials and Methods section for all protocol details. Major differences between these study protocols include the following: the filter applied for allele frequency was ≥ 1% with the exception of *AR* which had a previously validated allele frequency threshold of ≥ 0.5% [16]. Additionally, false positive variant calls arising due to the given sequencing run were assessed, tracked, and filtered out using 11 negative controls sequenced in this study. For patients with allelic fractions of ClinVar [54] pathogenic or likely pathogenic *BRCA1* or *BRCA2* mutations that were ≥ 20%, germline information was obtained through clinical records or by sequencing germline leukocyte DNA obtained from isolated buffy coat.

CN Variation

NGS-based CN detection was performed using an in-house developed algorithm, TMM-CNV and third-party tool, CNVKit [55]. TMM-CNV calculates trimmed mean and corresponding two standard deviations from mean relative coverage depths obtained for the sample and a mean of multiple references including sequence of 9 healthy controls (pool of controls). Data distribution at the gene-level was used to apply a trimmed mean of 0.2, 0.1, and corresponding standard deviation to calculate and set the lower and upper thresholds for calling focal deletions and focal amplifications, respectively. For autosomes a $\log_2$ value of mean relative coverage depth between sample and pool of controls was used, whereas for chromosome X, logarithmic value of mean relative coverage depth between sample and pool of controls was used. Final CN calls between TMM-CNV and CNVKit were compared for consensus. Conservative thresholds based on heterozygous SNP fractions of control cfDNA were used to call CN gain and deletion. Given that a targeted gene panel was used for sequencing and tumor cellularity varies in cfDNA sequencing, two thresholds were applied to detect copy gains and losses. CN gain for autosomes was defined by a $\log_2$ ratio of mean relative sequencing coverage at the gene level ≥ 0.4 and ≥ 1.2. CN loss for autosomes was defined by a $\log_2$ ratio of mean relative sequencing coverage at the gene level ≤ -0.4 and ≤ -0.6. For chromosome X, CN gain was defined by a logarithmic ratio of mean relative sequencing coverage at the gene level ≥ 0.7 and ≥ 1.2, and CN loss was defined by a logarithmic ratio of mean relative sequencing coverage at the gene level ≤ -0.4 and ≤ -0.6.

Estimation of ctDNA Fraction

Estimation of high verse low ctDNA fraction was based upon both mutant allele fraction (MAF) and CN alterations. The fraction of ctDNA (% ctDNA) was estimated based upon the highest autosomal variant allele fraction. ctDNA burden was dichotomized into high and low for statistical analyses. Patients with low ctDNA burden had a ClinVar pathogenic missense or truncating MAF < 7%. Conversely, patients with a high ctDNA burden had a ClinVar pathogenic missense or truncating MAF ≥ 7% and/or a CN loss ≤ -0.55 and/or a CN gain ≥ 1.0.

Statistical Analyses

Sample size estimate of 60 informative patients was calculated prior to study initiation. Power and confidence bounds were calculated using PASS 11 (NCSS Software). Chi-squared tests and logistic regression were used to determine associations between genomic status and PSA response. Kaplan-Meier methods and log-rank tests were used to estimate survival functions. Cox proportional-hazard modeling was used to estimate PFS and OS. Due to small sample size, clinical variables were dichotomized. PSA was dichotomized at 20ng/mL based on the median PSA of 19.3ng/mL. Age was dichotomized at 72 years based on the median age of 71.5 years. Prior abiteraterone and enzalutamide was dichotomized as yes or no, visceral metastases was dichotomized as yes or no, and ctDNA burden was dichotomized as low or high. Multivariable models included only two variables to reduce the likelihood of

overfitting. Statistical analyses were performed using STATA SE/15.1, and

GraphPad Prism 5 was used for figure generation.

Table 2.1. Patient Characteristics (n=62)

Characteristics	Total Cohort (n=62)	Abiraterone (n=35)	Enzalutamide (n=25)	Abiraterone plus Enzalutamide (n=2)
Age, years				
Median (range)	71.5 (41-90)	71 (51-90)	73 (41-90)	79 (70-87)
Race, n (%)				
White	51 (82.3)	27 (77.1)	24 (96.0)	0 (0)
Black	7 (11.3)	6 (17.1)	0 (0)	1 (50)
Other	4 (6.5)	2 (5.7)	1 (4.0)	1 (50)
Local Treatment for Prostate Cancer, n (%)				
Radical Prostatectomy	24 (38.7)	14 (40.0)	9 (36.0)	1 (50)
Radiation	9 (14.5)	3 (8.6)	5 (20.0)	1 (50)
Other	4 (6.5)	3 (8.6)	1 (4.0)	0 (0)
None	24 (38.7)	14 (40.0)	10 (40.0)	0 (0)
Not Available	1 (1.6)	1 (2.9)	0 (0)	0 (0)
Gleason Sum, n (%)				
≤7	14 (22.6)	10 (28.6)	2 (8.0)	2 (100)
≥8	42 (67.7)	22 (62.9)	20 (80.0)	0 (0)
Not Available	6 (9.7)	3 (8.6)	3 (12.0)	0 (0)
Prior Treatment for Metastatic Prostate Cancer, n (%)				
Prior Chemotherapy	13 (21.0)	5 (14.3)	8 (32.0)	0 (0)
Prior Abiraterone	10 (16.1)	2 (5.7)	8 (32.0)	0 (0)
Prior Enzalutamide	5 (8.1)	4 (11.4)	1 (4.0)	0 (0)
PSA, ng/mL				
Median (range)	19.3 (0.6-1966)	18.2 (0.6-1966)	18.9 (0.9-205.9)	102.6 (54.2-151.0)
Site of Metastases, n (%)				
Bone Only	34 (54.8)	21 (60.0)	13 (52.0)	0 (0)
Visceral Only	3 (4.8)	0 (0)	3 (12.0)	0 (0)
Lymph Node Only	4 (6.5)	1 (2.9)	3 (12.0)	0 (0)
Bone and Visceral	3 (4.8)	1 (2.9)	1 (4.0)	1 (50)
Bone and Lymph Node	18 (29.0)	12 (34.3)	5 (20.0)	1 (50)
Study Therapy, n (%)				
Abiraterone plus Prednisone	35 (56.5)	35 (100)	0 (0)	0 (0)
Enzalutamide	25 (40.3)	0 (0)	25 (100)	0 (0)
Abiraterone plus Prednisone and Enzalutamide	2 (3.2)	0 (0)	0 (0)	2 (100)
Progression Free Survival, weeks				
Median (range)	25.9 (2.3-162.7)	26.1 (3.7-162.7)	24.7 (2.3-103.4)	7.9 (4.6-11.1)
Prostate Cancer Specific Mortality, n (%)	30 (48.4)	11 (31.4)	17 (68.0)	2 (100)
Follow-up, weeks				
Median (range)	74.0 (4.7-182.1)	74.6 (4.7-182.1)	76.9 (21.4-144.9)	35.6 (16.4-54.7)

Table 22 Response to Therapy: Univariate and Multivariable Logistic Regression Analyses (n=62)

Univariate

		≥30% Decrease in PSA from Baseline			≥50% Decrease in PSA from Baseline		
	Patients (n)	OR	95% CI	P	OR	95% CI	P
Prior Abiraterone or Enzalutamide	15	1.54	0.48-5.01	0.469	2.41	0.74-7.93	0.146
PSA ≥20 ng/mL	30	1.46	0.52-4.07	0.470	1.67	0.61-4.59	0.323
Age ≥72 years	32	1.18	0.42-3.29	0.749	1.32	0.48-3.63	0.586
Visceral Metastasis	6	0.77	0.13-4.58	0.776	0.62	0.10-3.67	0.598
ctDNA High	27	3.61	1.24-10.56	**0.019**	3.17	1.11-9.05	**0.031**
AR CN Gain and/or LBD Mutation	34	1.67	0.59-4.73	0.337	1.80	0.65-5.01	0.261
AR LBD Mutation	8	6.00	1.10-32.76	**0.039**	4.71	0.87-25.28	0.072
AR CN Gain	32	2.06	0.72-5.85	0.176	2.27	0.81-6.34	0.119
TP53 Mutation and/or CN Loss	23	1.37	0.48-3.94	0.554	1.32	0.47-3.72	0.602
RB1 Mutation and/or CN Loss	17	2.25	0.72-7.01	0.162	2.35	0.75-7.35	0.141
TP53 and RB1 Mutation and/or CN Loss	6	9.74	1.06-89.40	**0.044**	7.73	0.85-70.65	0.070
PI3K Pathway Defect	15	7.19	1.94-26.68	**0.003**	8.53	2.09-34.81	**0.003**
WNT Pathway Defect	9	3.89	0.87-17.39	0.076	3.05	0.69-13.53	0.143
BRCA1/BRCA2/ATM Mutation and/or CN Loss	24	1.63	0.57-4.63	0.362	1.53	0.55-4.30	0.417
BRCA1/BRCA2/ATM Truncating Mutations	14	1.25	0.37-4.19	0.718	0.96	0.29-3.21	0.953

Multivariable

		≥30% Decrease in PSA from Baseline			≥50% Decrease in PSA from Baseline		
	Patients (n)	OR	95% CI	P	OR	95% CI	P
AR LBD Mutation	8	6.52	1.10-38.67	**0.039**	4.88	0.85-28.08	0.076
TP53 and RB1 Mutation and/or CN Loss	6	6.68	0.69-65.03	0.102	5.40	0.56-52.15	0.145
PI3K Pathway Defect	15	5.17	1.12-23.91	**0.035**	7.09	1.40-35.94	**0.018**

Significant P values in bold. Multivariable analyses controlled for ctDNA High.
OR: odds ratio; CI: confidence interval; PSA: prostate-specific antigen; ctDNA: cell-free tumor DNA; AR: androgen receptor; CN: copy number; LBD: ligand-binding domain; TP53: tumor protein 53; RB1: retinoblastoma-associated protein 1; PI3K: phosphoinositide 3-kinase; WNT: wingless-type MMTV integration site; BRCA1/2: breast cancer gene 1/2; ATM: ataxia-telangiectasia mutated gene.

Table 2.3. PFS and OS: Univariate and Multivariable Cox Regression Analyses (n=62)

	Patients (n)	Progression-free Survival						Overall Survival					
		Univariate			Multivariable			Univariate			Multivariable		
		HR	95% CI	P	HR	95% CI	P	HR	95% CI	P	HR	95% CI	P
Prior Abiraterone or Enzalutamide	15	1.17	0.63-2.14	0.620	1.25	0.67-2.31	0.480	1.95	0.71-3.24	0.284	1.95	0.89-4.29	0.095
PSA ≥20 ng/mL	30	1.43	0.83-2.45	0.193	1.51	0.88-2.60	0.137	1.56	0.70-2.95	0.326	1.56	0.75-3.25	0.231
Age ≥72 years	32	1.04	0.60-1.78	0.895	1.07	0.62-1.84	0.805	1.08	0.50-2.12	0.925	1.08	0.52-2.22	0.835
Visceral Metastasis	6	1.29	0.51-3.26	0.595	1.44	0.56-3.69	0.450	3.09	0.95-6.63	0.064	3.09	1.14-8.36	**0.026**
ctDNA High	27	1.76	1.03-3.01	**0.039**	-	-	-	2.92	1.40-6.11	**0.004**	-	-	-
AR CN Gain and/or LBD Mutation	34	2.00	1.15-3.47	**0.014**	1.74	0.95-3.19	0.072	2.07	1.36-6.36	**0.006**	2.07	0.87-4.89	0.099
AR LBD Mutation	8	2.39	1.11-5.14	**0.026**	2.51	1.15-5.45	**0.020**	1.64	0.56-4.82	0.364	1.69	0.57-4.97	0.345
AR CN Gain	32	2.07	1.20-3.57	**0.009**	1.82	0.98-3.40	0.060	3.26	1.52-7.00	**0.002**	2.33	0.96-5.62	0.060
TP53 Mutation and/or CN Loss	23	1.33	0.77-2.30	0.314	1.26	0.73-2.19	0.406	3.19	1.53-6.64	**0.002**	2.70	1.27-5.72	**0.009**
RB1 Mutation and/or CN Loss	17	0.94	0.52-1.70	0.849	0.69	0.36-1.32	0.265	1.47	0.68-3.18	0.321	0.99	0.43-2.24	0.974
TP53 and RB1 Mutation and/or CN Loss	6	1.66	0.71-3.91	0.246	1.58	0.67-3.73	0.299	4.50	1.79-11.28	**0.001**	4.56	1.78-11.71	**0.002**
PI3K Pathway Defect	15	1.77	0.97-3.22	0.064	1.40	0.71-2.77	0.327	3.64	1.69-7.86	**0.001**	2.62	1.12-6.10	**0.026**
WNT Pathway Defect	9	1.32	0.64-2.73	0.450	1.13	0.54-2.39	0.746	2.92	1.28-6.68	**0.011**	2.36	0.995-5.60	0.051
BRCA1/BRCA2/ATM Mutation and/or CN Loss	24	0.95	0.55-1.64	0.855	0.89	0.52-1.54	0.683	1.45	0.69-3.06	0.326	0.87	0.37-2.08	0.770
BRCA1/BRCA2/ATM Truncating Mutations	14	0.89	0.47-1.68	0.715	0.86	0.45-1.63	0.641	1.03	0.41-2.57	0.948	0.97	0.39-2.44	0.952

Significant P values in bold. Multivariable analyses controlled for ctDNA High.
HR: hazard ratio; CI: confidence interval; PSA: prostate-specific antigen; ctDNA: cell-free tumor DNA; AR: androgen receptor; CN: copy number; LBD: ligand-binding domain; TP53: tumor protein 53; RB1: retinoblastoma-associated protein 1; PI3K: phosphoinositide 3-kinase; WNT: wingless-type MMTV integration site; BRCA1/2: breast cancer gene 1/2; ATM: ataxia-telangiectasia mutated gene.

Table 2.4. Patient Samples with *AR* Genetic Alterations

	Pre-therapy (n=62)	Progression (n=26)
AR Genetic Alteration, n (%)	34 (54.8)	15 (57.7)
AR Copy Number Gain, n (%)	32 (51.6)	15 (57.7)
AR Mutation, n (%)	8 (12.9)	4 (15.4)
≥2 *AR* Mutations, n (%)	0 (0)	1 (3.8)
AR Copy Number Gain and Mutation, n (%)	6 (9.7)	4 (15.4)

	Pre-therapy			Progression	
Patient	*AR* LBD Mutation	Allelic Fraction (%)	Therapy	*AR* LBD Mutation	Allelic Fraction (%)
26	W742C	1.4	ENZA	No Response	
38	-	-	ABI	L702H T878A	1.5 9.4
52	-	-	ABI	L702H	18.5
54	T878I	0.8	ABI	No Response	
63	H875Y	0.6	ABI	No Sample	
70	L702H	74.6	ENZA	No Response	
82	T878A	1.3	ABI	No Response	
83	L702H	27.3	ENZA	No Response	
86	-	-	ENZA	H875Y	1.3
91	-	-	ABI	T878A	1.7
97	V731M	1.5	ABI	No Response	
105	H875Y	5.3	ABI	No Sample	

AR: androgen receptor; LBD: ligand-binding domain.

Table 2.5. Response to Therapy: Additional Multivariable Logistic Regression Analyses (n=62)

	Multivariable			
	≥30% Decrease in PSA from Baseline			
	Patients (n)	OR	95% CI	P
AR LBD Mutation	8	2.51	1.15-5.45	**0.020**
ctDNA High	27	1.81	1.05-3.11	0.032
AR LBD Mutation	8	5.76	1.02-32.60	**0.048**
Prior Abiraterone or Enzalutamide	15	1.15	0.32-4.12	0.827
AR LBD Mutation	8	5.78	1.05-31.79	**0.044**
PSA ≥ 20 ng/mL	30	1.32	0.45-3.84	0.616

Significant P values in bold.
PSA: prostate-specific antigen; OR: odds ratio; CI: confidence interval; AR: androgen receptor; ctDNA: cell-free tumor DNA; LBD: ligand-binding domain.

Table 2.6. OS: Multivariable Logistic Regression Analyses (n=62) for *TP53* Genetic Aberrations

	Patients (n)	OR	95% CI	P
			Overall Survival	
TP53 Mutation and/or CN Loss	22	2.70	1.29-5.62	**0.008**
ctDNA High	27	2.59	1.22-5.49	**0.013**
TP53 Mutation and/or CN Loss	22	3.02	1.46-6.23	**0.003**
Prior Abiraterone or Enzalutamide	15	1.47	0.69-3.15	0.322
TP53 Mutation and/or CN Loss	22	3.35	1.59-7.05	**0.001**
PSA ≥ 20 ng/mL	30	1.00	1.0004-1.003	**0.005**

Significant P values in bold.
OR: odds ratio; CI: confidence interval; PSA: prostate-specific antigen; ctDNA: cell-free tumor DNA; CN: copy number; TP53: tumor protein 53.

Table 2.7. OS: Multivariable Logistic Regression Analyses (n=62) for PI3K Pathway Defects

	Patients (n)	OR	95% CI	P
			Overall Survival	
PI3K Pathway Defect	15	2.62	1.12-6.10	**0.026**
ctDNA High	27	2.17	0.96-4.92	0.063
PI3K Pathway Defect	15	3.50	1.59-7.71	**0.002**
Prior Abiraterone or Enzalutamide	15	1.89	0.54-2.62	0.669
PI3K Pathway Defect	15	4.05	1.85-8.85	**<0.001**
PSA ≥ 20 ng/mL	30	1.00	1.0004-1.003	**0.005**

Significant P values in bold.
OR: odds ratio; CI: confidence interval; PSA: prostate-specific antigen; ctDNA: cell-free tumor DNA; CN: copy number; PI3K: phosphoinositide 3-kinase.
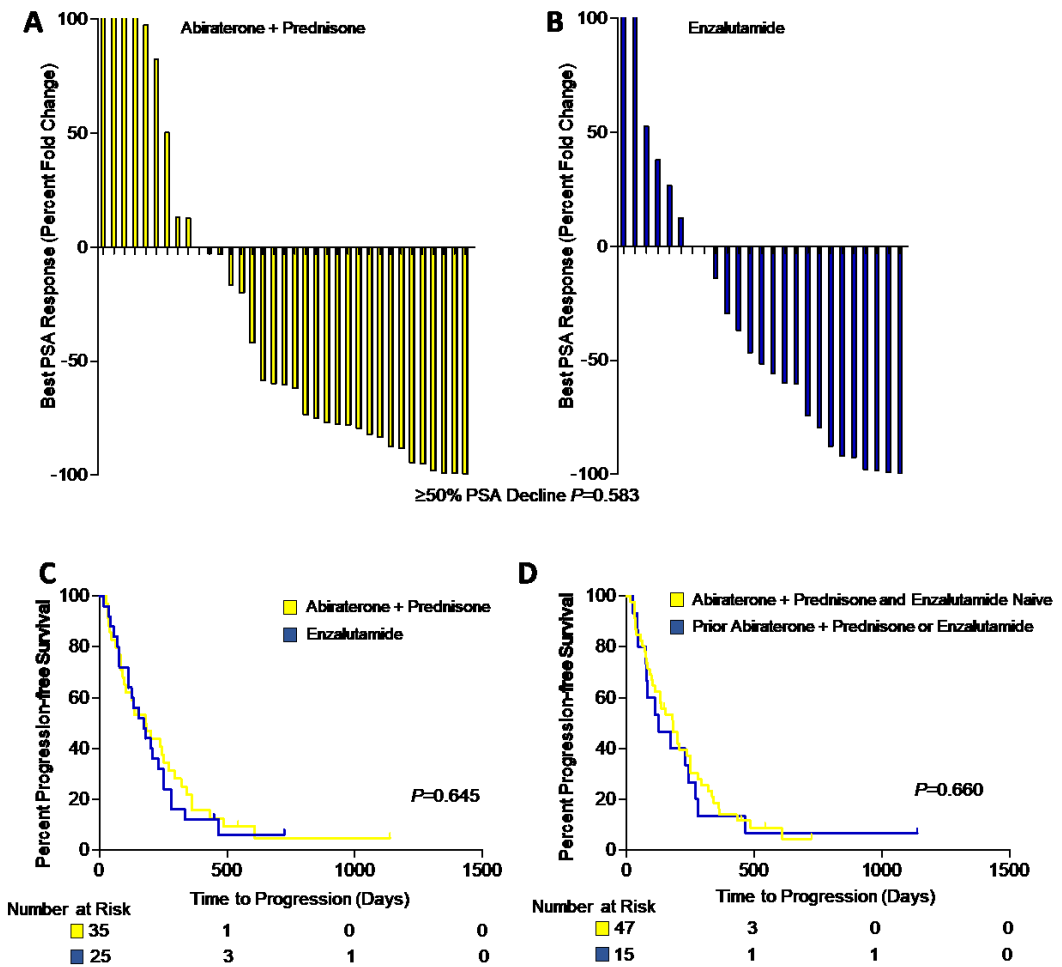
Figure 2.1. PSA response and PFS were similar between patients on

abiraterone + prednisone and patients on enzalutamide. (A) Waterfall plot of best

PSA response for patients receiving abiraterone + prednisone therapy (n=35) as

determined by best percentage fold change in PSA. (B) Waterfall plot of best

PSA response for patients receiving enzalutamide therapy (n=25) as determined

by best percentage fold change in PSA. Chi-squared analysis of PSA response

in patients receiving abiraterone + prednisone compared to patients on

enzalutamide (*P*=0.583). (C) Kaplan-Meier method and log-rank test to determine median time to progression for patients who were treated with abiraterone + prednisone (n=35) compared to patients who were treated with enzalutamide (n=25) therapy (26.1 weeks vs. 24.7 weeks; *P*=0.645). (D) Kaplan-Meier method and log-rank test to determine median time to progression for patients who had prior abiraterone + prednisone or enzalutamide therapy (n=15) compared to patients who were abiraterone + prednisone and enzalutamide naïve (n=47) (17.9 weeks vs. 26.0 weeks; *P*=0.660).

65
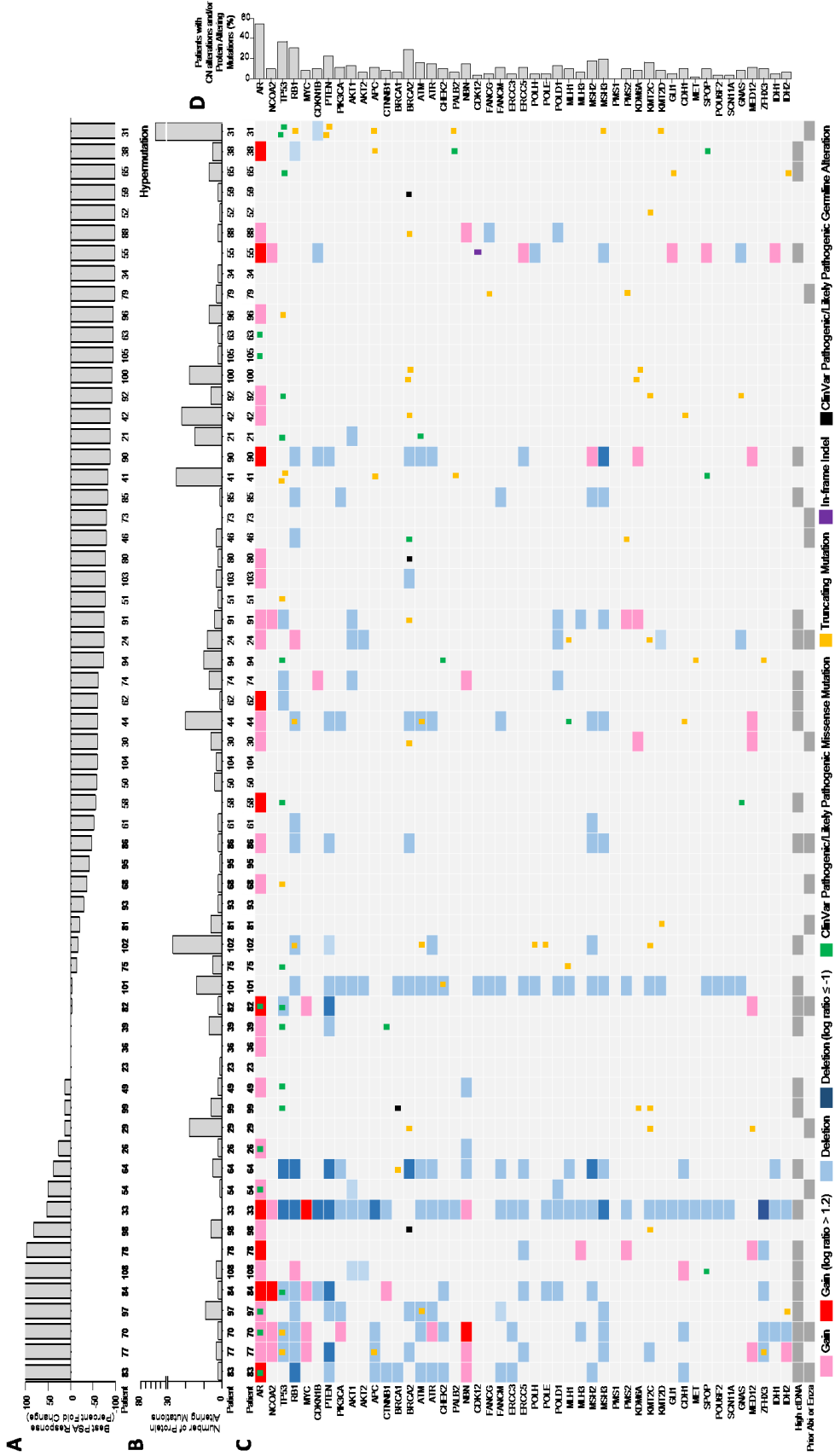
Figure 2.2. Genetic alterations detected in cfDNA prior to therapy and best PSA response. (A) Waterfall plot of best PSA response for all patients (n=62) following therapy as determined by best percentage fold change in PSA. (B) Total number of protein altering genetic changes in 47 genes detected by NGS of cfDNA from 62 patients prior to abiraterone and enzalutamide therapy. (C) Genetic alterations (CN status, ClinVar pathogenic/likely pathogenic missense and germline mutations, and truncating mutations) in 47 genes detected by NGS of cfDNA from 62 patients prior to abiraterone and enzalutamide therapy in order of best PSA response. (D) The total number of genetic alterations (CN and mutations) in 47 genes detected by NGS of cfDNA from 62 patients prior to abiraterone and enzalutamide therapy.

Figure 2.3. Genetic alterations detected in cfDNA following progression. Genetic

alterations (CN status, ClinVar pathogenic/likely pathogenic missense and

germline mutations, and truncating mutations) in 47 genes detected by NGS of

cfDNA from 26 patients following progression on abiraterone + prednisone or enzalutamide therapy.
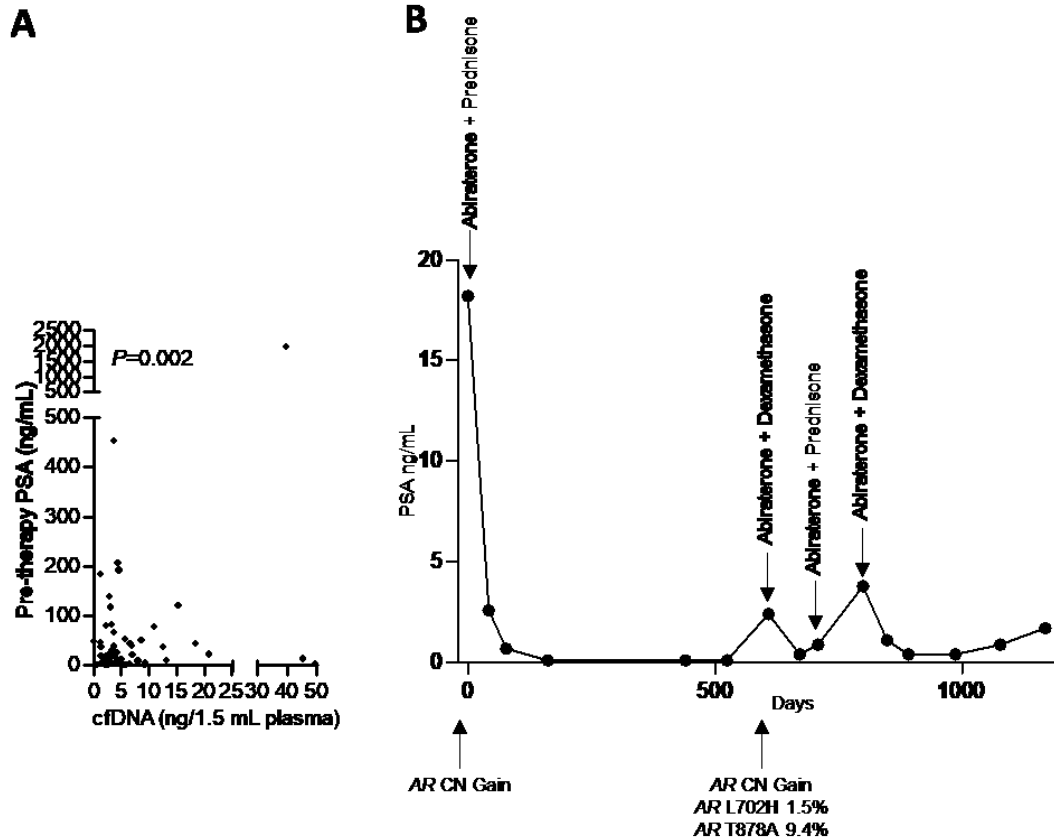

Figure 2.4. Pre-therapy PSA is associated with cfDNA concentration prior to therapy and a patient's PSA changes while progressing on treatment. (A) Pre-therapy PSA is associated with cfDNA concentration prior to therapy as determined using Pearson correlation (r=0.40; *P*=0.002). Pre-therapy PSA was compared with the amount of cfDNA isolated per 1.5mL plasma prior to therapy. (B) PSA for a patient progressing on abiraterone + prednisone with a detectable *AR* L702H mutation and then switched to abiraterone + dexamethasone.
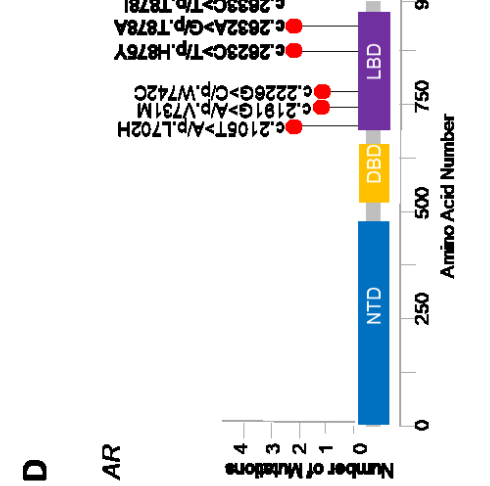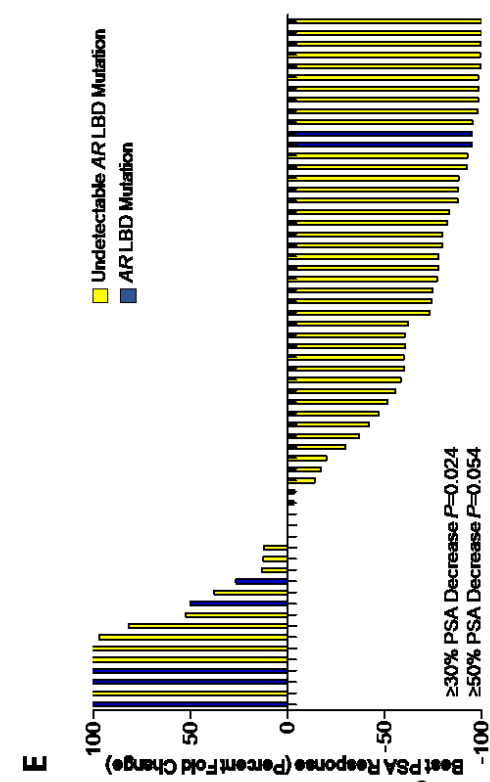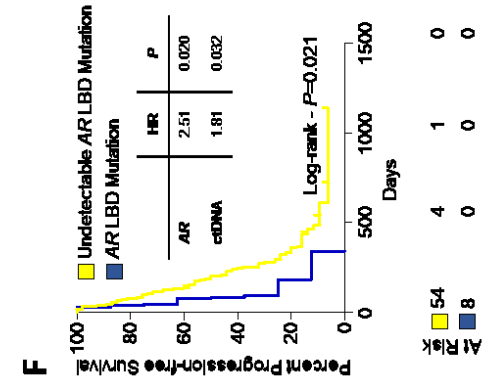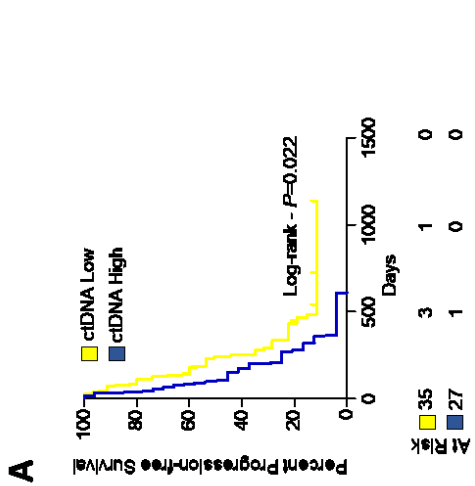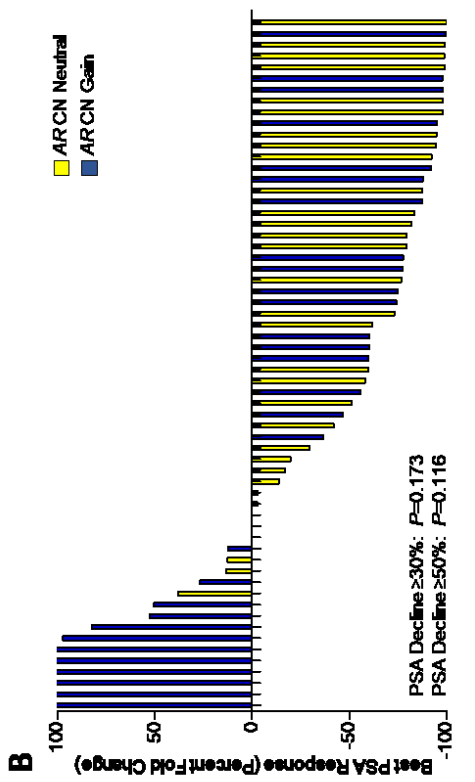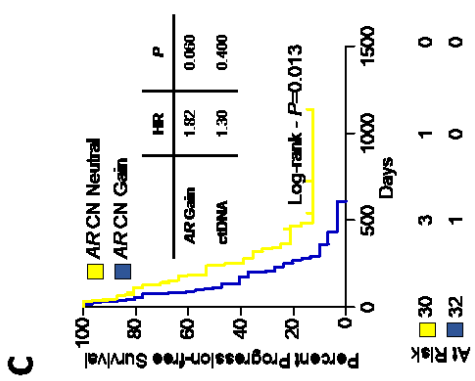
Figure 2.5. PFS: pathogenic *AR* LBD mutations are associated with a shorter time to progression. (A) Kaplan-Meier method and log-rank test to determine median time to progression for patients who had high vs. low ctDNA prior to therapy. (B) Waterfall plot of best PSA response for all patients (n=62) following therapy as determined by best percentage fold change in PSA. *AR* CN gain determined by deep NGS of cfDNA prior to therapy. Chi-squared analyses for a ≥ 30% and ≥ 50% PSA decrease. (C) Kaplan-Meier method and log-rank test to determine median time to progression for patients who were positive vs. negative for *AR* CN gain prior to therapy. The association of *AR* LBD mutations with PFS controlled for ctDNA burden using multivariable proportional hazards modeling. (D) Gene schematic illustrating pathogenic *AR* LBD mutations detected by targeted NGS of cfDNA prior to abiraterone and enzalutamide therapies (NTD=N-terminal domain, DBD=DNA binding domain). (E) Waterfall plot of best PSA response for all patients (n=62) following therapy as determined by best percentage fold change in PSA. *AR* LBD mutations determined by deep NGS of cfDNA prior to therapy. Chi-squared analyses for a ≥ 30% and ≥ 50% PSA decrease. (F) Kaplan-Meier method and log-rank test to determine median time to progression for patients who were positive vs. negative for *AR* LBD mutations prior to therapy. The association of *AR* LBD mutations with PFS controlled for ctDNA burden using multivariable proportional hazards modeling.
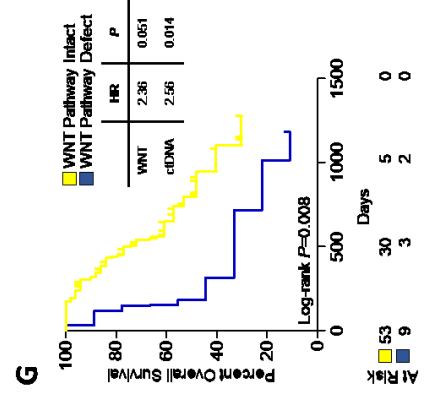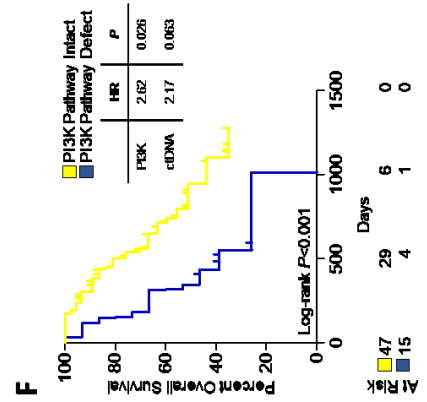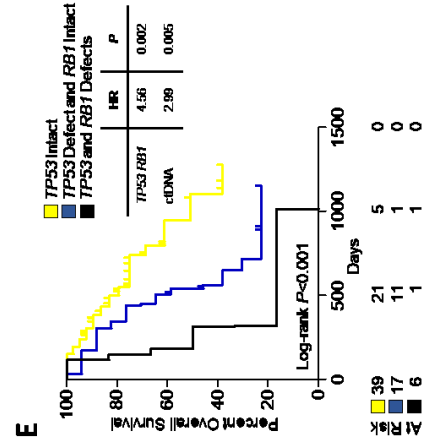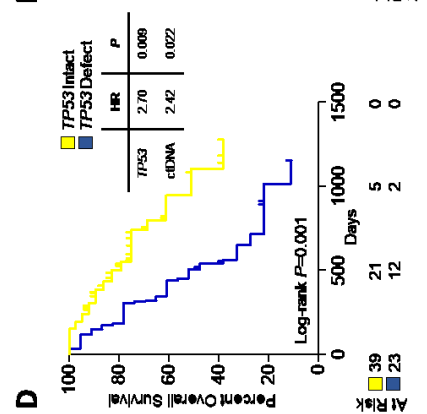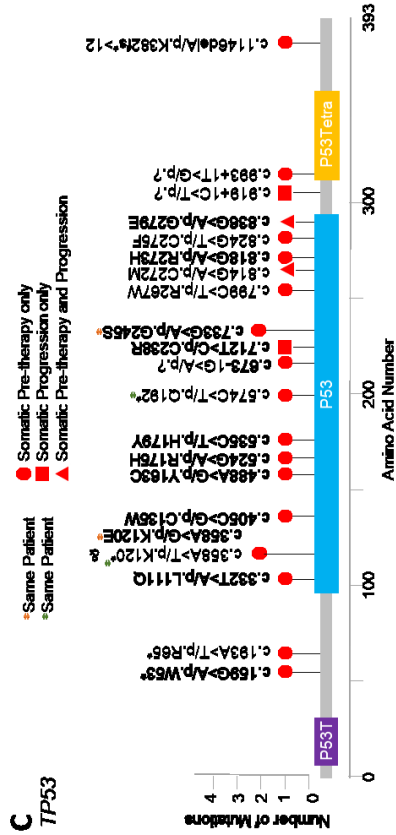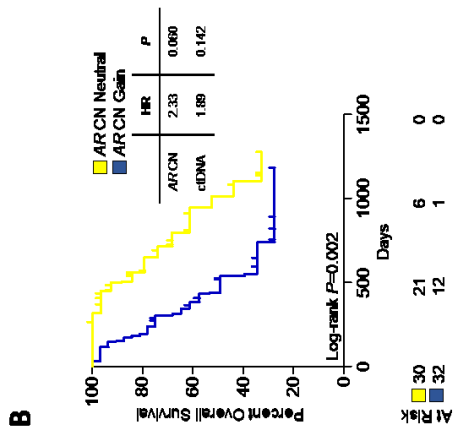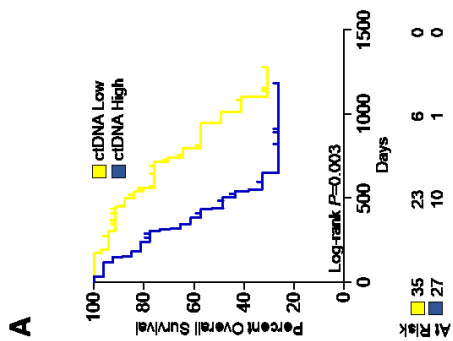
Figure 2.6. OS: *TP53* and PI3K pathway defects are associated with worse OS. (A) Kaplan-Meier method and log-rank test to determine median OS for patients who had high vs. low ctDNA prior to therapy. (B) Kaplan-Meier method and log-rank test to determine median OS for patients who had *AR* CN gain prior to therapy. Association of *AR* CN gain with OS controlled for ctDNA burden using multivariable proportional hazards modeling. (C) Gene schematic illustrating deleterious *TP53* mutations detected by deep NGS of cfDNA prior to abiraterone and enzalutamide therapies and at disease progression while on therapy (P53T=P53 transactivation motif, P53=P53 DNA-binding domain, P53Tetra=P53 tetramerization motif). (D) Kaplan-Meier method and log-rank test to determine median OS for patients who had *TP53* defects (CN loss and or ClinVar pathogenic/likely pathogenic mutations) prior to therapy. Association of *TP53* defects with OS controlled for ctDNA burden using multivariable proportional hazards modeling. (E) Kaplan-Meier method and log-rank test to determine median OS for patients who had both *TP53* and *RB1* defects compared to patients who had *TP53* defects but were *RB1* intact (CN loss and or ClinVar pathogenic/likely pathogenic mutations) prior to therapy. Association of dual *TP53* and *RB1* defects with OS controlled for ctDNA burden using multivariable proportional hazards modeling. (F) Kaplan-Meier method and log-rank test to determine median OS for patients who had PI3K pathway defects (CN loss and/or truncating mutations in *PTEN* and/or CN gain of *PIK3CA*) prior to therapy. Association of PI3K defects with OS controlled for ctDNA burden using multivariable proportional hazards modeling. (G) Kaplan-Meier method and log-

rank test to determine median OS for patients who had WNT pathway defects

(CN loss and/or truncating mutations in *APC* and/or CN gain and/or pathogenic

missense mutations in *CTNNB1*) prior to therapy. Association of WNT defects

with OS controlled for ctDNA burden using multivariable proportional hazards

modeling.

A *BRCA2*

B *BRCA1*

C *ATM*

Legend:
- Germline (black circle)
- Somatic Pre-therapy only (red circle)
- Somatic Progression only (red square)
- Somatic Pre-therapy and Progression (red triangle)
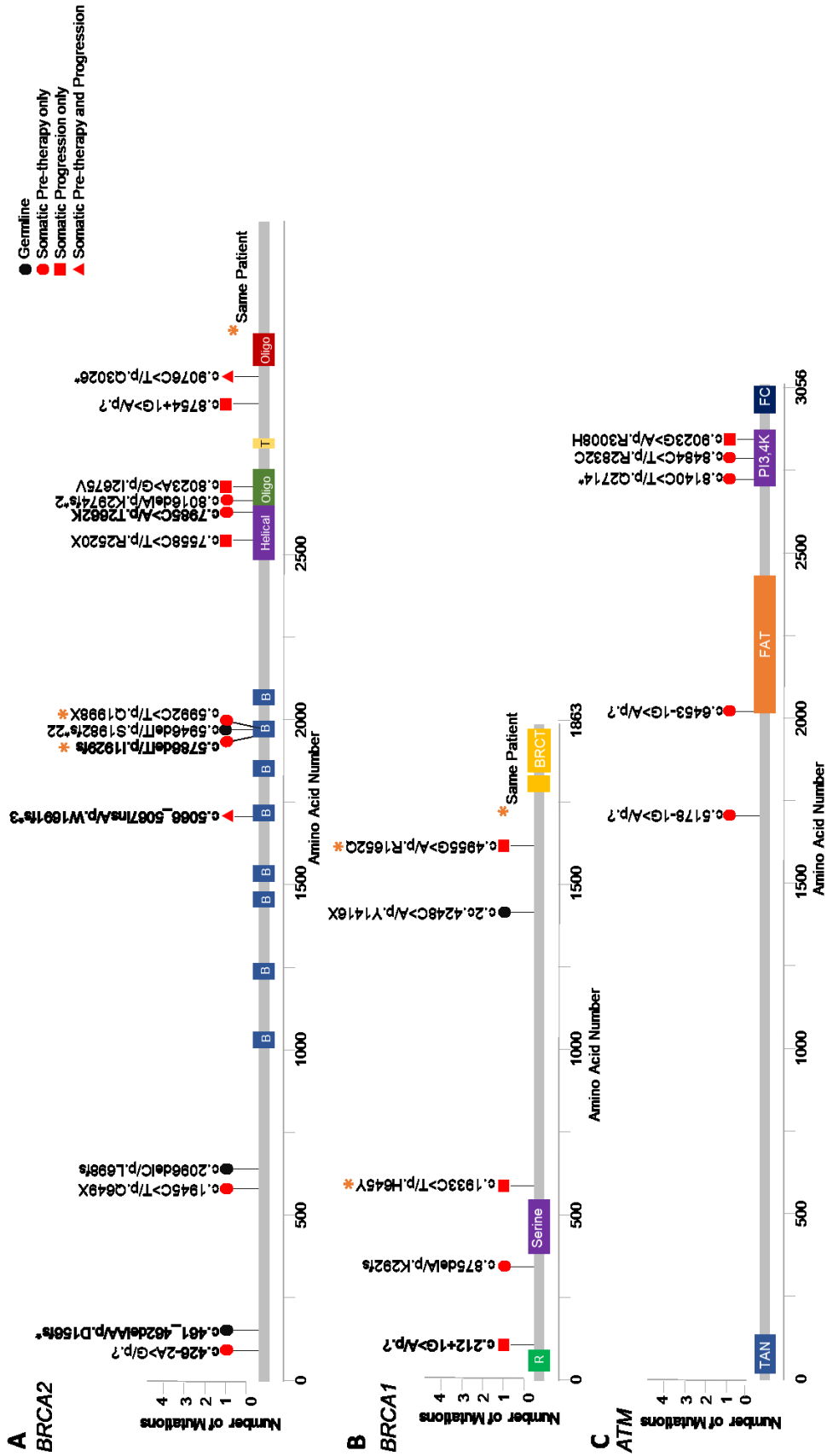
Figure 2.7. Mutations detected in *BRCA1*, *BRCA2*, and *ATM* prior to therapy and at progression. A-C, Gene schematics illustrating deleterious germline and somatic mutations in (A) BRCA2 (B=BRC repeats, Helical=helical domain, Oligo=oligonucleotide-binding domain, T=tower domain), (B) BRCA1 (R=Ring finger domain, Serine=Serine rich domain associated with BRCT, BRCT=BRCA1 C terminus domain) and (C) ATM (TAN=Telomere length maintenance and DNA damage repair, FAT=FAT domain, PI3,4K=Phosphatidylinositol 3- and 4-kinase, FC=FATC domain) and as detected by deep, targeted NGS of cfDNA prior to abiraterone + prednisone and enzalutamide therapies and at progression while on therapy.

References

1. de Bono JS, Logothetis CJ, Molina A, Fizazi K, North S, Chu L, Chi KN, Jones RJ, Goodman OB, Jr., Saad F, et al. Abiraterone and increased survival in metastatic prostate cancer. *The New England journal of medicine*. 2011;364(21):1995-2005.

2. Ryan CJ, Smith MR, de Bono JS, Molina A, Logothetis CJ, de Souza P, Fizazi K, Mainwaring P, Piulats JM, Ng S, et al. Abiraterone in metastatic prostate cancer without previous chemotherapy. *The New England journal of medicine*. 2013;368(2):138-48.

3.   Scher HI, Fizazi K, Saad F, Taplin ME, Sternberg CN, Miller K, de Wit R, Mulders P, Chi KN, Shore ND, et al. Increased survival with enzalutamide in prostate cancer after chemotherapy. *The New England journal of medicine*. 2012;367(13):1187-97.

4.   Beer TM, Armstrong AJ, Rathkopf DE, Loriot Y, Sternberg CN, Higano CS, Iversen P, Bhattacharya S, Carles J, Chowdhury S, et al. Enzalutamide in metastatic prostate cancer before chemotherapy. *The New England journal of medicine*. 2014;371(5):424-33.

5.   Cancer Genome Atlas Research N. Comprehensive molecular characterization of urothelial bladder carcinoma. *Nature*. 2014;507(7492):315-22.

6.   Baca SC, Prandi D, Lawrence MS, Mosquera JM, Romanel A, Drier Y, Park K, Kitabayashi N, MacDonald TY, Ghandi M, et al. Punctuated evolution of prostate cancer genomes. *Cell*. 2013;153(3):666-77.

7.   Taylor BS, Schultz N, Hieronymus H, Gopalan A, Xiao Y, Carver BS, Arora VK, Kaushik P, Cerami E, Reva B, et al. Integrative genomic profiling of human prostate cancer. *Cancer cell*. 2010;18(1):11-22.

8.   Grasso CS, Wu YM, Robinson DR, Cao X, Dhanasekaran SM, Khan AP, Quist MJ, Jing X, Lonigro RJ, Brenner JC, et al. The mutational landscape of lethal castration-resistant prostate cancer. *Nature*. 2012;487(7406):239-43.

9.   Kumar A, Coleman I, Morrissey C, Zhang X, True LD, Gulati R, Etzioni R, Bolouri H, Montgomery B, White T, et al. Substantial interindividual and limited intraindividual genomic diversity among tumors from men with metastatic prostate cancer. *Nature medicine*. 2016;22(4):369-78.

10.   Robinson D, Van Allen EM, Wu YM, Schultz N, Lonigro RJ, Mosquera JM, Montgomery B, Taplin ME, Pritchard CC, Attard G, et al. Integrative clinical genomics of advanced prostate cancer. *Cell*. 2015;161(5):1215-28.

11.   Abida W, Armenia J, Gopalan A, Brennan R, Walsh M, Barron D, Danila D, Rathkopf D, Morris M, Slovin S, et al. Prospective Genomic Profiling of Prostate Cancer Across Disease States Reveals Germline and Somatic Alterations That May Affect Clinical Decision Making. *JCO precision oncology*. 2017;2017.

12.   Gao J, Aksoy BA, Dogrusoz U, Dresdner G, Gross B, Sumer SO, Sun Y, Jacobsen A, Sinha R, Larsson E, et al. Integrative analysis of complex cancer genomics and clinical profiles using the cBioPortal. *Science signaling*. 2013;6(269):pl1.

13.   Cerami E, Gao J, Dogrusoz U, Gross BE, Sumer SO, Aksoy BA, Jacobsen A, Byrne CJ, Heuer ML, Larsson E, et al. The cBio cancer genomics portal: an open platform for exploring multidimensional cancer genomics data. *Cancer discovery*. 2012;2(5):401-4.

14.   Romanel A, Gasi Tandefelt D, Conteduca V, Jayaram A, Casiraghi N, Wetterskog D, Salvi S, Amadori D, Zafeiriou Z, Rescigno P, et al. Plasma AR and abiraterone-resistant prostate cancer. *Science translational medicine*. 2015;7(312):312re10.

15.   Azad AA, Volik SV, Wyatt AW, Haegert A, Le Bihan S, Bell RH, Anderson SA, McConeghy B, Shukin R, Bazov J, et al. Androgen Receptor Gene Aberrations in Circulating Cell-Free DNA: Biomarkers of Therapeutic Resistance

in Castration-Resistant Prostate Cancer. *Clinical cancer research: an official journal of the American Association for Cancer Research*. 2015;21(10):2315-24.

16.   Goldstein A, Valda Toro P, Lee J, Silberstein JL, Nakazawa M, Waters I, Cravero K, Chu D, Cochran RL, Kim M, et al. Detection fidelity of AR mutations in plasma derived cell-free DNA. *Oncotarget*. 2017.

17.   Annala M, Vandekerkhove G, Khalaf D, Taavitsainen S, Beja K, Warner EW, Sunderland K, Kollmannsberger C, Eigl BJ, Finch D, et al. Circulating tumor DNA genomics correlate with resistance to abiraterone and enzalutamide in prostate cancer. *Cancer discovery*. 2018.

18.   Salvi S, Casadio V, Conteduca V, Burgio SL, Menna C, Bianchi E, Rossi L, Carretta E, Masini C, Amadori D, et al. Circulating cell-free AR and CYP17A1 copy number variations may associate with outcome of metastatic castration-resistant prostate cancer patients treated with abiraterone. *British journal of cancer*. 2015;112(10):1717-24.

19.   Conteduca V, Wetterskog D, Sharabiani MTA, Grande E, Fernandez-Perez MP, Jayaram A, Salvi S, Castellano D, Romanel A, Lolli C, et al. Androgen receptor gene status in plasma DNA associates with worse outcome on enzalutamide or abiraterone for castration-resistant prostate cancer: a multi-institution correlative biomarker study. *Annals of oncology*. 2017;28(7):1508-16.

20.   Wyatt AW, Azad AA, Volik SV, Annala M, Beja K, McConeghy B, Haegert A, Warner EW, Mo F, Brahmbhatt S, et al. Genomic Alterations in Cell-Free DNA and Enzalutamide Resistance in Castration-Resistant Prostate Cancer. *JAMA oncology*. 2016.

21.   Antonarakis ES, Lu C, Wang H, Luber B, Nakazawa M, Roeser JC, Chen Y, Mohammad TA, Chen Y, Fedor HL, et al. AR-V7 and resistance to enzalutamide and abiraterone in prostate cancer. *The New England journal of medicine*. 2014;371(11):1028-38.

22.   Qu F, Xie W, Nakabayashi M, Zhang H, Jeong SH, Wang X, Komura K, Sweeney CJ, Sartor O, Lee GM, et al. Association of AR-V7 and prostate specific antigen RNA levels in blood with efficacy of abiraterone acetate and enzalutamide treatment in men with prostate cancer. *Clinical cancer research: an official journal of the American Association for Cancer Research*. 2016.

23.   Antonarakis ES, Lu C, Luber B, Wang H, Chen Y, Zhu Y, Silberstein JL, Taylor MN, Maughan BL, Denmeade SR, et al. Clinical Significance of Androgen Receptor Splice Variant-7 mRNA Detection in Circulating Tumor Cells of Men With Metastatic Castration-Resistant Prostate Cancer Treated With First- and Second-Line Abiraterone and Enzalutamide. *Journal of clinical oncology: official journal of the American Society of Clinical Oncology*. 2017;35(19):2149-56.

24.   Henzler C, Li Y, Yang R, McBride T, Ho Y, Sprenger C, Liu G, Coleman I, Lakely B, Li R, et al. Truncation and constitutive activation of the androgen receptor by diverse genomic rearrangements in prostate cancer. *Nature communications*. 2016;7:13668.

25.   Watson PA, Arora VK, and Sawyers CL. Emerging mechanisms of resistance to androgen receptor inhibitors in prostate cancer. *Nature reviews Cancer*. 2015;15(12):701-11.

26.   Ku SY, Rosario S, Wang Y, Mu P, Seshadri M, Goodrich ZW, Goodrich MM, Labbe DP, Gomez EC, Wang J, et al. Rb1 and Trp53 cooperate to suppress prostate cancer lineage plasticity, metastasis, and antiandrogen resistance. *Science*. 2017;355(6320):78-83.

27.   Mu P, Zhang Z, Benelli M, Karthaus WR, Hoover E, Chen CC, Wongvipat J, Ku SY, Gao D, Cao Z, et al. SOX2 promotes lineage plasticity and antiandrogen resistance in TP53- and RB1-deficient prostate cancer. *Science*. 2017;355(6320):84-8.

28.   Shen MM, and Abate-Shen C. Pten inactivation and the emergence of androgen-independent prostate cancer. *Cancer research*. 2007;67(14):6535-8.

29.   Jiao J, Wang S, Qiao R, Vivanco I, Watson PA, Sawyers CL, and Wu H. Murine cell lines derived from Pten null prostate cancer show the critical role of PTEN in hormone refractory prostate cancer development. *Cancer research*. 2007;67(13):6083-91.

30.   Mulholland DJ, Tran LM, Li Y, Cai H, Morim A, Wang S, Plaisier S, Garraway IP, Huang J, Graeber TG, et al. Cell autonomous role of PTEN in regulating castration-resistant prostate cancer growth. *Cancer cell*. 2011;19(6):792-804.

31.   Carver BS, Chapinski C, Wongvipat J, Hieronymus H, Chen Y, Chandarlapaty S, Arora VK, Le C, Koutcher J, Scher H, et al. Reciprocal feedback regulation of PI3K and androgen receptor signaling in PTEN-deficient prostate cancer. *Cancer cell*. 2011;19(5):575-86.

32.   Hussain M, Daignault-Newton S, Twardowski PW, Albany C, Stein MN, Kunju LP, Siddiqui J, Wu YM, Robinson D, Lonigro RJ, et al. Targeting Androgen Receptor and DNA Repair in Metastatic Castration-Resistant Prostate Cancer: Results From NCI 9012. *Journal of clinical oncology: official journal of the American Society of Clinical Oncology*. 2017;JCO2017757310.

33.   Antonarakis ES, Changxue, L., Luber, B., Liang, C., Wang, H., Chen, Y., Silberstein, J.L., Piana, D., Lai, Z., Chen, Y., Isaacs, W.B. Germline DNA-repair Gene Mutations and Outcomes in Men with Metastatic Castration-resistant Prostate Cancer Receiving First-lin Abiraterone and Enzalutamide. *European urology*. 2018.

34.   Landrum MJ, Lee JM, Benson M, Brown G, Chao C, Chitipiralla S, Gu B, Hart J, Hoffman D, Hoover J, et al. ClinVar: public archive of interpretations of clinically relevant variants. *Nucleic acids research*. 2016;44(D1):D862-8.

35.   Salvi S, Casadio V, Conteduca V, Lolli C, Gurioli G, Martignano F, Schepisi G, Testoni S, Scarpi E, Amadori D, et al. Circulating AR copy number and outcome to enzalutamide in docetaxel-treated metastatic castration-resistant prostate cancer. *Oncotarget*. 2016.

36.   Lallous N, Volik SV, Awrey S, Leblanc E, Tse R, Murillo J, Singh K, Azad AA, Wyatt AW, LeBihan S, et al. Functional analysis of androgen receptor mutations that confer anti-androgen resistance identified in circulating cell-free DNA from prostate cancer patients. *Genome biology*. 2016;17:10.

37.   Pritchard CC, Mateo J, Walsh MF, De Sarkar N, Abida W, Beltran H, Garofalo A, Gulati R, Carreira S, Eeles R, et al. Inherited DNA-Repair Gene

Mutations in Men with Metastatic Prostate Cancer. *The New England journal of medicine*. 2016;375(5):443-53.

38.   Na R, Zheng SL, Han M, Yu H, Jiang D, Shah S, Ewing CM, Zhang L, Novakovic K, Petkewicz J, et al. Germline Mutations in ATM and BRCA1/2 Distinguish Risk for Lethal and Indolent Prostate Cancer and are Associated with Early Age at Death. *European urology*. 2017;71(5):740-7.

39.   Cohen JD, Li L, Wang Y, Thoburn C, Afsari B, Danilova L, Douville C, Javed AA, Wong F, Mattox A, et al. Detection and localization of surgically resectable cancers with a multi-analyte blood test. *Science*. 2018.

40.   Leary RJ, Sausen M, Kinde I, Papadopoulos N, Carpten JD, Craig D, O'Shaughnessy J, Kinzler KW, Parmigiani G, Vogelstein B, et al. Detection of chromosomal alterations in the circulation of cancer patients with whole-genome sequencing. *Science translational medicine*. 2012;4(162):162ra54.

41.   Webb S. The cancer bloodhounds. *Nature biotechnology*. 2016;34(11):1090-4.

42.   Wyatt AW, Annala M, Aggarwal R, Beja K, Feng F, Youngren J, Foye A, Lloyd P, Nykter M, Beer TM, et al. Concordance of Circulating Tumor DNA and Matched Metastatic Tissue Biopsy in Prostate Cancer. *Journal of the National Cancer Institute*. 2017;109(12).

43.   Beaver JA, Jelovac D, Balukrishna S, Cochran RL, Croessmann S, Zabransky DJ, Wong HY, Valda Toro P, Cidado J, Blair BG, et al. Detection of cancer DNA in plasma of patients with early-stage breast cancer. *Clinical cancer*

research: an official journal of the American Association for Cancer Research. 2014;20(10):2643-50.

44.   Schweizer MT, and Antonarakis ES. Liquid biopsy: Clues on prostate cancer drug resistance. *Science translational medicine*. 2015;7(312):312fs45.

45.   Beltran H, Prandi D, Mosquera JM, Benelli M, Puca L, Cyrta J, Marotz C, Giannopoulou E, Chakravarthi BV, Varambally S, et al. Divergent clonal evolution of castration-resistant neuroendocrine prostate cancer. *Nature medicine*. 2016;22(3):298-305.

46.   Jamaspishvili T, Berman DM, Ross AE, Scher HI, De Marzo AM, Squire JA, and Lotan TL. Clinical implications of PTEN loss in prostate cancer. *Nature reviews Urology*. 2018;15(4):222-34.

47.   de Bono JS, De Giorgi U., Massard, C, Bracarda, S., Rodrigues, D.N., Kocak, I., Font, A., Arija, J.A., Shih, K., Radavoi, G.D., Yu, W., Chan, W., Gendreau, S. Zhang, L., Riisnaes, R., Wongchenko, M.J., Maslyar, D., Jinga, V. PTEN loss as a predictive biomarker for the Akt inhibitor ipatasertib combined with abiraterone acetate in patients with metastatic castration-resistant prostate cancer (mCRPC). *Annals of Oncology*. 2016;27(suppl_6):7180.

48.   Mateo J, Carreira S, Sandhu S, Miranda S, Mossop H, Perez-Lopez R, Nava Rodrigues D, Robinson D, Omlin A, Tunariu N, et al. DNA-Repair Defects and Olaparib in Metastatic Prostate Cancer. *The New England journal of medicine*. 2015;373(18):1697-708.

49.   Cheng HH, Pritchard CC, Boyd T, Nelson PS, and Montgomery B. Biallelic Inactivation of BRCA2 in Platinum-sensitive Metastatic Castration-resistant Prostate Cancer. *European urology*. 2016;69(6):992-5.

50.   Brahmer JR, Drake CG, Wollner I, Powderly JD, Picus J, Sharfman WH, Stankevich E, Pons A, Salay TM, McMiller TL, et al. Phase I study of single-agent anti-programmed death-1 (MDX-1106) in refractory solid tumors: safety, clinical activity, pharmacodynamics, and immunologic correlates. *Journal of clinical oncology: official journal of the American Society of Clinical Oncology*. 2010;28(19):3167-75.

51.   Kwon ED, Drake CG, Scher HI, Fizazi K, Bossi A, van den Eertwegh AJ, Krainer M, Houede N, Santos R, Mahammedi H, et al. Ipilimumab versus placebo after radiotherapy in patients with metastatic castration-resistant prostate cancer that had progressed after docetaxel chemotherapy (CA184-043): a multicentre, randomised, double-blind, phase 3 trial. *The Lancet Oncology*. 2014;15(7):700-12.

52.   Le DT, Uram JN, Wang H, Bartlett BR, Kemberling H, Eyring AD, Skora AD, Luber BS, Azad NS, Laheru D, et al. PD-1 Blockade in Tumors with Mismatch-Repair Deficiency. *The New England journal of medicine*. 2015;372(26):2509-20.

53.   Guedes LB, Antonarakis ES, Schweizer MT, Mirkheshti N, Almutairi F, Park JC, Glavaris S, Hicks J, Eisenberger MA, De Marzo AM, et al. MSH2 Loss in Primary Prostate Cancer. *Clinical cancer research: an official journal of the American Association for Cancer Research*. 2017;23(22):6863-74.

54.   Pritchard CC, Morrissey C, Kumar A, Zhang X, Smith C, Coleman I, Salipante SJ, Milbank J, Yu M, Grady WM, et al. Complex MSH2 and MSH6 mutations in hypermutated microsatellite unstable advanced prostate cancer. *Nature communications*. 2014;5:4988.

55.   Talevich E, Shain AH, Botton T, and Bastian BC. CNVkit: Genome-Wide Copy Number Detection and Visualization from Targeted DNA Sequencing. *PLoS computational biology*. 2016;12(4):e1004873.

3 Isogenic Modeling of Androgen Receptor Ligand-binding Domain Mutations

Introduction

The Androgen Receptor (AR)

The AR is a member of the steroid and nuclear receptor superfamily [1, 2] and is mainly expressed in androgen-target tissues, such as prostate, skeletal muscle, and liver [3]. AR functions as an intracellular transcriptional factor and is regulated by the binding of its ligands: androgens, such as testosterone (T) and 5-alpha-dihydrotesterone (DHT). Androgen-AR interactions initiate conformational changes of the receptor such that receptor-protein and receptor-DNA interactions are affected and the transcription of androgen-responsive genes can commence [2]. In utero, the AR is responsible for male sexual differentiation, and during adolescence, it plays a role in male pubertal changes. In adult males, androgen-AR interactions are involved in spermatogenesis, muscle mass maintenance, and libido [4, 5].

The human *AR* gene is located on the X chromosome, contains eight exons, and encodes a protein that is 920 amino acids long [6, 7]. The three main functional domains of AR are the N-terminal domain (NTD, exon 1), DNA-binding domain (DBD, exons 2-3), and ligand-binding domain (LBD, exons 4-8) (Figure 3.1). The protein's hinge region (exon 4) is located between the DBD and LBD. The nuclear localization signal (NLS, exons 3-4) spans across the DBD and hinge region. AR has two transactivation functions. The N-terminal activation function 1 (AF1) is not conserved across other steroid receptors, and the C-

terminal activation function (AF2) is ligand-dependent and more conserved in sequence across other steroid receptors [8].

When AR is not bound to an agonist, it is mainly located in the cytoplasm, where its LBD associates with a complex of heat shock proteins (HSPs) [9]. Once a ligand or agonist binds to the receptor, AR dissociates from the HSPs and undergoes a series of conformational changes, including dimerization, phosphorylation, and nuclear translocation. Once in the nucleus, the ligand-activated AR can bind to an androgen response element (ARE), which is located in the promoter or enhancer region of AR-targeted genes. ARE-bound ARs can also recruit other transcription co-regulators (such as co-activators and co-repressors) [10] and transcriptional machinery [11], all of which further regulate target gene expression.

Androgen-AR Interactions and Their Role in CRPC

Androgen synthesis is initially regulated by the hypothalamic-pituitary-testicular axis [7]. The adrenal glands are then responsible for *de novo* steroidogenesis and the prostate is where these newly synthesized steroids are finally converted to DHT [7]. DHT and T are canonical AR ligands such that when they interact with the AR, they can initiate receptor signaling. Just 15 years ago, it was thought that AR signaling was not involved in castration-resistant prostate cancer (CRPC) biology [7]. However, studies from the past decade have shown that androgens remaining after both physical and chemical castration and the AR itself continue to contribute to CRPC biology and progression [12, 13]. These

studies identified the need for antiandrogen therapies for patients with CRPC.

Through a drug discovery screen, the next-generation therapy and AR

antagonist, enzalutamide, was identified [14]. Abiraterone acetate is another

antiandrogen therapy that was developed for metastatic CRPC patients and

specifically inhibits CYP17A1, thereby preventing *de novo* steroidogenesis [15].

Both of these next-generation therapies have been successful in treating CRPC

patients; however, overcoming the inherent or acquired resistance to these

therapies remains a major clinical challenge.

Resistance Mechanisms to Next-Generation Therapies

Resistance mechanisms to therapies targeting the androgen-AR axis can

be broadly categorized into three classes (restored AR signaling, AR bypass

signaling, and complete AR independence) based upon clinical relapse profiles

and histological and molecular features (Table 3.1) [7]. Restored AR signaling

clinically involves AR-positive disease and a rising PSA with histological features

of adenocarcinoma. Molecular features characteristic to this class include *AR*

genetic alterations such as amplification and mutation, *AR* splice variants, and

intratumoral DHT synthesis. Similar to restored AR signaling, AR bypass

signaling is characterized by AR-positive adenocarcinomas with a rising PSA;

however, the oncogenic addiction to AR signaling is bypassed by upregulation of

glucocorticoid receptor signaling [7]. Complete AR independence has histological

features of small cell carcinoma (SSC) or neuroendocrine prostate cancer

(NEPC) and is characterized clinically by being AR-low or negative with a low

PSA and molecularly by retinoblastoma-associated protein (*RB1*) deletion, tumor protein p53 (*TP53*) deletion/mutation, neuroblastoma MYC oncogene (*MYCN*) gain, and/or aurora kinase A (*AURKA*) gain [7].

Currently, it is difficult to fully discern the role of *AR* mutations in therapy resistance due to several confounding variables. To date, five hotspot LBD mutations have been identified (L702H, W742C, H875Y, F877L, and T878A) in patients [16-20]. Despite having an elevated frequency in CRPC compared to primary prostate cancer (PCa) [16, 17, 21, 22], the overall prevalence of each individual *AR* mutation remains low. Therefore, it is difficult to determine their individual association with therapeutic response. This is further complicated by the fact that *AR* mutations are often detected along with *AR* amplification and/or other *AR* mutations [23]. Additionally, the emergence of both AR bypass signaling and SCC/NEPC in patients with CRPC may hinder our ability to determine the clinical significance of *AR* mutations alone as predictors of therapeutic response to enzalutamide and abiraterone.

Our current understanding of how hotspot *AR* mutations may mediate therapeutic resistance is based upon limited clinical data and pre-clinical studies. Pre-clinical models have shown that AR antagonists can paradoxically function as agonists in the context of certain *AR* LDB mutations [24, 25]. In *in vitro* overexpression studies, the AR antagonist bicalutamide has been shown to have either partial or full agonistic activity to AR L702H, W742C, H875Y and T878A [24] while the next generation therapy enzalutamide has partial agonist activity to AR H875Y, F877L, and T878A [24]. This phenomena has been supported

clinically by some patients who showed clinical improvement following discontinuation of flutamide therapy [7]. Alternatively, some LBD mutations may allow for the promiscuous activation of AR by other steroid ligands such as estrogen, progesterone, and glucocorticoids [7, 24]. A better understanding of this non-specific activity may be of particular importance as the glucocorticoid prednisone is given to patients being treated with abiraterone to prevent mineralocorticoid excess syndrome. In preclinical studies, AR L702H is activated by glucocorticoids and has been found in patients treated with abiraterone. These prior pre-clinical studies examining the role of both hotspot and non-hotspot *AR* mutations have been mostly limited to exogenous *AR* overexpression [24], which less than half the time recapitulates findings in the clinic. Studies have shown that strikingly distinct phenotypes exist between models of exogenous overexpression of gene mutations and gene editing to introduce the mutation [26, 27]. For example, overexpression of *HER2* missense mutations which are rarely seen amplified in patients are far more oncogenic than heterozygous *HER2* missense mutations introduced by gene editing which better recapitulate clinical findings [27]. Overall, these data highlight the need to develop pre-clinical models that reflect patient findings for rigorous investigations of *AR* LBD mutations and therapy resistance.

The CRISPR/Cas System

Clustered regularly interspaced short palindromic repeats (CRISPR) and CRISPR-associated (Cas) genes are the main elements of a microbial adaptive

immune system [28-32]. To date, three types (I-III) of CRISPR/Cas systems have been identified across bacteria and archaea [30]. However, every system ultimately involves the cleavage of foreign nucleic acids by RNA-guided nucleases, which are encoded for in the Cas genes. It was discovered that microbes contain genetic loci with distinctive repetitive elements interspaced with short variable sequences or protospacers [33]. These protospacers were found to be derived from exogenous DNA sources, such as viruses or plasmids, and each protospacer was always associated with a protospacer adjacent motif (PAM) [34-36]. The sequence of the PAM was also discovered to be specific to the type of CRISPR/Cas system being utilized by that given species of bacteria or archaea [35, 36]. Together, the protospacers, PAMs, and interspersed foreign genetic elements constitute the CRISPR RNA (crRNA) array. The crRNA array encodes the guide RNAs or the sequences that the Cas nuclease will use in order to recognize and target foreign nucleic acids for cleavage [35]. The CRISPR/Cas systems also require a trans-activating crRNA (trcrRNA), which facilitates the processing of the crRNA into discrete units [32, 37]. Once the Cas protein associates with the trcrRNA and guide RNA, it can target an invading pathogen for destruction by creating a Watson-Crick base pairing between its specific guide RNA and the pathogen's complementary nucleic acid sequence.

The Type II CRISPR system specifically consists of the Cas9 nuclease and guide RNAs that are 20 nucleotides in length [32, 37-40]. Additionally, the wild-type (WT) Cas9 derived from *Streptococcus pyogenes* targets the complementary foreign DNA of its guide RNA for cleavage when the sequence

immediately precedes a 5′-NGG PAM, thereby making a blunt cut between the 17th and 18th bases in the target sequence (or three base pairs 5′ of the PAM) [38]. To date, the Cas9 protein has been optimized for expression in mammalian cells, where it has been shown to maintain its nuclease function [41-44]. Furthermore, Jinek et al. (2012) showed that the required crRNA and trcrRNA for Cas9 function could be fused together, creating one single-guide RNA (sgRNA) [38]. Thus, by altering the 20-nucleotide guide sequence within the sgRNA, Cas9 can target any sequence of interest for cleavage in mammalian cells as long as it falls within the vicinity of the PAM sequence. The HNH and RuvC nuclease domains of Cas9 are responsible for its ability to target sequences for cleavage and, hence, create double strand breaks (DSBs) [39]. Meanwhile, an aspartate-to-alanine mutation in the RuvC catalytic domain (D10A) causes the Cas9 mutant to nick rather than cleave the nucleic acid sequence of interest [37, 38]. Thus, the Cas9 nickase mutant (Cas9n) yields single-strand breaks, and in particular, the SpCas9n only nicks between the 17th and 18th bases in the target sequence.

DSBs in DNA can be particularly harmful for a cell if no attempt to repair them is made [45]. Thus, two main DNA repair mechanisms in order to correct DSBs have evolved in eukaryotic cells [45, 46]. The first mechanism of DSB repair is non-homologous end joining (NHEJ). NHEJ involves the broken ends of DNA being ligated, often resulting in INDEL mutations. The second mechanism of DSB repair is homology-directed repair (HDR). HDR is the precise editing of a damaged locus when a sister chromosome or homologous template is available.

CRISPR/Cas9 gene editing studies have exploited these two types of DSB repair in order to create knockout and knock-in (KI) mutations in genetic loci of interest [41-44, 47]. However, many CRISPR/Cas9 studies have also illustrated that while each base within the 20-nucleotide guide sequence contributes to overall Cas9 specificity, multiple mismatches between the sgRNA and a particular nucleotide sequence can be tolerated, leading to many off-target DSBs and unwanted INDEL mutations [41, 48-50]. Single-strand nicks are usually repaired by the base excision repair (BER) pathway, which potentially results in decreased off-target INDEL mutations [51]. However, while targeting a region of interest with one nickase limits off-target effects of the CRISPR/Cas9 gene editing system, it does not necessarily result in a desired knockout or KI mutation of the targeted locus due to the fact that the cell will preferentially use BER to resolve this lesion.

Ran et al. (2013) developed a double nickase strategy that involves two Cas9n plasmids, each with sgRNAs that are slightly off-set and complementary to opposite strands of the target site [52, 53]. Nicking both DNA strands simultaneously by a pair of Cas9 nickases leads to a site-specific DSB. This DSB can then be repaired by either NHEJ or HDR. Thus, the CRISRP/Cas9 double nickase system increases the specificity of Cas9n's target recognition, while also allowing Cas9n to modify a region of interest at a rate similar to WT Cas9.

Translational Relevance of the Isogenic Models with AR LBD Mutations

Due to the increased Cas9n specificity and similar rates of genome modification with WT Cas9, the CRISPR/Cas9 double nickase system was chosen to generate a novel, isogenic panel of PCa cell lines, all of which contain hotspot *AR* LBD mutations. The four PCa cell lines that were chosen for *AR* gene editing were LNCaP, LAPC-4, VCaP, and CWR22Rv1 (or 22Rv1). These androgen responsive cell lines were chosen for this panel because they are commonly used in research and recapitulate a spectrum of *AR* genomic statuses seen in patients with CRPC. The experimental goal of this study was to first introduce individual missense mutations into the *AR* genetic locus in all of these cell lines using two Cas9n-sgRNA complexes and a repair template (RT) containing a particular *AR* LBD mutation (Figure 3.2A). In other words, after a DSB is created by the double nickases within the *AR* genetic locus, the cell would preferentially repair this damage by HDR (i.e. using the provided RT) and, thereby, KI to its genome the desired *AR* LBD mutation.

Currently, it is unknown if any single and/or combination of *AR* LBD mutations detected in patient cell-free DNA by next-generation sequencing are predictive of either innate or acquired resistance to next-generation therapies. Consequently, how *AR* mutational status should influence therapy selection for men with CRPC has not been determined. By generating novel isogenic cell line models, the biologic role of these *AR* mutations as well as their role in resistance to contemporary androgen-AR axis therapies can be elucidated. Thus, the

findings from these isogenic models have the ability to influence the clinical management of men with metastatic PCa who have somatic *AR* mutations.

Materials and Methods

CRISPR/Cas9 Double Nickase Design and Preparation

The pSpCas9n(BB)-2A-Puro (PX462) V2.0 nickase plasmid was originally purchased by Dr. Ben H. Park (Johns Hopkins School of Medicine (JHSoM), Baltimore, MD) from Addgene. PX462 was then molecularly cloned, purified, and digested with BbsI (New England Biolabs, Inc.) by Dr. W. Brian Dalton. Since a CRISPR/Cas9 double nickase stategy was determined to be ideal for *AR* genomic targeting, the digested PX462 was used to create two, guide-specific Cas9 plasmids (or Cas9 protein guides). In order to transform PX462 into two Cas9 protein guides, the online CRISPR Design Tool (http://tools.genome-engineering.org) was used to determine the optimal, offset 20-nucleotide guide sequences within the given *AR* genomic target sequence of interest. These two Cas9 Guides were designed 18 nucleotides apart in *AR*, intron 7 and were confirmed to not be in a region involved in splicing by the online Human Splicing Finder (www.umd.be/HSF/). The CRISPR Design Tool identified two PAMs (CCC and GGG) and the 20-base sequences (5'-aggaagtacggggaagggg-3' and 5'-agaccaaaaatcagaggttg-3') downstream and upstream of the PAMs for the generation of Cas9 Guide 1A and 1B, respectively. From these two, 20-base

sequences, the sgRNAs sequences were designed and purchased as oligos from IDT as follows: Guide 1A forward: 5'-caccgcccccttccccgtacttcct-3'; Guide 1A reverse: 5'-aaacaggaagtacggggaagggggc-3'; Guide 1B forward: 5'-caccgagaccaaaaatcagaggttg-3' Guide 1B reverse: 5'-aaaccaacctctgattttttggtctc-3'. Each forward and reverse oligo for a given Cas9 Guide was annealed in a PNK buffer reaction provided by Dr. W. Brian Dalton and using the following cycling conditions: (1) 95°C for 5 minutes; (2) ramp down to 25°C at 5°C per minute; (3) dilute annealed oligos 1:200 with UltraPure™ Distilled Water (Invitrogen). Each diluted, annealed oligo pairing of sgRNAs was ligated to PX462 separately, using New England Biolab, Inc.(NEB)'s Quick Ligase as per the manufacturer's protocol. The ligation reactions were cleaned up by a QIAquick PCR Purification Kit (Qiagen), transformed into Invitrogen's One Shot® TOP10 Electrocomp™ E. coli, and plated on LB-Ampicillin (50µg/mL) plates overnight. Colonies were PCR-screened by Phusion® Hot Start Flex DNA Polymerase (NEB) as per the manufacturer's protocol and using the following primers: forward primer 216 (5'-cctctgacttgagcgtcgat-3') and reverse primer 871 (5'-ggggcgtacttggcatatgata-3'). The annealing temperature for these primes was 66.3°C with an extension time of 30 seconds. All positive colonies were prepared using Qiagen's Plasmid Maxi Kit, thereby creating Cas9n Guide 1A and 1B. Glycerol stocks of each positive colony were also prepared and stored at -80°C.

CRISPR/Cas9 RT Design and Preparation

The first two, hotspot mutations in *AR*, exon 8 to be chosen for targeting by the CRISPR/Cas9 double nickase system were F877L and T878A. Three, 323-base pair RTs were generated for this region, each spanning the *AR*, intron 7/exon 8 boundary of interest (gBlocks Gene Fragments, IDT). The gBlock RTs were homologous to the region except for the single nucleotide missense mutation of interest, the inclusion of the M13F primer sequence (5'-tgtaaaacgacggccagt-3') to be inserted into the intron in order to mutate Guide 1A's PAM and for target-specific PCR amplification, and the sequence (TTA) to mutate the PAM sequence of Guide 1B to prevent re-targeting after incorporation. The gBlock RT names and sequences are as follows (with mutated bases in **bold**): (1) RT1-WT: 5'-agcacaagctggagaagtcttgagtcagagagcttacaatggtataagacatctcttgggagccctcagtgact ccatggagaccatttctttctctctctctcgctgtctctctctaacacacacacacacacacgacctcatgggggg agga**tgtaaaacgacggccagt**gggggaggaaacaaaaggctgaaagaccaaaaatcagaggttt**tta**g aagaggctagcagaggccacctccttgtcaaccctgtttttctccctcttattgttccctacagattgcgagagagct gcatcagttcacttttgacctgctaatcaagtcacacatggtgagcgtggactttccggaaatgatggcagagatc atctctgtgcaagtgcccaagatcctttctgggaaagtcaagcccatctatttccacacccagtgaagcattggaa a-3' (2) RT2-F877L: 5'-agcacaagctggagaagtcttgagtcagagagcttacaatggtataagacatctcttgggagccctcagtgact ccatggagaccatttctttctctctctctcgctgtctctctctaacacacacacacacacacgacctcatgggggg agga**tgtaaaacgacggccagt**gggggaggaaacaaaaggctgaaagaccaaaaatcagaggttt**tta**g aagaggctagcagaggccacctccttgtcaaccctgtttttctccctcttattgttccctacagattgcgagagagct

gcatcag**c**tcacttttgacctgctaatcaagtcacacatggtgagcgtggactttccggaaatgatggcagagat

catctctgtgcaagtgcccaagatcctttctgggaaagtcaagcccatctatttccacacccagtgaagcattgga

aa-3' (3) RT3-T878A: 5'-

agcacaagctggagaagtcttgagtcagagagcttacaatggtataagacatctcttgggagccctcagtgact

ccatggagaccatttctttctctctctctcgctgtctctctctaacacacacacacacacacacgacctcatgggggg

agga**tgtaaaacgacggccagt**gggggaggaaacaaaaggctgaaagaccaaaaatcag**tta**ttgggg

aagaggctagcagaggccacctccttgtcaaccctgtttttctccctcttattgttccctacagattgcgagagagct

gcatcagttc**g**cttttgacctgctaatcaagtcacacatggtgagcgtggactttccggaaatgatggcagagatc

atctctgtgcaagtgcccaagatcctttctgggaaagtcaagcccatctatttccacacccagtgaagcattggaa

a-3'. All gBlock RTs were PCR-amplified by Phusion® Hot Start Flex DNA

Polymerase (NEB) as per the manufacturer's protocol and then validated by

Sanger sequencing (JHSoM Genetic Recourses Core Facility). The forward

primer (gBlock-F1) for PCR amplification was 5'-

tctttctctctctctcgctgtctctctctaacacacacacacacacacacgacctcatgg-3' and the reverse

primer (gBlock-R1) was 5'-ccaatgcttcactgggtgtgg-3'. These primers had an

annealing temperature of 67°C with an extension time of 30 seconds and

extended each gBlock RT to a size of 359 nucleotides. PCR reactions were

cleaned up using a QIAquick PCR Purification Kit (Qiagen) as per the

manufacturer's protocol, and both gBlock-F1 and gBlock-R1 were used as

sequencing primers in the Sanger sequencing reactions.

Cell Lines and Culture

22Rv1, LAPC-4, and VCaP cells were gifts of Dr. John Isaacs (The Johns Hopkins University, Baltimore, MD). LNCaP cells were obtained from the American Type Culture Collection (ATCC; Manassas, VA). LNCaP and 22Rv1 cells were cultured in growth medium (RPMI-1640 (Gibco) supplemented with 10% (vol/vol) FBS (Corning) and 1% (vol/vol) Pen Strep (P/S; Gibco)). LAPC-4 cells were cultured in growth medium (IMDM (Gibco) supplemented with 10% (vol/vol) FBS and 1% (vol/vol) P/S). VCaP cells were cultured in growth medium (DMEM, High Glucose (ATCC) with 10% (vol/vol) FBS and 1% (vol/vol) P/S).

Cell Line Transfections with CRISPR/Cas9 Reagents

All cell lines were plated in 6-wells at a concentration of 6×10^5 cells per well in their respective growth medium. When cells reached 80% confluency (24 to 48 hours after being plated), each well was washed with 1X PBS (Gibco). Cells were then incubated for two hours in antibiotic-free growth medium with 10% (vol/vol) FBS only. Transfection reactions were set up according to Promega's FuGENE HD Transfection Reagent Technical Manual. Each 150uL transfection reaction for a given 6-well contained a total of 2.85ug total DNA (1250ng RT, 800ng Guide 1A, and 800ng Guide 1B), 11.4uL FuGENE HD (which is a 4:1 ratio of ug total DNA to uL FuGENE HD), and remaining amount of Opti-MEM I (Gibco). Each transfection reaction incubated for 5 minutes at room temperature. After the two-hour incubation, the antibiotic-free growth media with 10% (vol/vol) FBS only was refreshed on each 6-well of cells, and the given

150uL transfection reaction was added to the well. After 48 hours, half the transfected cells of a 6-well were taken for genomic DNA (gDNA) isolation, meanwhile the remaining half of the transfected cells were maintained in cell culture for single cell isolations.

gDNA Isolations and Single Cell Isolations

All gDNA isolations of transfected cell pools were performed with Qiagen's DNeasy Blood and Tissue Kit as per the manufacturer's protocol. As for single cell isolations, each pool of transfected cells was counted, and serial dilutions were performed in respective media in order to plate 48, 96, 192, or 288 cells per 96-well plate (or 0.5, 1, 2, or 3 cells per 96-well). Plates were checked and marked weekly for wells that contained the growth of single cell colonies. Once wells containing a single cell colony had reached greater than 50% confluency (2-4 weeks depending on the given cell line), the cells of a given well were trypsinized (0.25% Trypsin, 2.21mM EDTA; Corning) and replica plated between two 96-well plates. Once the cells in the duplicated 96-well plates reached greater than 80% confluency, gDNA was isolated from an entire 96-well plate, using Promega's Wizard SV 96 Genomic DNA Purification System as per the manufacturer's protocol. The gDNA was then PCR-screened for positive clones that had successfully undergone HDR with the CRISPR RTs. All positive clones were taken from the duplicated and remaining 96-well plate and expanded, maintained, and frozen down for experimental purposes.

PCR Screens for CRISPR-positive Clones

Due to difficulty amplifying the region of interest from these 96-well plates, all gDNA isolated from these transfected cell lines underwent nested PCR amplification in order to initially screen for the single cell isolated clones that successfully underwent HDR, utilizing the provided gBlock RTs. First, a region of 874 bases was PCR-amplified from the gDNA using Invitrogen's Platinum™ *Taq* DNA Polymerase as per the manufacturer's protocol. This region completely surrounds the PAM sites in *AR*, intron 7, the single base substitution site in *AR,* exon 8, and the gBlock RTs. The forward primer (F1) sequence for this PCR is as follows: 5'-GTGGTGAAGAAAAGAACACGG-3'. The reverse primer (R1) sequence for this PCR is as follows: 5'-GCCCAGCAAATAGAATTCAGG-3'. The annealing temperature for this primer pair was 58.8°C with an extension time of one minute. Then, the PCR product from this first PCR was used as the product for the second, nested PCR and amplified using Invitrogen's Platinum™ *Taq* DNA Polymerase as per the manufacturer's protocol. The product size for the nested PCR is 442 bases, which still encompasses the majority of the gBlock RT design. The forward primer (M13F) sequence for the nested PCR is as follows: 5'-TGTAAAACGACGGCCAGT-3', which contains the mutated PAM 1 sequence in the gBlock RTs. The reverse primer sequence for this nested PCR is the same as R1. The annealing temperature for this primer pair was 56.5°C with an extension time of 30 seconds. Single cell colonies containing the positive, 442-base band were trypsinized from the duplicated 96-well plates and expanded for experimental purposes. Please note that isolated gDNA from the transfected cell

pools only underwent the one, nested PCR with primers M13F and R1 for screening purposes. The nested PCR product from both the 96-well plates and the transfected cell pools was gel isolated using Qiagen's QIAquick Gel Extraction Kit as per manufacturer's protocol and sent for Sanger sequencing. The M13F or the R1 primer was used as the sequencing primer in these reactions. As the single cell clones were expanded and maintained, gDNA was continuously isolated, nested PCR-screened, and Sanger sequenced to confirm CRISPR/Cas9-edited genomic status.

Droplet Digital PCR (ddPCR)

ddPCR for determining the *AR* copy number of parental cell lines and CRISPR/Cas9-edited cell clones was performed largely as described previously [23, 54]. In order to confirm the *AR* genomic status as either WT or mutant of all parental and CRISPR/Cas9-edited cell lines, isolated gDNA was digested with MseI (NEB) and cleaned using a QIAquick PCR Purification Kit (Qiagen) as per the manufacturer's protocol. WT and mutant probes to AR, exon 8 were designed and ordered from IDT as follows: WT probe (HEX): ATCAGTTCACTTTTGACCTGCTA; F877L probe (FAM): ATCAGCTCACTTTTGACCTGCTA; and T878A probe (FAM): ATCAGTTCGCTTTTGACCTGCTA. WT control genomic female and male DNA (Promega) digested with MseI as well as the gBlock RTs for the particular mutation were used as ddPCR controls. ddPCR (Bio-Rad) was performed in a dedicated, ultraviolet (UV)-equipped hood and according to the manufacturer's

protocol. Total molecules were quantified and analyzed by the QX200 Droplet Reader software.

Results

Initial Nested PCR Screens of All Transfected Cell Lines

Initial nested PCR screens of LNCaP, LAPC-4, 22Rv1, and VCaP gDNA successfully amplified the expected, 442-base pair (bp) band from the CRISPR/Cas9n reagent-transfected cell line pools and did not amplify any DNA fragment from the non-transfected cell line pools (i.e. negative controls; Figure 3.2B). Sanger sequencing of the gel isolated, nested PCR product showed both the parental *AR*, intron 7 and exon 8 sequences as well as the expected KI point mutations provided by the RTs. Both parental and KI RT mutations are present in the transfected cell line gDNA because the transfection rate of any population of cells is not 100%, and therefore, these cell pools still contain both transfected and non-transfected cells. In addition, the CRISPR/Cas9n reagent-transfected cells within these pools may not have completely utilized the RT to repair the *AR* genomic locus after the DNA had been nicked; hence, this gDNA may also contain cells with complete and incomplete RT KIs.

LNCaP-CRISPRed Cell Lines

Sixteen, 96-well plates for single cell dilutions were used for each of the transfected LNCaP cell pools. Since there was a separate transfection for each RT (WT, F877L, and T878A), a total of 48 plates were created and then visually screened by an inverted microscope over a period of four weeks for wells containing single cell colonies. From these 48 plates, only a total of 480 wells contained single cell colonies and were, therefore, replicated between two 96-well plates. Thus, it is estimated that 160 single cell colonies were replica plated for each RT transfection. All of these 480 single cell colonies (growing in a total of 5, 96-well plates) were screened by two PCRs (including the nested PCR) for cells that had successfully undergone HDR with the provided RT. From the LNCaP cells transfected with the WT RT (LNCaP-WT), only 1 single cell colony was found by this PCR screen. For the LNCaP cells transfected with the F877L and T878A RTs (LNCaP-F877L and LNCaP-T878A, respectively), two LNCaP-F877L and three LNCaP-T878A clones were identified. Thus, a total of 6 clones (out of a total of 480 or 1.3% of clones) were found to have utilized the provided RT to repair the double-stranded nicks created by Guides 1A and 1B within *AR*, intron 7. Each CRISPR-positive, 442-bp band amplified from these six single cell colonies in the second PCR (or nested PCR) was gel isolated and sent for Sanger sequencing. The gDNA from these same six cell lines was also digested in order to determine the genomic status of the entire cell colony by ddPCR. In the meantime, it took two months to expand these six cell colonies from the second replica plate. When cell lines were at a point of freezing down, gDNA was

again isolated in order to perform a nested PCR screen as well as additional Sanger sequencing and ddPCR assessments.

It was determined by Sanger sequencing and ddPCR that not one of these six, CRISPR-positive LNCaP colonies was a homogeneous cell population (i.e. a cell line that was expanded from a single cell). Therefore, an aliquot of each line was taken before completing freezing them down and single cell dilutions into 96-well plates were performed for a second time. Four, 96-well plates (each diluted at 1 cell per well) were created for each CRISPR-positive cell line. From a total of 24 plates, only a combined total of two 96-well plates were created for replication. Thus, only 12-32 single cell colonies were isolated per original CRISPR-positive cell line. Interestingly, when both of these 96-well plates were PCR-screened, the single cell colonies from four of these six original CRISPR-positive cell lines screened completely negative (i.e. did not amplify the 442-bp band). In fact, only single cell colonies from two of these original CRISPR-positive cell lines amplified the 442-bp band. Thus, the second single cell dilutions of the original six CRISPR-positive LNCaP cell lines yielded only a total of six CRISPR-positive colonies from the LNCaP-WT line and one CRISPR-positive colony from a LNCaP-T878A line. These seven, CRISPR-positive colonies from the second attempt at single cell dilutions were expanded and frozen down.

The 442-bp bands amplified from the six, second dilution LNCaP-WT cell lines during the nested PCR screen were gel isolated and Sanger sequenced. From these results, it was concluded that these cell lines were still not

homogeneous populations and that isolating single LNCaP cells in 96-well plates may be more difficult than originally anticipated. Therefore, an original stock of the LNCaP-WT clone was defrosted for a third single cell isolation. For this third attempt at single cell isolations, the LNCaP-WT cells were diluted across 16, 96-well plates (i.e. four plates per cell dilution) containing a feeder layer of irradiated NIH 3T3 cells. From these 16 plates, a total of four, 96-well plates of single cell clones were created for replication. Interestingly, when these four plates were screened by nested PCR, the majority (>90%) of the wells were CRISPR-positive (i.e. most of the colonies contained cells that had utilized the RT during HDR). Twenty-one single cell colonies were chosen randomly from these four plates and taken for expansion. The 442-bp bands from the nested PCR screen of these 21 colonies were gel isolated and Sanger sequenced. The gDNA from nine of these 21 colonies was also digested for ddPCR. Since all of these LNCaP-WT colonies had very similar Sanger sequencing and ddPCR results (Figure 3.3A), it was concluded that there was most likely not an issue with how the cells were single cell isolated for the third time. In fact, ddPCR results of the parental LNCaP cell lines (i.e. before transfection with the CRISPR/Cas9n reagents) confirm that these cells have two copies of the *AR* gene (Table 3.2). Thus, the single cell colonies isolated from LNCaP-WT for the third time are most likely homogeneous populations of cells where only one of the *AR* alleles has been targeted by the nickases and repaired using the WT RT. Additionally, RNA was isolated and cDNA was synthesized from two of these LNCaP-WT single cell colonies. The cDNA from these two colonies was assessed by ddPCR in order to

determine which allele (WT or T878A) is being expressed. While the majority of the cDNA being expressed by these colonies contained the parental sequence (T878A), these colonies were also expressing the knocked-in WT allele at very low levels (Figure 3.4A).

LAPC-4-CRISPRed Cell Lines

The first set of LAPC-4 single cell dilution plates (total=16, 96-well plates per RT) were set up similarly to the first set of LNCaP single cell dilution plates. However, for the LAPC-4 single cell isolations, only a total of 430 single cell colonies (or ~140 colonies per RT transfection) were replica plates into an initial 4.5, 96-well plates. Interestingly, a total of 6 clones (out of a total of 430 or 1.4% of clones) were found by PCR screening to have utilized the provided RT to repair the double-stranded nicks created by Guides 1A and 1B within *AR*, intron 7. From the LAPC-4 cells transfected with the WT RT (LAPC-4-WT), only 1 single cell colony was found by this PCR screen. For the LAPC-4 cells transfected with the F877L and T878A RTs (LAPC-4-F877L and LAPC-4-T878A, respectively), two LAPC-4-F877L and three LAPC-4-T878A clones were identified. Each CRISPR-positive, 442-bp band amplified from these six single cell colonies in the nested PCR was gel isolated and sent for Sanger sequencing, while the gDNA from these same six cell lines was also digested in order to determine the genomic status of the entire cell colony by ddPCR (Figure 3.3B). In the meantime, it took 3.5 months to expand these six LAPC-4 cell colonies from the second replica plate. When cell lines were at a point of freezing down, gDNA

was again isolated in order to perform a nested PCR screen as well as additional Sanger sequencing and ddPCR assessments.

Since it was determined by Sanger sequencing and ddPCR that not one of these six, CRISPR-positive LAPC-4 colonies was a homogeneous cell population, an aliquot of each line was taken before completely freezing them down and single cell dilutions into 96-well plates for a second time were performed. Similar to the second single cell dilutions of LNCaP cells, only a combined total of two 96-well plates were created for replication. Thus, only 12-32 single cell colonies were isolated per original CRISPR-positive cell line. Interestingly, when both of these 96-well plates were PCR-screened, the single cell colonies from three of these six original CRISPR-positive cell lines screened completely negative. In fact, only single cell colonies from three of these original CRISPR-positive cell lines amplified the 442-bp band. Thus, the second single cell dilutions of the original six CRISPR-positive LAPC-4 cell lines yielded only a total of one CRISPR-positive colonies from LAPC-4-WT, 12 CRISPR-positive colonies from a LAPC-4-F877L line, and nine CRISPR-positive colonies from a LAPC-4-T878A line. However, only seven and nine colonies of these second dilution LAPC-4-F877L and T878A lines, respectively, were able to be expanded and frozen down. The 442-bp bands amplified by the nested PCR screen from these 16, second dilution LAPC-4-F877L and T878A cell lines were gel isolated and Sanger sequenced. From these results, it was concluded that all seven of the LAPC-4-F877L cell lines contained gDNA with the F877L missense mutation as well as the parental cell line's sequence, making it a heterogeneous or mixed

population of cells. However, all nine of the LAPC-4-T878A cell lines looked like homogeneous cell populations as they only contained the T878A missense mutation in their Sanger sequencing results. However, these results still need to be confirmed by ddPCR.

ddPCR results of the parental LAPC-4 cell lines (i.e. before transfection with the CRISPR/Cas9n reagents) confirm that these cells have one copy of the *AR* gene (Table 3.2). Thus, the single cell colonies isolated from the first single cell dilutions of the transfected LAPC-4 cells as well as the LAPC-4-F877L cell lines from the second attempt at dilutions are most likely heterogeneous or mixed populations of cells. Additionally, RNA was isolated and cDNA was synthesized from two of these single cell colonies isolated from LAPC-4-F877L for the second time. The cDNA from these two colonies was then assessed by ddPCR in order to determine if there were cells in these populations expressing *AR* WT or F877L. The cDNA being expressed by both of these colonies contained the parental sequence (WT) and the mutated sequence (F877L) at very similar levels (Figure 3.4B).

22Rv1-CRISPRed Cell Lines

A total of 24, 96-well plates (or eight plates per RT) were originally set up for single cell dilutions of all 22Rv1 cell lines transfected with CRISPR/Cas9n reagents. Within five weeks, 200 single cell colonies per RT were replica plated. From initial PCR screens, two WT, five F877L, and five T878A colonies were CRISPR-positive. These 12 colonies (or 2% of the total colonies) were

expanded over four weeks. Of these 12 CRISPR-transfected cell lines, only 1 targeted WT, four F877L, and two T878A cell lines were able to be grown and expanded. Through Sanger sequencing, it was discovered that two of the 22Rv1-F877L lines did not contain the intended F877L mutation, thereby creating CRISPR-targeted controls for the 22Rv1 cell lines. Sanger sequencing results for the five other CRISPR-positive cell lines show that both the particular knocked-in missense mutation and parental line sequences are present. Thus, these five CRISPR-positive 22RVI cell lines remain as mixed cell populations with targeted and non-targeted cells or as homogeneous cell populations with at least one *AR* allele targeted. Since the *AR* copy number status for parental 22Rv1 cells is still being assessed (Table 3.2), no conclusions about these lines have been made as of yet.

VCaP-CRISPRed Cell Lines

A total of 36, 96-well plates (or 12 plates per RT) were originally set up for single cell dilutions of all VCaP cell lines transfected with CRISPR/Cas9n reagents. It took two months to collect ~75 single cell colonies per RT for replication, and it was an additional five months after replication before these single cell colonies grew to about 80% confluency and could be screened. Through PCR screening, three WT, five F877L and 10 T878A CRISPR-positive colonies were initially discovered. However, it took an additional six months to expand these single cell colonies from the 96-well replica plates and not every colony survived. From these 18 original CRISPR-positive VCaP colonies, only

three WT, two F877L, and seven T878A colonies survived the process of expansion. From these 12 single cell colonies, gDNA was isolated before freezing stocks of each CRISPR-positive cell line. However, it was decided to delay additional screens on these CRISPR-positive cell lines since these particular cell lines took over a year to grow. Interestingly, when a second transfection of VCaP cells with the CRISPR/Cas9n reagents was performed, an additional eight, 96-well plates per RT (i.e. a total of 24 plates) were created; however, no single cell colonies were visible after three months. Thus, no replica plates could be made or screened. In addition to growing poorly after transfection, parental VCaP cell lines were found to contain increased *AR* copy number by ddPCR (Table 3.2). It is still being considered whether or not this copy number gain could be interfering with the targeting of the *AR* genetic locus by the CRISPR/Cas9n system.

Discussion and Future Directions

CRISPR/Cas9 is a relatively new gene editing method and consequently protocols for using this system are still being optimized. While this study demonstrates that the CRISPR/Cas9n system can be used to introduce *AR* genetic mutations in several PCa cell lines (including LNCaP, LAPC-4, 22Rv1, and VCaP), there are a few limitations of this study that need to be addressed since none of the generated cell lines can be utilized in experiments as of yet.

The first limitation of this study is the type of CRISPR/Cas9n system that was utilized. While the double nickase system does limit off-target mutagenesis, a recent study has suggested that the efficiency of the system could be further increased if the Cas9n plasmids directly target the region of interest's exon for nicking and if the provided RTs are much shorter [55]. Another study has suggested combining CRISPR/Cas9 gene editing technology with recombinant adeno-associated virus (rAAV) genome editing technology such that the designed RT contains a selection cassette in addition to the mutations of interest [56]. This technique would then allow for the selection of cells that specifically utilized the RT to repair the double-strand break introduced by the nickases and would, thereby, also increase the rate of finding CRISPR-positive single cell clones after the initial transfections.

Another limitation of this study was the initial single cell isolation protocol that was used. This protocol originally involved the significant dilution of the cell population across 96-well plates; however, it became evident that after transfection, these PCa cell lines were very sensitive and seemed to only grow in a non-single cell state. The best single cell isolation results in this study were seen with the LNCaP-WT line, which was single cell isolated for a third time in plates containing a feeder layer of irradiated NIH 3T3 cells. In addition to using feeder layer cells, cloning cylinder technology could also be employed to isolate single, CRISPR-positive cells. This technique involves cells being distributed across a large enough surface area so that individual cells can grow without interacting with other growing colonies and in continuously conditioned media.

This method is particularly useful when single cells cannot grow without paracrine signaling. Thus, all of the remaining CRISPR-positive LNCaP, LAPC-4, and 22Rv1 cell lines will need to be properly single cell isolated using a different protocol.

In addition to re-isolating single cell clones from each of the CRISPR-positive lines and redesigning the CRISPR/Cas9 gene editing system, the LNCaP-WT cell line that has already been properly single cell isolated (and all other CRISPR-positive LNCaP cell lines that will undergo single cell dilution) will need to endure further gene editing in order to introduce the *AR* LBD sequences of interest into the second *AR* allele. Once the entire panel of isogenic PCa cell lines with *AR* LBD mutations has been generated, a unique and valuable resource will be available for many future studies. Future studies will comprehensively examine these cell lines for genetic and epigenetic alterations as well as differences in overall gene expression. These cell lines will also be valuable pre-clinical substrates for drug design and testing. Ultimately, by generating novel isogenic cell line models, the biologic role of these *AR* mutations as well as their role in resistance to contemporary androgen-AR axis therapies can be elucidated. Consequently, how *AR* mutational status should influence therapy selection for men with CRPC can be determined.
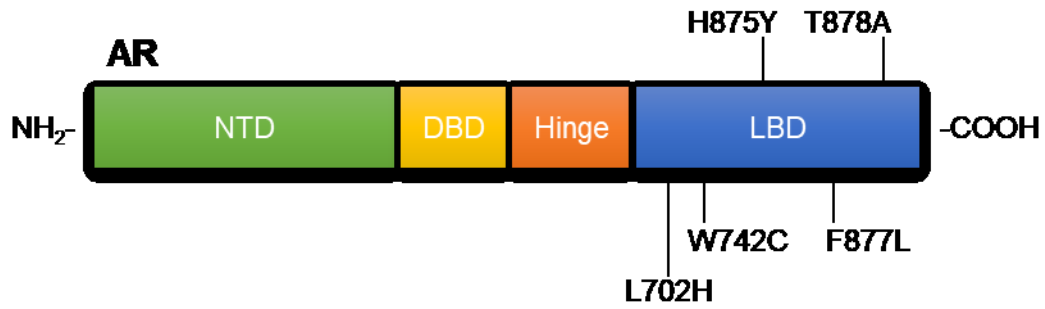
Figure 3.1. Schematic of the domain structure of AR, highlighting the location of cancer-associated LBD hotspot mutations.
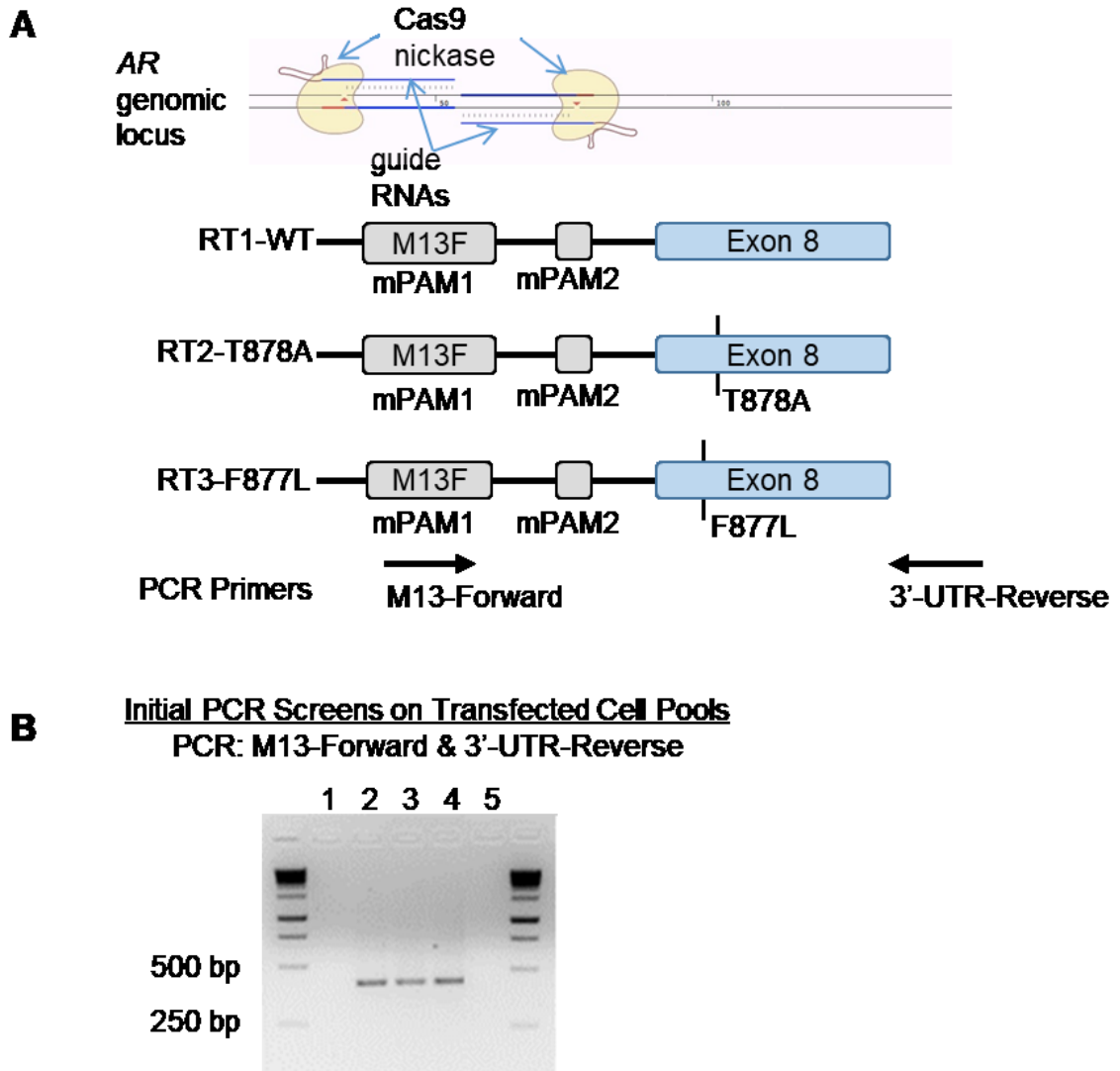
Figure 3.2. Schematic of CRISPR/Cas9n gene targeting scheme for *AR* in PCa

cell lines. A) CRISPR-targeting strategy for *AR* WT, T878A, and F877L. Intronic

barcodes for amplification were introduced into the *AR* genetic locus for targeted

parental identification (mPAM1-M13F and mPAM2-TTA). B) Representative

image of PCR-amplified gDNA using the M13-Forward internal barcode specific

primer and the 3'-UTR-Reverse primer outside of the targeting region. The gDNA

in this particular PCR was from VCaP cells either not transfected with

CRISPR/Cas9n reagents (i.e. negative control; Lane 1) or transfected with

CRISPR/Cas9n reagents (WT, F877L, and T878A RTs; Lanes 2-5, respectively).

Lane 5 represents a water (or negative) control.
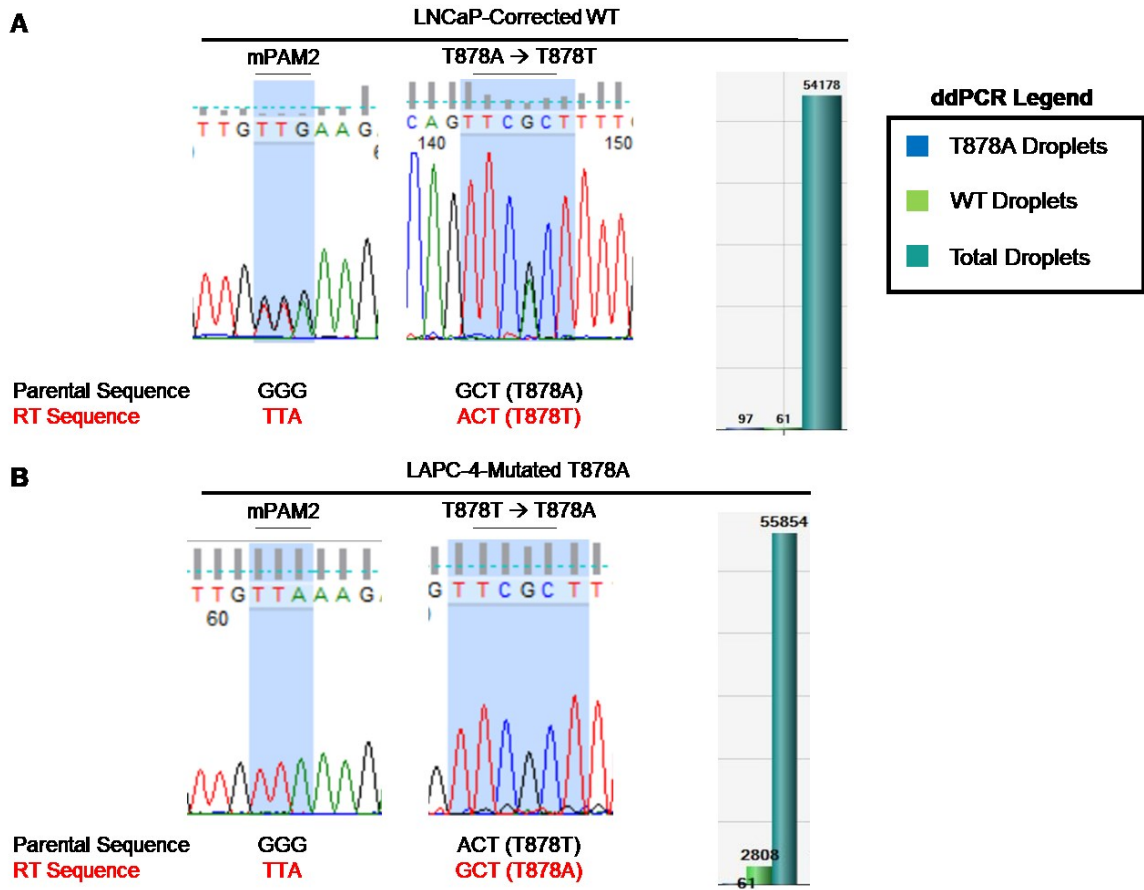
Figure 3.3. Representative Sanger sequencing and ddPCR results for PCa cell

lines, all of which were single cell isolated after transfection with CRISPR/Cas9n

reagents. A) Results for a LNCaP cell line transfected with the WT RT. B)

Results for a LAPC-4 cell line transfected with the T878A RT.
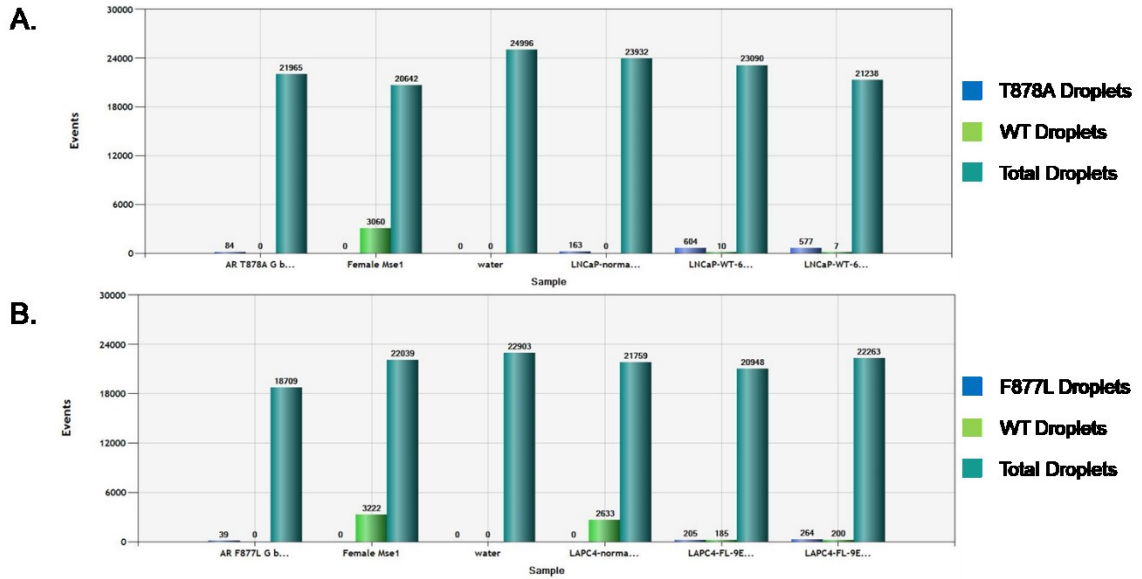
Figure 3.4. Determining the *AR* gene expression status of CRISPR/Cas9n-transfected PCa cell lines by assessing cDNA via ddPCR. ddPCR results for (A) two LNCaP-WT cell lines that were single cell isolated during the third attempt and for (B) two LAPC-4-F877L cell lines that were originally thought to be single cell isolated during the second attempt, but most likely remained a mixed population of targeted and non-targeted cells. Positive controls for both ddPCRs include: AR T878A and F877L gBlocks (mutant probe controls), Female gDNA digested by MseI (WT probe control), and a given cDNA control for each of the parental cell lines. A water (or negative) control was also utilized.

Table 3.1. Three Categories of Resistance Mechanisms to Next-generation AR-targeted Therapies for CRPC. (Adapted from Watson PA, et al. (2015) [7].)

	Restored AR Signaling	AR Bypass Signaling	Complete AR Independence
Clinical Relapse Profile	• AR+ • Rising PSA	• AR+ • Rising PSA	• AR-low or AR- • Low PSA
Histological Features	• Adenocarcinoma	• Adenocarcinoma	• SCC/NEPC • Unknown Subtypes
Molecular Features	• AR-activating mutations • AR-active splice variants • Intratumoral DHT Synthesis from Adrenal Precursors	• Glucocorticoid Receptor Upregulation	• *RB1* Deletion • *TP53* Deletion or Mutation • *MYCN* Gain • *AURKA* Gain

Table 3.2. AR Status of PCa Cell Lines.

Cell Line	AR Status	*AR* Genotype	*AR* Copy Number
LNCaP	Positive	Mutant: T878A	2
LAPC4	Positive	WT	1
VCaP	Positive; *AR* Gene Amplification; Splice Variant Positive	WT	>25
CWR 22Rv1	Positive; Splice Variant Positive	Mutant: H875Y	To Be Determined

References:

1.   Freedman, LP. Molecular Biology of Steroid and Nuclear Hormone Receptors. Birkhauser; Boston, MA: 1998.

2.   Gao W, Bohl CE, and Dalton JT. Chemistry and Structural Biology of Androgen Receptor. *Chemical reviews*. 2005;105(9):3352-3370.

3.   Keller ET, Ershler WB, and Chang C. The androgen receptor: a mediator of diverse responses. *Frontiers in bioscience: a journal and virtual library*. 1996;1:d59-71.

4.   J. G. Hardman, L. E. Limbird, and A. G. Gilman (ed). Goodman & Gilman's the pharmacological basis of therapeutics. 10th edition. McGraw-Hill Medical Publication Division; New York: 2001.

5.   Johansen KL. Testosterone metabolism and replacement therapy in patients with end-stage renal disease. *Seminars in dialysis*. 2004;17(3):202-8.

6.   Migeon BR, Brown TR, Axelman J, and Migeon CJ. Studies of the locus for androgen receptor: localization on the human X chromosome and evidence for homology with the Tfm locus in the mouse. *PNAS USA*. 1981;78(10):6339-43.

7.   Watson PA, Arora VK, and Sawyers CL. Emerging mechanisms of resistance to androgen receptor inhibitors in prostate cancer. *Nature reviews Cancer*. 2015;15(12):701-11.

8.   Chawnshang, C. Androgens and androgen receptor: mechanisms, functions, and clinical applications. Kluwer Academic Publishers; Boston, MA: 2002.

9.   Pratt WB and Toft DO. Steroid receptor interactions with heat shock protein and immunophilin chaperones. *Endocrine reviews*. 1997;18(3):306-60.

10.   Heinlein CA and Chang C. Androgen receptor (AR) coregulators: an overview. *Endocrine reviews*. 2002;23(2):175-200.

11.   Shang Y, Myers M, and Brown M. Formation of the androgen receptor transcription complex. *Molecular cell*. 2002;9(3):601-10.

12.   Visakorpi T, Hyytinen E, Koivisto P, Tanner M, et al. In vivo amplification of the androgen receptor gene and progression of human prostate cancer. *Nature genetics*. 1995;9(4):401-406.

13.   Chen CD, Welsbie DS, Tran C, Baek SH, Chen R, et al. Molecular determinants of resistance to antiandrogen therapy. *Nature medicine*. 2004;10(1):33-39.

14.   Tran C, Ouk S, Clegg NJ, Chen Y, Watson PA, Arora V, et al. Development of a second-generation antiandrogen for treatment of advanced prostate cancer. *Science*. 2009;324(5928):787-790.

15.   Attard G, Belldegrun AS, and de Bono JS. Selective blockade of androgenic steroid synthesis by novel lyase inhibitors as a therapeutic strategy for treating metastatic prostate cancer. *BJU international*. 2005;96(9):1241-1246.

16.   Grasso CS, Wu YM, Robinson DR, Cao X, et al. The mutational landscape of lethal castration-resistant prostate cancer. *Nature*. 2012;487(7406):239-43.

17.   Robinson D, Van Allen EM, Wu YM, Schultz N, et al. Integrative clinical genomics of advanced prostate cancer. *Cell*. 2015;161(5):1215-28.

18.   Azad AA, Volik SV, Wyatt AW, Haegert A, Le Bihan S, et al. Androgen Receptor Gene Aberrations in Circulating Cell-Free DNA: Biomarkers of Therapeutic Resistance in Castration-Resistant Prostate Cancer. *Clinical cancer research: an official journal of the American Association for Cancer Research*. 2015;21(10):2315-24.

19.   Romanel A, et al. Plasma AR and abiraterone-resistant prostate cancer. *Science translational medicine*. 2015;7(312):312re10.

20.   Wyatt AW, Azad AA, Volik SV, Annala M, Beja K1, et al. Genomic Alterations in Cell-Free DNA and Enzalutamide Resistance in Castration-Resistant Prostate Cancer. *JAMA oncology*. 2016;2(12):1598-1606.

21.   Kumar A, Coleman I, Morrissey C, Zhang X, et al. Substantial interindividual and limited intraindividual genomic diversity among tumors from men with metastatic prostate cancer. *Nature medicine*. 2016;22(4):369-78.

22.   Cancer Genome Atlas Research Network. The Molecular Taxonomy of Primary Prostate Cancer. *Cell*. 2015;163(4):1011-25.

23.   Torquato S, Pallavajjala A, Goldstein A, Toro PV, Silberstein JL, et al. Genetic Alterations Detected in Cell-free DNA are Associated with Enzalutamide and Abiraterone Resistance in Castration-resistant Prostate Cancer. [Submitted]

24.   Lallous N, Volik SV, Awrey S, Leblanc E, et al. Functional analysis of androgen receptor mutations that confer anti-androgen resistance identified in circulating cell-free DNA from prostate cancer patients. *Genome biology*. 2016;17:10.

25.   Veldscholte J, Ris-Stalpers C, Kuiper GG, Jenster G, et al. A mutation in the ligand binding domain of the androgen receptor of human LNCaP cells affects steroid binding characteristics and response to anti-androgens. *Biochemical and biophysical research communications*. 1990;173(2):534-40.

26.   Konishi H, Karakas B, Abukhdeir AM, Lauring J, et al. Knock-in of mutant K-ras in nontumorigenic human epithelial cells as a new model for studying K-ras mediated transformation. *Cancer research*. 2007;67(18):8460-7.

27.   Zabransky DJ, Yankaskas CL, Cochran RL, Wong HY, et al. HER2 missense mutations have distinct effects on oncogenic signaling and migration. *PNAS USA*. 2015;112(45):E6205-14.

28.   Deveau H, Garneau JE, and Moineau S. CRISPR/Cas system and its role in phage-bacteria interactions. *Annual review of microbiology*. 2010;64:475-493.

29.   Horvath P and Barrangou R. CRISPR/Cas, the immune system of bacteria and archaea. *Science*. 2010;327(5962):167-170.

30.   Makarova KS, Haft DH, Barrangou R, Brouns SJ, et al. Evolution and classification of the CRISPR-Cas systems. *Nature reviews Microbiology*. 2011;9(6):467-477.

31.   Bhaya D, Davison M, and Barrangou R. CRISPR-Cas systems in bacteria and archaea: versatile small RNAs for adaptive defense and regulation. *Annual review of genetics*. 2011;45:273-297.

32.   Garneau JE, Dupuis MÈ, Villion M, Romero DA, et al. The CRISPR/Cas bacterial immune system cleaves bacteriophage and plasmid DNA. *Nature*. 2010;468(7320):67-71.

33.   Makarova KS, Haft DH, Barrangou R, Brouns SJ, et al. Evolution and classification of the CRISPR-Cas systems. *Nature reviews Microbiology*. 2011;9(6):467-477.

34.   Marraffini LA and Sontheimer EJ. CRISPR interference limits horizontal gene transfer in staphylococci by targeting DNA. *Science*. 2008;322(5909):1843-1845.

35.   Brouns SJ, Jore MM, Lundgren M, Westra ER, et al. Small CRISPR RNAs guide antiviral defense in prokaryotes. *Science*. 2008;321(5891):960-964.

36.   Barrangou R, Fremaux C, Deveau H, Richards M, et al. CRISPR provides acquired resistance against viruses in prokaryotes. *Science*. 2007;315(5819):1709-1712.

37.   Gasiunas G, Barrangou R, Horvath P, and Siksnys V. Cas9-crRNA ribonucleoprotein complex mediates specific DNA cleavage for adaptive immunity in bacteria. *PNAS USA*. 2012;109(39):E2579-E2586.

38.   Jinek M, Chylinski K, Fonfara I, Hauer M, et al. A programmable dual-RNA-guided DNA endonuclease in adaptive bacterial immunity. *Science*. 2012;337(6096):816-821.

39.   Sapranauskas R, Gasiunas G, Fremaux C, Barrangou R, et al. The Streptococcus thermophilus CRISPR/Cas system provides immunity in Escherichia coli. *Nucleic acids research*. 2011;39(21):9275-9282.

40.   Magadán AH, Dupuis M-È, Villion M, and Moineau S. Cleavage of phage DNA by the Streptococcus thermophilus CRISPR3-Cas system. *PLoS ONE*. 2012;7(7):e40913.

41.   Cong L, , Ran FA, Cox D, Lin S, Barretto R, et al. Multiplex genome engineering using CRISPR/Cas systems. *Science*. 2013;339(6121):819-823.

42.   Mali P, Yang L, Esvelt KM, Aach J, Guell M, et al. RNA-guided human genome engineering via Cas9. *Science*. 2013;339(6121):823-826.

43.   Jinek M, East A, Cheng A, Lin S, et al. RNA-programmed genome editing in human cells. *eLife*. 2013;2:e00471.

44.   Cho SW, Kim S, Kim JM, and Kim JS. Targeted genome engineering in human cells with the Cas9 RNA-guided endonuclease. *Nature biotechnology*. 2013;31(3):230-232.

45.   Chapman JR, Taylor MR, and Boulton SJ. Playing the end game: DNA double-strand break repair pathway choice. *Molecular cell*. 2012;47(4):497-510.

46.   Lieber MR. The mechanism of double-strand DNA break repair by the nonhomologous DNA end joining pathway. *Annual review of biochemistry*. 2010;79:181-211.

47.   Hwang WY, Fu Y, Reyon D, Maeder ML, et al. Efficient genome editing in zebrafish using a CRISPR-Cas system. *Nature biotechnology*. 2013;31(3):227-229.

48.   Fu Y, Foden JA, Khayter C, Maeder ML, et al. High-frequency off-target mutagenesis induced by CRISPR-Cas nucleases in human cells. *Nature biotechnology*. 2013;31(9):822-6.

49.   Jiang W, Bikard D, Cox D, Zhang F, and Marraffini LA. RNA-guided editing of bacterial genomes using CRISPR-Cas systems. *Nature biotechnology*. 2013;31(3):233-9.

50.   Hsu PD, Scott DA, Weinstein JA, Ran FA, et al. DNA targeting specificity of RNA-guided Cas9 nucleases. *Nature biotechnology*. 2013;1(9):827-32.

51.   Dianov GL and Hübscher U. Mammalian base excision repair: the forgotten archangel. *Nucleic acids research*. 2013;41(6):3483-90.

52.   Ran FA, Hsu PD, Lin CY, Gootenberg JS, et al. Double nicking by RNA-guided CRISPR Cas9 for enhanced genome editing specificity. *Cell*. 2013;154(6):1380-1389.

53.   Ran FA, Hsu PD, Wright J, Agarwala V, et al. Genome engineering using the CRISPR-Cas9 system. *Nature protocols*. 2013;8(11):2281-2308.

54.   Goldstein A, Valda Toro P, Lee J, Silberstein JL, Nakazawa M, Waters I, et al. Detection fidelity of AR mutations in plasma derived cell-free DNA. *Oncotarget*. 2017;8(9):15651-62.

55.   Paquet D, Kwart D, Chen A, Sproul A, et al. Efficient introduction of specific homozygous and heterozygous mutations using CRISPR/Cas9. *Nature*. 2016;533(7601):125-9.

56.   Kaulich M, Lee YJ, Lönn P, Springer AD, et al. Efficient CRISPR-rAAV engineering of endogenous genes to study protein function by allele-specific RNAi. *Nucleic acids research*. 2015;43(7):e45.

Samantha Danielle Torquato
Curriculum Vitae
1550 Orleans Street, Baltimore, MD 21287
(443) 287 – 0877 || storqua1@jhmi.edu

EDUCATION

Johns Hopkins School of Medicine, Baltimore, MD   2014 – 2018
　　Ph.D. in Cellular and Molecular Medicine
　　Preparing Future Faculty Teaching Academy Certificate

Smith College, Northampton, MA   2007 – 2011
　　B.A. in Biological Sciences and Mathematics
　　High Honors in Biological Sciences
　　Associate Member of Sigma Xi, The Scientific Research Society
　　First Group Scholar 2009 – 2011 (top 10% of the Class of 2011)
　　Dean's List 2008 – 2011
　　Massachusetts Initial Teacher License in Mathematics – Grades 8-12

RESEARCH EXPERIENCE

Johns Hopkins School of Medicine, Baltimore, MD   2015 – 2018
　　Ph.D. Candidate in the Laboratory of Paula J. Hurley, Ph.D.
　　Dissertation Title: *Genetic Alterations in Prostate Cancer: Evaluating Their Biomarker Potential and Roles in Therapeutic Response and Resistance*

Brigham and Women's Hospital, Department of Medicine – Cardiovascular Medicine, Boston, MA   2012 – 2014
　　Technical Research Assistant II in the Laboratory of Jane A. Leopold, M.D.

Brigham and Women's Hospital, Department of Medicine – Gastroenterology, Boston, MA   2011 – 2012
　　Technical Research Assistant II in the Laboratory of Richard Blumberg, M.D.

AB Biosciences, Inc., Allston, MA, **Research Assistant**   2011

Smith College, Northampton, MA   2008 – 2011
　　Honors Thesis Student in the Laboratory of Robert Merritt, Ph.D.
　　Honors Thesis in Biological Sciences: *An Exploration of Restricted Lactate Dehydrogenase Subunit Association*

University of Massachusetts, Amherst, MA, **Laboratory Assistant**   2010

Smith College participates in the Summer Black-Footed Ferret Survey,
Logan County, KS   2009
    Student Research Assistant in the Laboratory of Steven Williams, Ph.D.

PUBLICATIONS

Torquato S, Pallavajjala A, Goldstein A, Toro PV, Silberstein JL, Lee J, Nakazawa M, Waters I, Chu D, Shinn D, Grogonski T, Hughes RM, Simons BW, Khan H, Feng Z, Carducci MA, Paller CJ, Denmeade SR, Kressel B, Eisenberger MA, Antonarakis ES, Trock BJ, Park BH, Hurley PJ. Androgen Receptor Ligand-binding Domain Mutations in Cell-free DNA are Associated with Enzalutamide and Abiraterone Resistance in Castration-resistant Prostate Cancer. (In Review)

Hughes RM, Simons BW, **Torquato S**, Miller R, Khan H, Theodros D, Haffner MC, Lotan T, Huang J, Davicioni E, An SS, Garraway IP, Fertig EJ, Isaacs JT, Brennen WN, Park BH, Hurley PJ. Asporin Restricts Mesenchymal Stromal Cell Differentiation and Drives Metastatic Progression. (In Review)

Goldstein A, Toro PV, Lee J, Silberstein JL, Nakazawa M, Waters I, Cravero K, Chu D, Cochran RL, Kim M, Shinn D, **Torquato S**, Hughes RM, Pallavajjala A, Carducci MA, Paller CJ, Denmeade SR, Kressel B, Trock BJ, Eisenberger MA, Antonarakis ES, Park BH, Hurley PJ. (2017). Detection fidelity of AR mutations in plasma derived cell-free DNA. *Oncotarget*, *8*(9), 15651–62. http://doi.org/10.18632/oncotarget.14926

Aguero J, Ishikawa K, Hadri L, Santos-Gallego C, Fish K, Hammoudi N, Chaanine A, **Torquato S**, Naim C, Ibanez B, Pereda D, García-Alvarez A, Fuster V, Sengupta PP, Leopold JA, Hajjar RJ. (2014). Characterization of right ventricular remodeling and failure in a chronic pulmonary hypertension model. *American Journal of Physiology - Heart and Circulatory Physiology*, *307*(8), H1204–15. http://doi.org/10.1152/ajpheart.00246.2014

ABSTRACTS & POSTER PRESENTATIONS

Torquato S, Pallavajjalla A, Goldstein A, Toro PV, Silberstein JL, Lee J, Nakazawa M, Waters I, Chu D, Shinn D, Groginski T, Hughes RM, Feng Z, Carducci MA, Paller CJ, Denmeade SR, Kressel B, Eisenberger MA, Antonarakis ES, Trock BJ, Park BH, Hurley PJ. "AR LBD mutations and resistance to enzalutamide and abiraterone in prostate cancer." Eleventh Annual Prostate Cancer Program Retreat. March, 2018. Fort Lauderdale, FL.

Torquato SD, Goldstein A, Toro PV, Dalton WB, Hughes RM, Silberstein JL, Carducci MA, Paller CJ, Denmeade SR, Kressel B, Trock B, Eisenberger MA, Antonarakis ES, Park BH, and Hurley PJ. "Androgen Receptor Missense

Mutations as Predictors of Therapeutic Response in Patients with Metastatic Castration-Resistant Prostate Cancer." Johns Hopkins Prostate Research Day. October 18, 2016. Baltimore, MD.

Torquato S, Ishikawa K, Aguero J, Maron BA, Loscalzo J, Hajjar RJ, and Leopold JA. "Downregulation of Pulmonary Artery Endothelial Catechol-o-methyltransferase Activity by Aldosterone Increases Norepinephrine Levels in Pulmonary Arterial Hypertension." American Heart Association Scientific Sessions 2014. November, 2014. Chicago, IL.

Torquato S, Maron B, Loscalzo J, and Leopold JA. "Aldosterone Increases Transforming Growth Factor-β Expression to Activate Autophagy and Increase Aortic Fibroblast Collagen Synthesis and Vascular Stiffness." American Heart Association Scientific Sessions 2013. November, 2013. Dallas, TX.

Torquato S, Lee HY, Maron B, Cottrill KA, Chan SY, Loscalzo J, and Leopold JA. "Network Analysis Identifies MicroRNA-22 as a Key Regulator of Vascular Calcification." American Heart Association Scientific Sessions 2013. November, 2013. Dallas, TX.

Torquato S, Maron B, Aghamohammadzadeh R, Loscalzo J, and Leopold JA. "Aldosterone Activates Autophagy to Increase Fibroblast Collagen Synthesis and Vascular Stiffness." Experimental Biology 2013. April, 2013. Boston, MA.

Torquato S, Katz L, and Merritt R. "Sequencing LDH in the Red-Spotted Newt: An Exploration of Restricted Subunit Association." Evolution 2010. June, 2010. Portland, OR.

TEACHING EXPERIENCE

The Johns Hopkins University Preparing Future Faculty Teaching Academy Certificate Program, Baltimore, MD, **Participant**   2017 – 2018

Johns Hopkins School of Medicine, Baltimore, MD, **Pollard Scholar**   2016

The College Success Initiative Summer Program, Bunker Hill Community College, Cambridge, MA, **Math Teacher**   2013

Northampton High School, Northampton, MA, **Student Teacher**   2011

Smith College Jacobson Center for Writing, Teaching, & Learning and Quantitative Learning Center, Northampton, MA, **Tutor**   2008 – 2010

2010 Science Teaching Fellowship, Clarke School for the Deaf, Northampton, MA, **Science Teaching Fellow**   2010

Smith College brings science to Springfield Renaissance School,
Springfield, MA, **Program Initiator** 2009

Smith College goes to Park Tudor School, Indianapolis, IN, **Intern** 2009

**Smith College's Urban Education Initiative with Springfield Renaissance
School**, Springfield, MA, **Urban Education Fellow** 2009

**Smith College's Summer Science and Engineering Program for High
School Girls**, Northampton, MA, **Program Intern** 2008

COMMUNITY SERVICE

Thread: The New Social Fabric, Baltimore, MD, **Mentor** 2014 – 2018

Cambridge Community Services, Cambridge, MA, **Mentor** 2013 – 2014

Charles River Watershed Association's Water Chestnut Program,
Newton, MA, **Volunteer** 2012

Habitat for Humanity, Western MA, **Volunteer** 2008